



12-2011

Immunity and Immunopathology in acute viral infections

Shalini Sharma
ssharma3@utk.edu

Recommended Citation

Sharma, Shalini, "Immunity and Immunopathology in acute viral infections." PhD diss., University of Tennessee, 2011.
https://trace.tennessee.edu/utk_graddiss/1225

This Dissertation is brought to you for free and open access by the Graduate School at Trace: Tennessee Research and Creative Exchange. It has been accepted for inclusion in Doctoral Dissertations by an authorized administrator of Trace: Tennessee Research and Creative Exchange. For more information, please contact trace@utk.edu.

To the Graduate Council:

I am submitting herewith a dissertation written by Shalini Sharma entitled "Immunity and Immunopathology in acute viral infections." I have examined the final electronic copy of this dissertation for form and content and recommend that it be accepted in partial fulfillment of the requirements for the degree of Doctor of Philosophy, with a major in Comparative and Experimental Medicine.

Barry T Rouse, Major Professor

We have read this dissertation and recommend its acceptance:

Timothy Sparer, Melissa Kennedy, Stephen Kennel

Accepted for the Council:

Carolyn R. Hodges

Vice Provost and Dean of the Graduate School

(Original signatures are on file with official student records.)

IMMUNITY AND IMMUNOPATHOLOGY IN ACUTE VIRAL INFECTIONS

A Dissertation Presented for the
Doctor of Philosophy Degree
The University of Tennessee, Knoxville

Shalini Sharma

December 2011

ACKNOWLEDGEMENTS

It gives me great pleasure to express sincere gratitude to my major advisor Dr. Barry T Rouse for his expert guidance, keen interest, constant encouragement, constructive criticism and suggestions which helped me immensely in executing the present work. I wish to thank my committee members, Dr. Melissa Kennedy, Dr. Stephen Kennel, Dr. Timothy Sparer, for their encouragement and interest in my research and their time and effort in reviewing this work.

I extend my sincere thanks to Dr. Paul Thomas, Dr. Mark Sangster and Dr. Robert Donnel for their scholarly suggestions, critical observation and kind help from time to time proved a great asset for me.

Thanks are also due to my colleagues Tamara Veiga Parga, Aarthi Sundararajan, Fernanda Gimenez, Sachin Mulik, Amol Suryawanshi, Naveen Rajasagi, Pradeep Reddy and Junwei Zeng for their help, exchanges of knowledge and frustrations during my graduate program. It has been a great pleasure to interact with other lab members and colleagues Pranay Dogra, Sidheshwar Bhela, Raphael Leon Richardson and Pranita Sarangi.

Finally, I express my deepest gratitude to my family for their constant encouragement, monumental patience and profound moral support.

ABSTRACT

Herpetic stromal keratitis (HSK) is an immunopathological and tissue destructive corneal lesion caused by herpes simplex virus (HSV) infection, which induces an intense inflammatory response and finally leads to blindness. Accumulating evidence using the murine model has shown that Th-1 phenotype CD4⁺ T cells orchestrating the inflammation mainly contribute to the immunopathological reaction in HSV-1 infected cornea. Initially various innate immune cells recruit and produce numerous inflammatory and angiogenic molecules into the corneal stroma those in turn drive the corneal immunopathology.

While the basic principles of immunity to the influenza A viruses (IAV) are probably similar for all vertebrates, detailed understanding is based largely on experiments in laboratory mice. Virus clearance is normally mediated via CD8⁺ effector T cells but, in their absence, the class-switched antibody response can ultimately achieve the same goal. Influenza virus-specific plasma cells and CD8⁺ T cells persist in the long term and the recall of the CD8⁺ T cell response can lead to earlier virus clearance.

The first part (Part I) of this dissertation focuses on the understanding of HSV-1 induced immunoinflammatory processes in the cornea and the secondary lymphoid tissues and the involvement of immuno-modulatory mechanisms following acute viral infections such as HSV and IAV. The next three parts (Part II-IV) focus on different inflammatory and counter-inflammatory mechanisms that

are activated following acute viral infections. Results in Part II evaluate the role of small molecule inhibitors of VEGFR2/src kinase inhibitors in controlling the progression of the inflammatory lesions after ocular HSV infection. Results of the third section show that the host counter inflammatory mechanisms inhibit tissue damage but these may also act to constrain the effectiveness of immunity to acute infections. The fourth section describes the functional significance of HVEM expression on regulatory T cell in their expansion following HSV-1 infection.

In this study, experiments were designed to understand the mechanisms involved in the regulation of immunity and resultant immunopathology using HSV-1 and IAV as the model systems and that modulation of these processes can enhance immune response and diminish immunopathology following acute infections.

TABLE OF CONTENTS

Part	Page
I Background and Overview.....	1
Animal models and pathogenesis of SK.....	3
Immunity and Immunopathology to IAV.....	12
Conclusion.....	19
List of references.....	20
Appendix.....	29
II An anti-inflammatory role of VEGFR2/src kinase inhibitor in HSV-1 induced immunopathology.....	34
Abstract.....	35
Introduction.....	36
Materials and Methods.....	38
Results.....	45
Discussion.....	53
List of references.....	59
Appendix.....	63
III Tim-3/Galectin-9 interaction regulates influenza A virus specific humoral and CD8 T cell responses.....	79

Abstract.....	80
Introduction.....	81
Materials and Methods.....	82
Results.....	88
Discussion.....	95
List of references.....	100
Appendix.....	104

IV Regulatory T cell expression of Herpes virus entry mediator (HVEM)

following HSV-1 infection and its functional significance..... 128

Abstract.....	129
Introduction.....	130
Materials and Methods.....	132
Results.....	136
Discussion.....	142
List of references.....	148
Appendix.....	151

V Conclusion..... 169

VITA..... 171

LIST OF FIGURES

Part	Figure	Page
I	Figure 1. Principal cellular events in herpetic SK pathogenesis.....	30
	Figure 2. Herpes virus entry mediator and its ligands.....	31
	Figure 3. Schematic representation of consequences of Tim-/Galectin-9 Interaction	32
II	Figure 2.1. Effect of topical administration of src kinase inhibitor (TG100801) on the severity of SK.....	65
	Figure 2.2. TG100801 inhibits FAK-y861 phosphorylation in the murine cornea.....	66
	Figure 2.3. TG100572 controls SK lesion severity independent of viral replication.....	67
	Figure 2.4. Effect of systemic administration of src kinase inhibitor (TG100572) on angiogenesis and SK lesion severity.....	69
	Figure 2.5. Representative eye photograph (at day 15 p.i.) of control (a) and TG100572 treated (b) mice.....	70
	Figure 2.6. Kinetics of Cellular infiltration in the corneas of control and TG100572 treated mice.....	72
	Figure 2.7. TG100572 treatment diminishes the infiltration of pathogenic Th1	

cells in the cornea.....74

Figure 2.8. TG100572 treatment results in the blockade of CXCL1 in the
cornea.....76

Figure 2.9. Src kinase inhibition may result in the attenuation of T cell
function.....78

III Figure 3.1. Tim-3 expression is up regulated on virus-specific CD8 T cells
after IAV infection.....106

Figure 3.2. Galectin 9 induces apoptosis of IAV NP tetramer specific and Tim-3⁺
CD8 T cells in vitro.....108

Figure 3.3. Gal-9 knockout animals mount stronger virus-specific CD8 T cell
responses in the acute phase.....110

Figure 3.4. Enhanced virus-specific antibody production in G9KO mice after
influenza infection.....112

Figure 3.5. Gal-9 knockout mice develop more robust recall responses to
influenza A virus upon heterologous challenge.....114

Figure 3.6. Administration of Tim-3 fusion protein in mice after IAV infection
enhances the magnitude and quality of IAV-specific CD8 T cells
responses.....116

Figure 3.7. Outcome of infection with IAV HKx31.....118

Figure 3.8. Cells obtained from broncho-alveolar lavage (BAL) were stained for
CD45⁺ and CD45⁺CD11b⁺Ly6G⁺120

Figure 3.9. Lung Histopathology.....	122
Figure 3.10. Characterization of CD4 ⁺ FoxP3 ⁺ regulatory T cells from WT and the G9KO mice.....	124
Figure 3.11. Adoptive transfer of memory CD8 T cells.....	127

IV Figure 4.1. HSV-1 infection results in the expansion of CD4 ⁺ FoxP3 ⁺ regulatory T cells.....	153
Figure 4.2. HVEM expression is up regulated on regulatory T Cells following HSV-1 infection and its viral ligand is expressed in PLN following infection.....	155
Figure 4.3. Primed cells stimulated with HSV causes HVEM up regulation on Tregs.....	157
Figure 4.4. Recombinant HSV-1 gD increases the proportions of FoxP3 ⁺ T cells among CD4 ⁺ T cells.....	159
Figure 4.5. HSV-1gD can help to expand Tregs.....	161
Figure 4.6. Diminished representations of CD4 ⁺ FoxP3 ⁺ regulatory T cells in the HVEM knockout mice.....	163
Figure 4.7. Reduced numbers of CD4 ⁺ FoxP3 ⁺ per CD4 ⁺ FoxP3 ⁻ T cells in HVEM knockout mice.....	165
Figure 4.8. Diminished frequencies of activated Tregs in HKO animals ...	167
Figure 4.9 Influence of HVEM expressing T regs on outcome of immune response to HSV.....	168

ABBREVIATIONS

APC.....	Antigen presenting cell
BTLA.....	B and T lymphocyte attenuator
CCL2, 5, 20.....	Chemokine (C-C motif) ligand 2, 5, 20
CD.....	Cluster of differentiation
CTL.....	Cytotoxic T lymphocyte
COX-2.....	Cyclooxygenase-2
CXCR2.....	CXC chemokines receptor 2
CXCL3, 8.....	CXC chemokine ligand 3, 8
DC.....	Dendritic cell
FGF.....	Fibroblast growth factor
Gal-9.....	Galectin-9
G9KO.....	Galectin-9 knockout
HKO.....	HVEM knockout
HVEM.....	Herpes virus entry mediator
HSV-1.....	Herpes simplex virus 1
HSV-1gD.....	Herpes simplex virus 1 glycoprotein D
HSK.....	Herpetic Stromal Keratitis
IAV.....	Influenza A virus
ICAM-1.....	Intercellular adhesion molecule 1
IFN- α , γ	Interferon alpha, gamma
IL-1, 2, 6, 12, 17, 18, 23... IL-18	Interleukin 1, 2, 6, 12, 17, 18, 23

BP.....Binding protein
IP-10.....Interferon inducible protein 10
KC.....Keratinocyte-derived chemokine
LT.....Lymphotoxin
LTa.....Lymphotoxin alpha
LTbR.....Lymphotoxin beta-receptor
MCP-1..... Monocyte chemoattractant protein 1
MIP-1, 2.....Macrophage inflammatory protein 1,2
MMP-9.....Matrix metalloproteinase-9
NFκB.....Nuclear factor- kappa B
PECAM.....Platelet endothelial cell adhesion molecule
PFU.....Plaque forming unit
PGE2.....Prostaglandin E2
PMN.....Polymorphonuclear leukocyte
PAMP.....Pathogen Associated Molecular Patterns
siRNA.....Small interfering RNA
SK.....Stromal Keratitis
SCID.....Severe combined immunodeficiency
TGF-β.....Transforming growth factor beta
TIMP.....Tissue inhibitors of metalloproteinases
TLR 2, 4, 9.....Toll like receptor 2, 4, 9
TNF-α.....Tumor necrosis factor alpha
VEGF.....Vascular endothelial growth factor

VEGFR2.....Vascular endothelial growth factor receptor 2
VLA4.....Very late antigen 4
Treg.....Regulatory T cell
Tim-3.....T cell immunoglobulin and mucin protein

PART I

BACKGROUND AND OVERVIEW

IMMUNOPATHOLOGY AND IMMUNITY TO HSV-1

Clinical Background

Herpes simplex virus (HSV) induced eye diseases are one of the commonest causes of unilateral infectious blindness in the western world. Epidemiological studies in the United States reveal that, 400,000 persons are affected, with 20,000 new cases occurring annually with the incidence ranging from 4.1- 20.7 cases/100 000 patients per year (9, 87). Results from surveys conducted by the National Health and Nutrition Examination between 1976 and 1980 (NHANES II) and again between 1988 and 1994 (NHANES III) showed a 30% increase in HSV-2 specific antibodies within the studied timeframe in the United States (67) . In contrast the age specific seroprevalence of HSV-1 has decreased in industrial countries with the exception of several developing countries (67) . Ocular lesions are mostly caused by HSV type 1 and very rarely by HSV type 2 infections. However, 80% of neonatal herpes infection is caused by HSV-2, although both strains can be involved.

Classically, the life cycle of HSV in the host is divided into four stages namely, entry, spread, establishment of latency and reactivation. After the primary infection of the skin or mucosal surfaces with HSV, it spreads to the neuronal cell bodies where latency is established. It is currently believed that the virus reactivation is kept in check by host immune cells in the sensory ganglion (82). The psychological and physical stresses that result in temporary impairment of the immune system facilitate the reactivation of HSV and subsequent release of the virus to the periphery (26). Most ocular HSV infections result in acute

epithelial keratitis that can be controlled with several antiviral drugs (42) . Twenty % of the patients infected ocularly with HSV develop, a chronic vision impairing stromal lesion known as herpetic stromal keratitis (HSK). In humans, approximately 50% of HSK occurs as a consequence of virus reactivation from the trigeminal ganglion and only ~2% of such cases result directly from primary HSV infection. The chances of developing SK are three times greater following a recurring herpetic keratitis than following a primary infection.

Symptoms of HSK lesions include corneal necrosis and ulceration along with stromal edema and neovascularization (16) . These lesions are shown to occur mainly as a result of T cell mediated immunopathological responses in the cornea whose pathogenesis is poorly understood. Forty to ninety percent of the patients with stromal keratitis may develop disciform keratitis (corneal endothelium is the main site of damage), while the rest of the patients may develop stromal opacities. If not treated properly, it may lead to corneal scarring and ulcerations warranting corneal transplantation. Apart from stromal keratitis, HSV infection can also result in viral retinitis and/or encephalitis in immunosuppressed and immunocompetent individuals. In some cases, infection with HSV-1 or 2 have also been reported to be associated with acute retinal necrosis syndrome.

Animal models and pathogenesis of SK

Most of the studies to elucidate the pathogenesis of HSK have been performed in animal models for human HSK. For primary infection, the mouse is the most studied animal species, while the rabbit is the preferred animal for

recurring infection. However similar types of lesions occur after primary or the recurrent infection (83). Understanding progressing events that finally lead to corneal inflammation has mainly come from primary ocular infection in mice. Several strains of mice including both immunocompromised and immunocompetent animals such as BALB/c, C57BL6, CAL-20, 129/SVEV have been described for studying HSK (16) . In immunocompetent animals SK lesions are evident within 6-7 days after ocular infection with HSV-1 that peak in severity between 15-21 days. The lesions are primarily caused by CD4⁺ T cells that are detected in abundance at day 7-8 pi and most of which are likely to be HSV reactive. Another model uses TCR transgenic mice on a RAG^{-/-} background, which have been shown to develop SK upon ocular infection with HSV, even though their CD4⁺ T cells were almost all reactive with OVA323-339 peptide and not detectably cross-reactive with HSV antigens (28). The CD4⁺ T cells in the ocular lesions of such animals were shown to react with the KJ1.26 mAb noted by others to react with the TCR of H-2d CD4⁺ T cells that recognize the OVA323-339 peptide (35) . Since this KJ⁺ TCR had no demonstrable reactivity with HSV, it was thought that the activation of KJ⁺ CD4⁺ T cells was not TCR mediated but involved activation by one or more cytokines (30) . This model was referred to as a bystander model of SK (29) . Yet another model that has been characterized is SK induced in SCID mice after reconstitution with CD4⁺ but not CD8⁺ T cells isolated from either HSV immune or naïve animals (80, 87, 93). All these animal models present typical SK lesions characterized by corneal haze, edema, necrosis, ulceration and neovascularization.

Ocular infection with HSV 1 in immunocompetent animals is followed by initial replication of virus especially in the corneal epithelium for up to 5-6 days. Live viral particles and the transcribed mRNA copies of viral genes can be detected from the corneal swabs during this time but not beyond 7 days post infection using conventional viral titration and RT-PCR assays respectively (9). However, viral DNA could be detected in the cornea even up to 21 days post infection (pi), the time when the disease is at its peak and spontaneous healing may start in a minority of animals. The nature and pathophysiological significance of the persisting viral genomic DNA in terms of its transcriptional and translational efficiency to make viral proteins is not yet elucidated. Studies focused on these aspects would shed light on some of the previously unknown players in the causation of SK.

After the initial phase of viral infection and replication in the cornea, there is a prominent infiltration of inflammatory cells near the corneal epithelium that mainly consists of neutrophils (PMN) (92). These cells could potentially exert anti-viral defense by producing nitric oxides, reactive oxygen species, TNF- α , IFN- γ or perhaps just by engulfing viral particles. Furthermore, the kinetics of their infiltration correlates with the clearance of replicating virus from the cornea as shown in Fig.1 (All figures are supplied in an appendix). Other studies where neutrophils were depleted prior to ocular HSV infection showed a delay in viral clearance from the cornea (96). In addition to their role in viral clearance, they may also provide conducive conditions for the ensuing inflammatory response by releasing mediators such as IL-1 β , IL-8 (MIP-1 α) IL-12 and TNF- α . Neutrophil

secreted NO could unmask corneal antigens that can be a continuous source for the influx of reactive T cells. The matrix metalloproteinases such as MMP-9 can cause break in stromal matrix and along with neutrophil or perhaps stromal cell secreted VEGF-A contribute to the neovascularisation of usually avascular cornea. Recently it has been shown that VEGF-A is indeed present in the cornea and being bound to a soluble form of the VEGF receptor-1 impedes its angiogenic activity. Ocular neovascularization resulting from HSV infection involves a change in the balance between VEGF-A and its soluble inhibitory receptor (85). Inhibition of angiogenesis by targeting MMP-9 and VEGF by siRNA approach were shown to reduce the extent of neovascularization (4, 44). Some additional angiokines such as bFGF, E-L-R motif containing chemokines (MIP-2) are also up regulated in cornea after HSV infection (107). In addition to PMNs, other cells such as DCs, NK cells, $\gamma\delta$ -T cells, macrophages etc. could contribute both towards viral clearance and the subsequent inflammation by secreting type I IFNs, and other cytokines as well as chemokines such as IL-6, IL-1 β , IL-12, MIP-2, TNF- α , IFN- γ , IL-23, IL-17 (9). Once the vascular bed is formed, there is continuous infiltration of cells because of leakage of newly formed vessels. IL-1 and IL-6 were shown to be the critical cytokines to initiate the subsequent inflammatory events and could be produced by epithelial cells initially after viral infection. HSV DNA and perhaps some of its other components expressing PAMPs can activate PRR such as toll like receptors (TLRs)-2,4 and 9 on the innate cells which provide stimulation for the activation of the NF κ B pathway (76). CpG motifs derived from viral DNA in the cornea could stimulate TLR 9 and

induce IL-1 and IL-6 which contribute to the immunopathological lesions along with an efficient induction of adaptive immune response (110). IL-6 could be produced by un-infected cells by IL-1 stimulation in a paracrine manner which in turn trigger MIP-2 (also known as CXCL8) production that is involved in the attraction of PMNs. COX-2, is another important mediator of inflammation that could be induced by IL-1 in the cornea and acts through production of PGE2 (23). Recent studies have shown the important role of TNF- α in the causation of SK. Animals lacking this cytokine were unable to control the virus in cornea and thus exhibited enhanced lesion severity (55).

IL-12 produced by PMNs, macrophages and Langerhans DCs was shown to be another important candidate cytokine involved in the pathogenesis of SK (48, 63). It is involved in the downstream production of IFN- γ by macrophages, NK cells, neutrophils and CD4+ T cells. Both proinflammatory and anti-inflammatory activities have been attributed to IFN- γ . It aids in the PMN influx by up regulating PECAM-1 and ICAM-1 on corneal epithelial cells (90, 108), endothelium cells and keratocytes needed for the exit of inflammatory cells. It also helps to prime the CD4+ T cell responses by up regulating MHC II on antigen presenting cells. The most important anti-inflammatory activity of IFN- γ is attributed to its potential of inducing anti-angiogenesis factors including, but probably not limited to, IP-10 (51). Its role in promoting Foxp3+ regulatory T cells induction was also described recently (21, 22, 99). IL-23/IL-17 axis is another identified pathway involved in pathogenesis of various types of autoimmune inflammatory lesions. IL-23 produced by innate cells such as DCs is responsible

for the stabilization of cells with the Th17 phenotype. IL-17 produced by inflammatory Th17 or perhaps fibroblast or neutrophils help recruit more PMNs. The role of IFN- γ producing Th1 cells is well studied in SK pathogenesis but a precise role of Th17 cells has not yet been described. In mouse SK lesion CD4+ T cell outnumbers CD8+ T cells but the reasons for their preferential accumulation remains unclear (61) . The inflammatory reaction in the trigeminal ganglion has a preponderance of CD8+ T cells in addition to CD4+ T cells. The antigen-specificity of CD4+ T cells that infiltrate cornea remains largely unknown because of a lack of specific CD4+ T cells epitope derived from HSV or the tetramer. It is anticipated that CD4+ T cells that infiltrate into cornea initially constitute a population enriched in HSV reactivity. Later on lesions would be dominated by bystander cell populations. Because of less stringent requirements of antigenic stimulation of Th17 cells (101), it is possible that the role of these cells in the pathogenesis of SK predominates in the later stages of inflammation where viral antigen availability is limited. Thus, one valid hypothesis could be that the acute phase is mainly dominated by Th1 cells while the chronicity of lesion is maintained by Th17 cells. Some of our initial published observations support this hypothesis (86).

Current treatment modalities

Presently the therapeutic agents used for treating acute keratitis include the administration of antivirals and corticosteroids and non-steroidal anti-inflammatory drugs such as Cyclooxygenase-2 (COX-2) blockers (7, 16, 105). Prolonged use of antivirals was shown to result in the development of resistance

particularly in immunocompromised individuals (10, 13). Similarly use of corticosteroids might give rise to numerous adverse effects (14, 45) and in some patients it may exacerbate HSK lesions due to enhanced HSV-1 replication (102). Animal studies in the mouse model of HSK have demonstrated that cytokine and chemokine blockers such as the IL-1 receptor antagonist are effective (8) . As neovascularization is an essential event for HSK pathogenesis, siRNA against VEGF was shown to be effective in reducing HSK lesions in the mouse (44) . Recent studies have shown that VEGF-induced vascular leakage is mediated by cytoplasmic protein kinase members of the Src proto-oncogene family in brain, heart, and other tissues (20, 109) (65, 103). Such vascular permeability is likely related to a loss of integrity in adherens junctions, which regulate cell-cell adhesion. VEGF has been shown to activate the Src family of tyrosine kinases (SFKs), leading to tyrosine phosphorylation of adhesion junction components, including VE-cadherin and its associated proteins β -catenin and γ -catenin, which are important to endothelial cell adhesion(20, 43, 64, 103, 104) . Abnormal vascular permeability is frequently associated with neovascularization (77). Endothelial cell barrier functions are disrupted by a number of viruses and a recent study suggests that VEGFR2 and SFK inhibitors may be of therapeutic utility in stabilizing vasculature during viral infections (33) . Furthermore, mouse model studies also support the effectiveness of regulatory T cell therapy in controlling HSK immunopathology (80) .

Regulatory T cells as an immunotherapeutic

The magnitude of a T cell mediated immune response to an acute viral infection may be influenced by the activity of one or more types of regulatory T cells (Tregs) (87, 88), particularly those that express FoxP3. For example HSV-1 infection results in the activation and expansion of regulatory T cells and the majority of expanded Tregs are not antigen specific. It is conceivable that the Treg expansion following an acute viral infection could be an immune evasion strategy employed by the virus to dampen the antiviral CD8 T cell responses (5) or conversely it could be a counter inflammatory mechanism imposed by the viral infected host itself to prevent the immune mediated collateral tissue damage (72). In addition to other mechanisms such as the cytokine IL-10 (71, 87) Treg are shown to be involved in controlling the ongoing inflammatory processes in the cornea (87) . In addition, these cells might help in the resolution of the clinical lesions and in model systems in which the activity of Treg cells can be inhibited, tissue-damaging immunopathological reactions to some viruses are increased (87). How HSV infection triggers Treg expansion and the molecular interactions responsible for their suppressive activity remains poorly understood. Additionally, since the expanded Treg population is largely non-specific to HSV, TCR (T cell receptor) mediated events likely play at most a minor role.

HSV entry into cells requires binding of the envelope glycoprotein D (gD) to HVEM (a TNF receptor family member) receptors on the cell (46). Besides being an entry receptor for HSV, HVEM is identified as a co-stimulatory molecule that is known to be constitutively expressed on the cells of immune compartment. HVEM can promote T cell activation by propagating signals from the TNF super

family member ligand, LIGHT, a lymphotoxin related inducible ligand (100) that competes with glycoprotein D for binding to HVEM on T cells or can deliver inhibitory signals upon binding with BTLA (B and T lymphocyte attenuator) (Fig 2). In a previous report HVEM knockout mice were shown to develop an unexpected enhancement of T cell responses (98), with increased susceptibility to autoimmunity and that over expression of HVEM enhances Treg suppressive function (91) suggesting a role of HVEM in Treg suppressive function. Importantly T cells from scurfy mice have been shown to lack HVEM expression even after activation (91), suggesting an involvement of FoxP3 in regulation of HVEM expression.

BTLA and CD160 binding to HVEM has an important role in antagonizing and down regulating effector cell function activated directly or indirectly by LIGHT and LT binding to HVEM or LTbR. The inhibitory functions of BTLA and CD160 may be distinct and non-redundant as suggested by their distinct expression. In addition, the TNF family ligands of HVEM (LIGHT and LTa) bind to LTbR and are important for immunoregulation by shaping the lymph node architecture and DC expansion and homeostasis. Therefore, HVEM may serve as a 'negotiator' balancing co-inhibition by BTLA / CD160 and co-stimulation by LIGHT / LTa / LTbR in order to achieve an immunobalance. But overall, the role of the newest ligand in the HVEM pathway, CD160, in these diseases remains to be determined and studies with mice deficient in CD160 and doubly deficient in CD160 / BTLA are needed to answer these questions (11). Taken together, although HVEM binding to LIGHT and LTa delivers a positive signal to T-cell

activation, the overall function of HVEM is inhibitory, suggesting the negative signals mediated by BTLA and CD160 are dominant. Therapies targeting the CRD1 of HVEM to block BTLA and CD160 binding are being developed to enhance immune responses and vaccination (50) and increasing BTLA expression levels in the cornea to prevent HSV-1 induced immunopathology (106).

IMMUNITY AND IMMUNOPATHOLOGY TO IAV

Respiratory virus infections are a major cause of morbidity and mortality throughout the world. A major challenge for immunologists is deciphering the underlying mechanisms of immune protection at mucosal surfaces such as the lung epithelium. Understanding the individual steps of an immune response in the lungs is essential if we are to develop vaccines that elicit effective immunity in the lung.

Influenza virus infections alone result in the deaths of about 36,000 people per year in the United States and there is tremendous concern that highly lethal variants of this virus may emerge and cause a major pandemic (39, 60). Moreover, the emergence of new respiratory pathogens, such as the corona virus associated with Severe Acute Respiratory Syndrome, poses a continual threat (66). Despite the medical significance of respiratory viral infections, satisfactory vaccines have not been developed. For example, in the case of influenza virus, the currently available vaccine elicits humoral immunity specific for viral coat proteins and must be reformulated yearly to be effective against

new viral strains (31). Recent progress in our understanding of cellular immune responses in the lung will facilitate the development of effective vaccines.

Immunity in the respiratory tract

Much of our understanding of immune responses to respiratory virus infections has been derived through experimental animal models. A particularly robust and well-characterized model is the infection of mice with mouse-adapted influenza virus(6, 18, 69). When introduced through the nose, the virus establishes infection of lung epithelial cells and elicits powerful cellular and humoral immune responses in the lung. CD8+ cytotoxic T cells first appear in the lung airways on day 7 post-infection and play a key role in clearing virus(24) . Typically, this effector T-cell response peaks around day 10 or 11 (24). Antibody is also generated in the response, but isotype switched antibody does not accumulate until day 7 and does not appear to play a critical role in the primary infection unless the viral titer is particularly high (34) . Following resolution of the infection, memory T cells persist in secondary lymphoid organs, such as the spleen and local draining lymph nodes, as well as a variety of peripheral sites, including the lung parenchyma and airways (38, 53). These memory cells retain the capacity to mediate accelerated recall responses due to their semi-activated status and increased precursor frequencies relative to naive T-cell populations (12, 24, 37, 38).

While the basic outline of T-cell immunity in the lung has been established, the specific details remain obscure. The advent of new technologies

for studying immune responses in vivo has allowed viral immunologists to begin to visualize key processes and dissect the underlying mechanisms.

Primary T-cell responses

The infection of respiratory epithelial cells initiates a cascade of events that culminate in the activation of a cellular immune response in the lung. The initial infection induces the production of inflammatory mediators by epithelial cells, which alert the innate immune response to the infection (17) . In addition, dendritic cells (DCs) lining the upper respiratory tract also detect the presence of an infection via toll-like receptors (TLRs), which detect viral proteins (49) or products of viral replication, such as double stranded RNA (2, 17, 36, 49, 95) . The combination of inflammation and TLR signaling activates DCs, increases their expression of class I and class II Major Histocompatibility Complex (MHC) molecules and induces a wide array of co-stimulatory and adhesion molecules as well as inflammatory cytokines that are required for the induction of T-cell responses (54, 56). Together, these changes in DC activity result in enhanced presentation of viral antigens to T cells (54). Finally, the DCs acquire the ability to traffic to the lymph nodes, migrate into T-cell areas and interact directly with naive T cells (52) . Once in the T-cell areas, mature DCs present antigen to naive T cells, which then initiate a program of proliferation and maturation (62) . This results in a massive increase in the number of antigen-specific T cells and the production of large numbers of effector cells with the capacity to lyse infected epithelial cells and secrete antiviral cytokines (70) . Finally, these effector cells

acquire the capacity to traffic and subsequently move to the site of infection in the lung where they effectively terminate the infection (70).

Animal models

Experimentally, the mouse model that is so familiar to immunologists provides a well-characterized system for analyzing acute and memory responses in this localized, non-persistent infection. Influenza can be controlled either by CD8+ T cells or by antibodies, but mice lacking both CD8+ T cells and antibodies succumb (19). Influenza viruses are not natural mouse pathogens, and viral spread between mice is minimal, despite the fact that substantial lung viral titers are achieved within 24 h of infection. Influenza infection in the ferret more closely resembles human influenza infection, but the ferret model has received little attention from immunologists, probably because of the lack of reagents and inbred ferret strains.

Influenza viruses grow rapidly in the human respiratory mucosa, allowing transmission to colleagues and family members via respiratory droplet inhalation (coughs and sneezes) even before the development of obvious symptoms. The net consequence is that influenza outbreaks tend to be 'explosive', moving rapidly through a community, and then dying out. Any given influenza A virus variant, however, can be sustained globally for at least 1–2 years in geographically dispersed communities.

Therapeutics and vaccines

X-ray crystallographic analysis of the structure of monoclonal antibody–NA complexes has helped the development of the 'rationally designed'

therapeutics zanamivir (Relenza) and oseltamivir (Tamiflu) (58, 97). Both influenza A and influenza B viruses find it difficult to 'escape' by altering the NA site targeted by these drugs. However, escape variants can emerge during severe H5N1 infection (15). These drugs are being stockpiled by national governments, but the real need is for an effective vaccine.

Adaptive immune responses to foreign antigens require precise regulation. If not, excessive bystander damage to host tissues may occur and an unlimited reaction could erode the size of the repertoire, limiting responses to other antigens. It is evident that the host possesses several mechanisms that control the size, composition and duration of immune reactions (113) . In consequence, after the primary response most cells die leaving a memory population that represents a fraction of the cells that responded initially to the antigen. Moreover, these memory cells rarely account for 10% of the total antigen reactive repertoire (1). In some circumstances, it would be desirable to expand the size of the memory population and perhaps extend the durability of effector cell activity, since this could improve immunity to certain pathogens. HIV is such an example (27) .

Some bystander tissue damage usually happens since several host defenses can destroy cells or orchestrate inflammatory reactions. With chronic infections, for example, immune mediated tissue damage would be more severe were it not for several cellular and chemical host components that inhibit inflammatory reaction (72). However, the activity of some of these counter inflammatory mechanisms could act to constrain the efficiency of protective

immune components (78). For instance, regulatory T cells (Treg) can inhibit inflammatory reactions associated with chronic virus infections (5), but the same Treg response can also limit the magnitude of protective immunity to a virus or induced by a vaccine (88, 94). Other host components may also function to limit and help resolve inflammatory reactions. These include some cytokines (84), groups of molecules derived from omega-3 polyunsaturated fatty acids (81), as well as some of the carbohydrate binding proteins of the galectin family (68). Galectin-9 (Gal-9), for example, upon binding to Tim-3 on T cells acts to limit the extent of immuno-pathological lesions in autoimmunity (47) as well as in some chronic infections (32, 41, 79).

Tim-3 was first discovered in 2002 as a molecule expressed on interferon (IFN)- γ -producing CD4⁺ T helper type 1 (Th1) and on CD8⁺ T cytotoxic type 1 (Tc1) cells (57). The S-type lectin galectin-9 (Gal-9) was then identified as a Tim-3 ligand. Gal-9 is a soluble molecule that is widely expressed, up regulated by IFN- γ (3), and binds to oligosaccharides on the Tim-3 IgV domain. Gal-9 triggering of Tim-3 on Th1 cells has been shown to induce cell death (112). Thus, Tim-3 came to be known as a negative regulatory molecule important for abrogating Th1- and Tc1-driven immune responses. Consistent with its role as an inhibitory molecule, blockade of the Tim-3 Tim-3L pathway in vivo by blocking antibody or soluble Tim-3 Ig fusion protein (Tim-3Ig), which serves to block Tim-3/Gal-9 interactions, exacerbates experimental allergic encephalomyelitis and type 1 diabetes (57, 75). Similarly, abrogation of Tim-3 signaling with blocking

antibody or by RNA interference increases the secretion of IFN- γ by activated human T cells.

Tim-3 is also involved in the induction of peripheral tolerance. Administration of Tim-3Ig abrogates the development of tolerance in Th1 cells and Tim-3-deficient mice are refractory to induction of tolerance by administration of high dose aqueous antigen (73). Of note, it has been shown that Tim-3 can regulate auto- and alloimmunity by modulating the capacity of regulatory T cells to dampen inflammatory responses (75). In addition, studies in a murine graft-versus-host disease model and a hepatitis B infection model support a role for Tim-3 in negatively regulating IFN- γ producing CD8⁺ Tc1 cells

New findings regarding the inhibitory role of Tim-3 have emerged over the past few years and it is now well established that Tim-3 is highly expressed on 'exhausted' or impaired CD8 T cells in various chronic viral infections (32, 40, 41) and in tumor-bearing hosts (25, 59, 74, 111). More importantly, the function of these impaired CD8 T cells can be restored by blocking the Tim-3/Tim-3L pathway. Recent studies have examined Tim-3 expression in acute and chronic models of viral infection. In acute Lymphocytic Choriomeningitis virus (LCMV) and herpes simplex virus (HSV) infection, Tim-3 is expressed on CD8⁺ T cells; however, this expression is transient and is found on only a small fraction of cells (78). Blockade of Tim-3/Gal-9 signals during the acute phase of HSV infection results in increased effector and memory CD8⁺ T cell responses and more efficient viral control (78). By contrast, virus-specific CD8⁺ T cells in chronic LCMV and Friend virus infection exhibit sustained high-level expression of Tim-3

on a large fraction of cells. These cells co express PD-1 and exhibit impaired effector cytokine production (40, 89). In these experimental models of viral infection, as well as in T cells from patients chronically infected with human immunodeficiency virus (HIV) and Hepatitis C virus (HCV), blocking both the Tim-3 and PD-1 pathways restores T cell proliferation and enhances cytokine production. Thus, in chronic viral infections, both the Tim-3 and PD-1 pathways seem to affect T cell exhaustion (Figure 3).

CONCLUSION

Understanding of the circumstances of infection and host-controlled factors that could explain why an infection can be resolved with minimal impact or cause substantial tissue damage could prove to be useful in the future for the control and perhaps prevention of tissue-damaging virus infection. Accordingly by inhibiting the factors involved in immunopathology following an acute viral infection or manipulating the immunomodulatory factors such as some cytokines, groups of molecules derived from omega-3 polyunsaturated fatty acids, as well as some of the carbohydrate binding proteins of the galectin family and co stimulatory molecules like HVEM could be beneficial in preventing immunopathology and to enhance immune responses to vaccines.

LIST OF REFERENCES

1. **Ahmed, R., and D. Gray.** 1996. Immunological memory and protective immunity: understanding their relation. *Science* **272**:54-60.
2. **Akira, S., and H. Hemmi.** 2003. Recognition of pathogen-associated molecular patterns by TLR family. *Immunol Lett* **85**:85-95.
3. **Asakura, H., Y. Kashio, K. Nakamura, M. Seki, S. Dai, Y. Shirato, M. J. Abedin, N. Yoshida, N. Nishi, T. Imaizumi, N. Saita, Y. Toyama, H. Takashima, T. Nakamura, M. Ohkawa, and M. Hirashima.** 2002. Selective eosinophil adhesion to fibroblast via IFN-gamma-induced galectin-9. *J Immunol* **169**:5912-5918.
4. **Azkur, A. K., B. Kim, S. Suvas, Y. Lee, U. Kumaraguru, and B. T. Rouse.** 2005. Blocking mouse MMP-9 production in tumor cells and mouse cornea by short hairpin (sh) RNA encoding plasmids. *Oligonucleotides* **15**:72-84.
5. **Belkaid, Y., and B. T. Rouse.** 2005. Natural regulatory T cells in infectious disease. *Nat Immunol* **6**:353-360.
6. **Bender, B. S., and P. A. Small.** 1992. Influenza: pathogenesis and host defense. *Semin Respir Infect* **7**:38-45.
7. **Biswas, P. S., K. Banerjee, B. Kim, P. R. Kinchington, and B. T. Rouse.** 2005. Role of inflammatory cytokine-induced cyclooxygenase 2 in the ocular immunopathologic disease herpetic stromal keratitis. *J Virol* **79**:10589-10600.
8. **Biswas, P. S., K. Banerjee, M. Zheng, and B. T. Rouse.** 2004. Counteracting corneal immunoinflammatory lesion with interleukin-1 receptor antagonist protein. *J Leukoc Biol* **76**:868-875.
9. **Biswas, P. S., and B. T. Rouse.** 2005. Early events in HSV keratitis--setting the stage for a blinding disease. *Microbes Infect* **7**:799-810.
10. **Biswas, S., L. Jennens, and H. J. Field.** 2007. Single amino acid substitutions in the HSV-1 helicase protein that confer resistance to the helicase-primase inhibitor BAY 57-1293 are associated with increased or decreased virus growth characteristics in tissue culture. *Arch Virol* **152**:1489-1500.
11. **Cai, G., and G. J. Freeman.** 2009. The CD160, BTLA, LIGHT/HVEM pathway: a bidirectional switch regulating T-cell activation. *Immunol Rev* **229**:244-258.
12. **Cauley, L. S., R. J. Hogan, and D. L. Woodland.** 2002. Memory T-cells in non-lymphoid tissues. *Curr Opin Investig Drugs* **3**:33-36.
13. **Chen, Y., C. Scieux, V. Garrait, G. Socié, V. Rocha, J. M. Molina, D. Thouvenot, F. Morfin, L. Hocqueloux, L. Garderet, H. Espérou, F. Sélimi, A. Devergie, G. Leleu, M. Aymard, F. Morinet, E. Gluckman, and P. Ribaud.** 2000. Resistant herpes simplex virus type 1 infection: an emerging concern after allogeneic stem cell transplantation. *Clin Infect Dis* **31**:927-935.
14. **Dahl, R.** 2006. Systemic side effects of inhaled corticosteroids in patients with asthma. *Respir Med* **100**:1307-1317.
15. **de Jong, M. D., T. T. Tran, H. K. Truong, M. H. Vo, G. J. Smith, V. C. Nguyen, V. C. Bach, T. Q. Phan, Q. H. Do, Y. Guan, J. S. Peiris, T. H. Tran, and J. Farrar.** 2005. Oseltamivir resistance during treatment of influenza A (H5N1) infection. *N Engl J Med* **353**:2667-2672.

16. **Deshpande, S., K. Banerjee, P. S. Biswas, and B. T. Rouse.** 2004. Herpetic eye disease: immunopathogenesis and therapeutic measures. *Expert Rev Mol Med* **6**:1-14.
17. **Diebold, S. S., M. Montoya, H. Unger, L. Alexopoulou, P. Roy, L. E. Haswell, A. Al-Shamkhani, R. Flavell, P. Borrow, and C. Reis e Sousa.** 2003. Viral infection switches non-plasmacytoid dendritic cells into high interferon producers. *Nature* **424**:324-328.
18. **Doherty, P. C., S. Hou, and R. A. Tripp.** 1994. CD8+ T-cell memory to viruses. *Curr Opin Immunol* **6**:545-552.
19. **Doherty, P. C., S. J. Turner, R. G. Webby, and P. G. Thomas.** 2006. Influenza and the challenge for immunology. *Nat Immunol* **7**:449-455.
20. **Eliceiri, B. P., R. Paul, P. L. Schwartzberg, J. D. Hood, J. Leng, and D. A. Cheresh.** 1999. Selective requirement for Src kinases during VEGF-induced angiogenesis and vascular permeability. *Mol Cell* **4**:915-924.
21. **Feng, G., W. Gao, T. B. Strom, M. Oukka, R. S. Francis, K. J. Wood, and A. Bushell.** 2008. Exogenous IFN-gamma ex vivo shapes the alloreactive T-cell repertoire by inhibition of Th17 responses and generation of functional Foxp3+ regulatory T cells. *Eur J Immunol* **38**:2512-2527.
22. **Feng, G., K. J. Wood, and A. Bushell.** 2008. Interferon-gamma conditioning ex vivo generates CD25+CD62L+Foxp3+ regulatory T cells that prevent allograft rejection: potential avenues for cellular therapy. *Transplantation* **86**:578-589.
23. **Fenton, R. R., S. Molesworth-Kenyon, J. E. Oakes, and R. N. Lausch.** 2002. Linkage of IL-6 with neutrophil chemoattractant expression in virus-induced ocular inflammation. *Invest Ophthalmol Vis Sci* **43**:737-743.
24. **Flynn, K. J., G. T. Belz, J. D. Altman, R. Ahmed, D. L. Woodland, and P. C. Doherty.** 1998. Virus-specific CD8+ T cells in primary and secondary influenza pneumonia. *Immunity* **8**:683-691.
25. **Fourcade, J., Z. Sun, M. Benallaoua, P. Guillaume, I. F. Luescher, C. Sander, J. M. Kirkwood, V. Kuchroo, and H. M. Zarour.** 2010. Upregulation of Tim-3 and PD-1 expression is associated with tumor antigen-specific CD8+ T cell dysfunction in melanoma patients. *J Exp Med* **207**:2175-2186.
26. **Freeman, M. L., B. S. Sheridan, R. H. Bonneau, and R. L. Hendricks.** 2007. Psychological stress compromises CD8+ T cell control of latent herpes simplex virus type 1 infections. *J Immunol* **179**:322-328.
27. **Gandhi, R. T., and B. D. Walker.** 2002. Immunologic control of HIV-1. *Annu Rev Med* **53**:149-172.
28. **Gangappa, S., J. S. Babu, J. Thomas, M. Daheshia, and B. T. Rouse.** 1998. Virus-induced immunoinflammatory lesions in the absence of viral antigen recognition. *J Immunol* **161**:4289-4300.
29. **Gangappa, S., S. P. Deshpande, and B. T. Rouse.** 1999. Bystander activation of CD4(+) T cells can represent an exclusive means of immunopathology in a virus infection. *Eur J Immunol* **29**:3674-3682.
30. **Gangappa, S., S. P. Deshpande, and B. T. Rouse.** 2000. Bystander activation of CD4+ T cells accounts for herpetic ocular lesions. *Invest Ophthalmol Vis Sci* **41**:453-459.

31. **Gerdil, C.** 2003. The annual production cycle for influenza vaccine. *Vaccine* **21**:1776-1779.
32. **Golden-Mason, L., B. E. Palmer, N. Kassam, L. Townshend-Bulson, S. Livingston, B. J. McMahon, N. Castelblanco, V. Kuchroo, D. R. Gretch, and H. R. Rosen.** 2009. Negative immune regulator Tim-3 is overexpressed on T cells in hepatitis C virus infection and its blockade rescues dysfunctional CD4+ and CD8+ T cells. *J Virol* **83**:9122-9130.
33. **Gorbunova, E. E., I. N. Gavrillovskaya, T. Pepini, and E. R. Mackow.** 2011. VEGFR2 and Src kinase inhibitors suppress Andes virus-induced endothelial cell permeability. *J Virol* **85**:2296-2303.
34. **Graham, M. B., and T. J. Braciale.** 1997. Resistance to and recovery from lethal influenza virus infection in B lymphocyte-deficient mice. *J Exp Med* **186**:2063-2068.
35. **Haskins, K., R. Kubo, J. White, M. Pigeon, J. Kappler, and P. Marrack.** 1983. The major histocompatibility complex-restricted antigen receptor on T cells. I. Isolation with a monoclonal antibody. *J Exp Med* **157**:1149-1169.
36. **Haynes, L. M., D. D. Moore, E. A. Kurt-Jones, R. W. Finberg, L. J. Anderson, and R. A. Tripp.** 2001. Involvement of toll-like receptor 4 in innate immunity to respiratory syncytial virus. *J Virol* **75**:10730-10737.
37. **Hogan, R. J., E. J. Usherwood, W. Zhong, A. A. Roberts, R. W. Dutton, A. G. Harmsen, and D. L. Woodland.** 2001. Activated antigen-specific CD8+ T cells persist in the lungs following recovery from respiratory virus infections. *J Immunol* **166**:1813-1822.
38. **Hogan, R. J., W. Zhong, E. J. Usherwood, T. Cookenham, A. D. Roberts, and D. L. Woodland.** 2001. Protection from respiratory virus infections can be mediated by antigen-specific CD4(+) T cells that persist in the lungs. *J Exp Med* **193**:981-986.
39. **Horimoto, T., and Y. Kawaoka.** 2001. Pandemic threat posed by avian influenza A viruses. *Clin Microbiol Rev* **14**:129-149.
40. **Jin, H. T., A. C. Anderson, W. G. Tan, E. E. West, S. J. Ha, K. Araki, G. J. Freeman, V. K. Kuchroo, and R. Ahmed.** 2010. Cooperation of Tim-3 and PD-1 in CD8 T-cell exhaustion during chronic viral infection. *Proc Natl Acad Sci U S A* **107**:14733-14738.
41. **Jones, R. B., L. C. Ndhlovu, J. D. Barbour, P. M. Sheth, A. R. Jha, B. R. Long, J. C. Wong, M. Satkunarajah, M. Schweneker, J. M. Chapman, G. Gyenes, B. Vali, M. D. Hyrcza, F. Y. Yue, C. Kovacs, A. Sassi, M. Loutfy, R. Halpenny, D. Persad, G. Spotts, F. M. Hecht, T. W. Chun, J. M. McCune, R. Kaul, J. M. Rini, D. F. Nixon, and M. A. Ostrowski.** 2008. Tim-3 expression defines a novel population of dysfunctional T cells with highly elevated frequencies in progressive HIV-1 infection. *J Exp Med* **205**:2763-2779.
42. **Kaufman, H. E.** 2002. Can we prevent recurrences of herpes infections without antiviral drugs? The Weisenfeld Lecture. *Invest Ophthalmol Vis Sci* **43**:1325-1329.
43. **Kevil, C. G., D. K. Payne, E. Mire, and J. S. Alexander.** 1998. Vascular permeability factor/vascular endothelial cell growth factor-mediated permeability

- occurs through disorganization of endothelial junctional proteins. *J Biol Chem* **273**:15099-15103.
44. **Kim, B., Q. Tang, P. S. Biswas, J. Xu, R. M. Schiffelers, F. Y. Xie, A. M. Ansari, P. V. Scaria, M. C. Woodle, P. Lu, and B. T. Rouse.** 2004. Inhibition of ocular angiogenesis by siRNA targeting vascular endothelial growth factor pathway genes: therapeutic strategy for herpetic stromal keratitis. *Am J Pathol* **165**:2177-2185.
 45. **Kolbe, L., A. M. Kligman, V. Schreiner, and T. Stoudemayer.** 2001. Corticosteroid-induced atrophy and barrier impairment measured by non-invasive methods in human skin. *Skin Res Technol* **7**:73-77.
 46. **Krummenacher, C., V. M. Supekar, J. C. Whitbeck, E. Lazear, S. A. Connolly, R. J. Eisenberg, G. H. Cohen, D. C. Wiley, and A. Carfi.** 2005. Structure of unliganded HSV gD reveals a mechanism for receptor-mediated activation of virus entry. *EMBO J* **24**:4144-4153.
 47. **Kuchroo, V. K., J. H. Meyers, D. T. Umetsu, and R. H. DeKruyff.** 2006. TIM family of genes in immunity and tolerance. *Adv Immunol* **91**:227-249.
 48. **Kumaraguru, U., and B. T. Rouse.** 2002. The IL-12 response to herpes simplex virus is mainly a paracrine response of reactive inflammatory cells. *J Leukoc Biol* **72**:564-570.
 49. **Kurt-Jones, E. A., L. Popova, L. Kwinn, L. M. Haynes, L. P. Jones, R. A. Tripp, E. E. Walsh, M. W. Freeman, D. T. Golenbock, L. J. Anderson, and R. W. Finberg.** 2000. Pattern recognition receptors TLR4 and CD14 mediate response to respiratory syncytial virus. *Nat Immunol* **1**:398-401.
 50. **Lasaro, M. O., N. Tatsis, S. E. Hensley, J. C. Whitbeck, S. W. Lin, J. J. Rux, E. J. Wherry, G. H. Cohen, R. J. Eisenberg, and H. C. Ertl.** 2008. Targeting of antigen to the herpesvirus entry mediator augments primary adaptive immune responses. *Nat Med* **14**:205-212.
 51. **Lee, S., M. Zheng, S. Deshpande, S. K. Eo, T. A. Hamilton, and B. T. Rouse.** 2002. IL-12 suppresses the expression of ocular immunoinflammatory lesions by effects on angiogenesis. *J Leukoc Biol* **71**:469-476.
 52. **Legge, K. L., and T. J. Braciale.** 2003. Accelerated migration of respiratory dendritic cells to the regional lymph nodes is limited to the early phase of pulmonary infection. *Immunity* **18**:265-277.
 53. **Marshall, D. R., S. J. Turner, G. T. Belz, S. Wingo, S. Andreansky, M. Y. Sangster, J. M. Riberdy, T. Liu, M. Tan, and P. C. Doherty.** 2001. Measuring the diaspora for virus-specific CD8⁺ T cells. *Proc Natl Acad Sci U S A* **98**:6313-6318.
 54. **Mellman, I., and R. M. Steinman.** 2001. Dendritic cells: specialized and regulated antigen processing machines. *Cell* **106**:255-258.
 55. **Minagawa, H., K. Hashimoto, and Y. Yanagi.** 2004. Absence of tumour necrosis factor facilitates primary and recurrent herpes simplex virus-1 infections. *J Gen Virol* **85**:343-347.
 56. **Moll, H.** 2003. Dendritic cells and host resistance to infection. *Cell Microbiol* **5**:493-500.

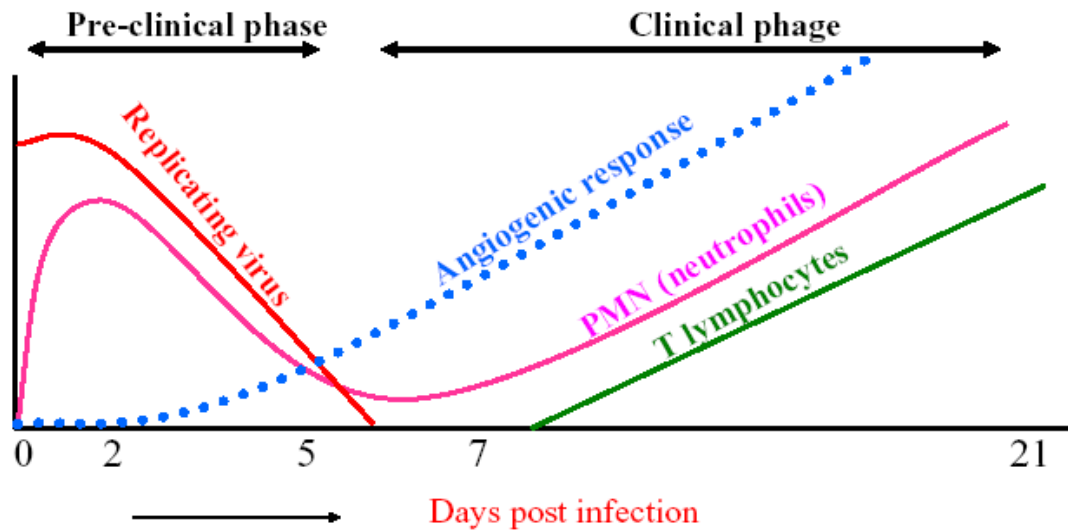
57. **Monney, L., C. A. Sabatos, J. L. Gaglia, A. Ryu, H. Waldner, T. Chernova, S. Manning, E. A. Greenfield, A. J. Coyle, R. A. Sobel, G. J. Freeman, and V. K. Kuchroo.** 2002. Th1-specific cell surface protein Tim-3 regulates macrophage activation and severity of an autoimmune disease. *Nature* **415**:536-541.
58. **Moscona, A.** 2005. Neuraminidase inhibitors for influenza. *N Engl J Med* **353**:1363-1373.
59. **Ngiow, S. F., B. von Scheidt, H. Akiba, H. Yagita, M. W. Teng, and M. J. Smyth.** 2011. Anti-TIM3 antibody promotes T cell IFN- γ -mediated antitumor immunity and suppresses established tumors. *Cancer Res* **71**:3540-3551.
60. **Nguyen-Van-Tam, J. S., and A. W. Hampson.** 2003. The epidemiology and clinical impact of pandemic influenza. *Vaccine* **21**:1762-1768.
61. **Niemialtowski, M. G., and B. T. Rouse.** 1992. Predominance of Th1 cells in ocular tissues during herpetic stromal keratitis. *J Immunol* **149**:3035-3039.
62. **Norbury, C. C., D. Malide, J. S. Gibbs, J. R. Bennink, and J. W. Yewdell.** 2002. Visualizing priming of virus-specific CD8⁺ T cells by infected dendritic cells in vivo. *Nat Immunol* **3**:265-271.
63. **Osorio, Y., S. L. Wechsler, A. B. Nesburn, and H. Ghiasi.** 2002. Reduced severity of HSV-1-induced corneal scarring in IL-12-deficient mice. *Virus Res* **90**:317-326.
64. **Owens, D. W., G. W. McLean, A. W. Wyke, C. Paraskeva, E. K. Parkinson, M. C. Frame, and V. G. Brunton.** 2000. The catalytic activity of the Src family kinases is required to disrupt cadherin-dependent cell-cell contacts. *Mol Biol Cell* **11**:51-64.
65. **Paul, R., Z. G. Zhang, B. P. Eliceiri, Q. Jiang, A. D. Boccia, R. L. Zhang, M. Chopp, and D. A. Cheresh.** 2001. Src deficiency or blockade of Src activity in mice provides cerebral protection following stroke. *Nat Med* **7**:222-227.
66. **Pearson, H., T. Clarke, A. Abbott, J. Knight, and D. Cyranoski.** 2003. SARS: what have we learned? *Nature* **424**:121-126.
67. **Pepose, J. S., T. L. Keadle, and L. A. Morrison.** 2006. Ocular herpes simplex: changing epidemiology, emerging disease patterns, and the potential of vaccine prevention and therapy. *Am J Ophthalmol* **141**:547-557.
68. **Rabinovich, G. A., and M. A. Toscano.** 2009. Turning 'sweet' on immunity: galectin-glycan interactions in immune tolerance and inflammation. *Nat Rev Immunol* **9**:338-352.
69. **Renegar, K. B.** 1992. Influenza virus infections and immunity: a review of human and animal models. *Lab Anim Sci* **42**:222-232.
70. **Román, E., E. Miller, A. Harmsen, J. Wiley, U. H. Von Andrian, G. Huston, and S. L. Swain.** 2002. CD4 effector T cell subsets in the response to influenza: heterogeneity, migration, and function. *J Exp Med* **196**:957-968.
71. **Rouse, B. T.** 2007. Regulatory T cells in health and disease. *J Intern Med* **262**:78-95.
72. **Rouse, B. T., and S. Sehrawat.** 2010. Immunity and immunopathology to viruses: what decides the outcome? *Nat Rev Immunol* **10**:514-526.
73. **Sabatos, C. A., S. Chakravarti, E. Cha, A. Schubart, A. Sánchez-Fueyo, X. X. Zheng, A. J. Coyle, T. B. Strom, G. J. Freeman, and V. K. Kuchroo.** 2003.

- Interaction of Tim-3 and Tim-3 ligand regulates T helper type 1 responses and induction of peripheral tolerance. *Nat Immunol* **4**:1102-1110.
74. **Sakuishi, K., L. Apetoh, J. M. Sullivan, B. R. Blazar, V. K. Kuchroo, and A. C. Anderson.** 2010. Targeting Tim-3 and PD-1 pathways to reverse T cell exhaustion and restore anti-tumor immunity. *J Exp Med* **207**:2187-2194.
75. **Sánchez-Fueyo, A., J. Tian, D. Picarella, C. Domenig, X. X. Zheng, C. A. Sabatos, N. Manlongat, O. Bender, T. Kamradt, V. K. Kuchroo, J. C. Gutiérrez-Ramos, A. J. Coyle, and T. B. Strom.** 2003. Tim-3 inhibits T helper type 1-mediated auto- and alloimmune responses and promotes immunological tolerance. *Nat Immunol* **4**:1093-1101.
76. **Sarangi, P. P., B. Kim, E. Kurt-Jones, and B. T. Rouse.** 2007. Innate recognition network driving herpes simplex virus-induced corneal immunopathology: role of the toll pathway in early inflammatory events in stromal keratitis. *J Virol* **81**:11128-11138.
77. **Scheppeke, L., E. Aguilar, R. F. Gariano, R. Jacobson, J. Hood, J. Doukas, J. Cao, G. Noronha, S. Yee, S. Weis, M. B. Martin, R. Soll, D. A. Cheresch, and M. Friedlander.** 2008. Retinal vascular permeability suppression by topical application of a novel VEGFR2/Src kinase inhibitor in mice and rabbits. *J Clin Invest* **118**:2337-2346.
78. **Sehrawat, S., P. B. Reddy, N. Rajasagi, A. Suryawanshi, M. Hirashima, and B. T. Rouse.** 2010. Galectin-9/TIM-3 interaction regulates virus-specific primary and memory CD8 T cell response. *PLoS Pathog* **6**:e1000882.
79. **Sehrawat, S., A. Suryawanshi, M. Hirashima, and B. T. Rouse.** 2009. Role of Tim-3/galectin-9 inhibitory interaction in viral-induced immunopathology: shifting the balance toward regulators. *J Immunol* **182**:3191-3201.
80. **Sehrawat, S., S. Suvas, P. P. Sarangi, A. Suryawanshi, and B. T. Rouse.** 2008. In vitro-generated antigen-specific CD4+ CD25+ Foxp3+ regulatory T cells control the severity of herpes simplex virus-induced ocular immunoinflammatory lesions. *J Virol* **82**:6838-6851.
81. **Serhan, C. N., S. Krishnamoorthy, A. Recchiuti, and N. Chiang.** 2011. Novel anti-inflammatory--pro-resolving mediators and their receptors. *Curr Top Med Chem* **11**:629-647.
82. **Sheridan, B. S., J. E. Knickelbein, and R. L. Hendricks.** 2007. CD8 T cells and latent herpes simplex virus type 1: keeping the peace in sensory ganglia. *Expert Opin Biol Ther* **7**:1323-1331.
83. **Shimeld, C., T. Hill, B. Blyth, and D. Easty.** 1989. An improved model of recurrent herpetic eye disease in mice. *Curr Eye Res* **8**:1193-1205.
84. **Sun, J., R. Madan, C. L. Karp, and T. J. Braciale.** 2009. Effector T cells control lung inflammation during acute influenza virus infection by producing IL-10. *Nat Med* **15**:277-284.
85. **Suryawanshi, A., S. Mulik, S. Sharma, P. B. Reddy, S. Sehrawat, and B. T. Rouse.** 2011. Ocular neovascularization caused by herpes simplex virus type 1 infection results from breakdown of binding between vascular endothelial growth factor A and its soluble receptor. *J Immunol* **186**:3653-3665.

86. **Suryawanshi, A., T. Veiga-Parga, N. K. Rajasagi, P. B. Reddy, S. Sehrawat, S. Sharma, and B. T. Rouse.** 2011. Role of IL-17 and Th17 cells in herpes simplex virus-induced corneal immunopathology. *J Immunol* **187**:1919-1930.
87. **Suvas, S., A. K. Azkur, B. S. Kim, U. Kumaraguru, and B. T. Rouse.** 2004. CD4+CD25+ regulatory T cells control the severity of viral immunoinflammatory lesions. *J Immunol* **172**:4123-4132.
88. **Suvas, S., U. Kumaraguru, C. D. Pack, S. Lee, and B. T. Rouse.** 2003. CD4+CD25+ T cells regulate virus-specific primary and memory CD8+ T cell responses. *J Exp Med* **198**:889-901.
89. **Takamura, S., S. Tsuji-Kawahara, H. Yagita, H. Akiba, M. Sakamoto, T. Chikaishi, M. Kato, and M. Miyazawa.** 2010. Premature terminal exhaustion of Friend virus-specific effector CD8+ T cells by rapid induction of multiple inhibitory receptors. *J Immunol* **184**:4696-4707.
90. **Tang, Q., and R. L. Hendricks.** 1996. Interferon gamma regulates platelet endothelial cell adhesion molecule 1 expression and neutrophil infiltration into herpes simplex virus-infected mouse corneas. *J Exp Med* **184**:1435-1447.
91. **Tao, R., L. Wang, K. M. Murphy, C. C. Fraser, and W. W. Hancock.** 2008. Regulatory T cell expression of herpesvirus entry mediator suppresses the function of B and T lymphocyte attenuator-positive effector T cells. *J Immunol* **180**:6649-6655.
92. **Thomas, J., S. Gangappa, S. Kanangat, and B. T. Rouse.** 1997. On the essential involvement of neutrophils in the immunopathologic disease: herpetic stromal keratitis. *J Immunol* **158**:1383-1391.
93. **Thomas, J., and B. T. Rouse.** 1998. Immunopathology of herpetic stromal keratitis: discordance in CD4+ T cell function between euthymic host and reconstituted SCID recipients. *J Immunol* **160**:3965-3970.
94. **Toka, F. N., S. Suvas, and B. T. Rouse.** 2004. CD4+ CD25+ T cells regulate vaccine-generated primary and memory CD8+ T-cell responses against herpes simplex virus type 1. *J Virol* **78**:13082-13089.
95. **Tripp, R. A., L. P. Jones, L. M. Haynes, H. Zheng, P. M. Murphy, and L. J. Anderson.** 2001. CX3C chemokine mimicry by respiratory syncytial virus G glycoprotein. *Nat Immunol* **2**:732-738.
96. **Tumpey, T. M., S. H. Chen, J. E. Oakes, and R. N. Lausch.** 1996. Neutrophil-mediated suppression of virus replication after herpes simplex virus type 1 infection of the murine cornea. *J Virol* **70**:898-904.
97. **von Itzstein, M., and P. Colman.** 1996. Design and synthesis of carbohydrate-based inhibitors of protein-carbohydrate interactions. *Curr Opin Struct Biol* **6**:703-709.
98. **Wang, Y., S. K. Subudhi, R. A. Anders, J. Lo, Y. Sun, S. Blink, J. Wang, X. Liu, K. Mink, D. Grandi, K. Pfeffer, and Y. X. Fu.** 2005. The role of herpesvirus entry mediator as a negative regulator of T cell-mediated responses. *J Clin Invest* **115**:711-717.
99. **Wang, Z., J. Hong, W. Sun, G. Xu, N. Li, X. Chen, A. Liu, L. Xu, B. Sun, and J. Z. Zhang.** 2006. Role of IFN-gamma in induction of Foxp3 and conversion of CD4+ CD25- T cells to CD4+ Tregs. *J Clin Invest* **116**:2434-2441.

100. **Ware, C. F., and J. R. Sedý.** 2011. TNF Superfamily Networks: bidirectional and interference pathways of the herpesvirus entry mediator (TNFSF14). *Curr Opin Immunol*.
101. **Weaver, C. T., R. D. Hatton, P. R. Mangan, and L. E. Harrington.** 2007. IL-17 family cytokines and the expanding diversity of effector T cell lineages. *Annu Rev Immunol* **25**:821-852.
102. **Weinstein, B. I., J. Schwartz, G. G. Gordon, M. O. Dominguez, S. Varma, M. W. Dunn, and A. L. Southren.** 1982. Characterization of a glucocorticoid receptor and the direct effect of dexamethasone on herpes simplex virus infection of rabbit corneal cells in culture. *Invest Ophthalmol Vis Sci* **23**:651-659.
103. **Weis, S., S. Shintani, A. Weber, R. Kirchmair, M. Wood, A. Cravens, H. McSharry, A. Iwakura, Y. S. Yoon, N. Himes, D. Burstein, J. Doukas, R. Soll, D. Losordo, and D. Cheresch.** 2004. Src blockade stabilizes a Flk/cadherin complex, reducing edema and tissue injury following myocardial infarction. *J Clin Invest* **113**:885-894.
104. **Weis, S. M., and D. A. Cheresch.** 2005. Pathophysiological consequences of VEGF-induced vascular permeability. *Nature* **437**:497-504.
105. **Whitley, R. J., and B. Roizman.** 2001. Herpes simplex virus infections. *Lancet* **357**:1513-1518.
106. **Xia, L., S. Zhang, J. Zhou, and Y. Li.** 2010. A crucial role for B and T lymphocyte attenuator in preventing the development of CD4⁺ T cell-mediated herpetic stromal keratitis. *Mol Vis* **16**:2071-2083.
107. **Yan, X. T., T. M. Tumpey, S. L. Kunkel, J. E. Oakes, and R. N. Lausch.** 1998. Role of MIP-2 in neutrophil migration and tissue injury in the herpes simplex virus-1-infected cornea. *Invest Ophthalmol Vis Sci* **39**:1854-1862.
108. **Yannariello-brown, J., C. K. Hallberg, H. Häberle, M. M. Brysk, Z. Jiang, J. A. Patel, P. B. Ernst, and S. D. Trocme.** 1998. Cytokine modulation of human corneal epithelial cell ICAM-1 (CD54) expression. *Exp Eye Res* **67**:383-393.
109. **Yuan, S. Y.** 2002. Protein kinase signaling in the modulation of microvascular permeability. *Vascul Pharmacol* **39**:213-223.
110. **Zheng, M., D. M. Klinman, M. Gierynska, and B. T. Rouse.** 2002. DNA containing CpG motifs induces angiogenesis. *Proc Natl Acad Sci U S A* **99**:8944-8949.
111. **Zhou, Q., M. E. Munger, R. G. Veenstra, B. J. Weigel, M. Hirashima, D. H. Munn, W. J. Murphy, M. Azuma, A. C. Anderson, V. K. Kuchroo, and B. R. Blazar.** 2011. Coexpression of Tim-3 and PD-1 identifies a CD8⁺ T-cell exhaustion phenotype in mice with disseminated acute myelogenous leukemia. *Blood* **117**:4501-4510.
112. **Zhu, C., A. C. Anderson, A. Schubart, H. Xiong, J. Imitola, S. J. Khoury, X. X. Zheng, T. B. Strom, and V. K. Kuchroo.** 2005. The Tim-3 ligand galectin-9 negatively regulates T helper type 1 immunity. *Nat Immunol* **6**:1245-1252.
113. **Zinkernagel, R. M.** 1996. Immunology taught by viruses. *Science* **271**:173-178.

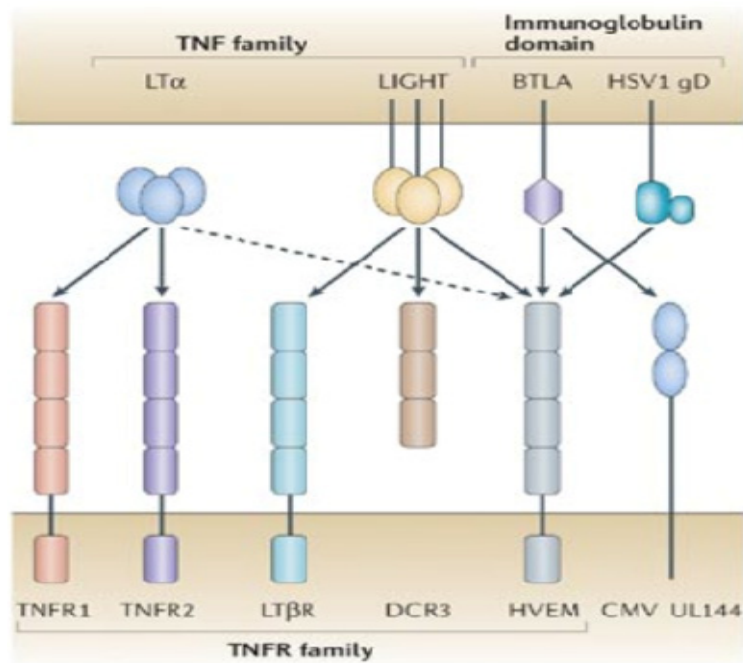
APPENDIX



CRUCIAL EVENTS IN HSK PATHOPHYSIOLOGY

Figure. 1. Principal events in herpetic SK pathogenesis

Following ocular HSV infection replicating virus could be detected in the cornea till 5-7 days p.i. Early inflammatory response in the cornea is dominated by the polymorphonuclear leukocytes (PMN). Infiltration of PMNs into the cornea is characterized by a typical biphasic influx. Angiogenesis or the process of new blood vessel development from the existing limbal vessels starts at 24h p.i. and peaks around 15 days p.i. Influx of pathogenic CD4+ T lymphocytes occurs in the clinical phase around 7-9 days p.i.



Copyright © 2006 Nature Publishing Group
 Nature Reviews | Immunology

Murphy et al. *Nature Reviews Immunology* 6, 671–681 (September 2006) | doi:10.1038/nri1917

Figure 2 | Molecular interactions between TNFRs, TNFs and immunoglobulin-domain-containing receptors. Tumour-necrosis factor (TNF) receptor (TNFR) family members predominantly interact with one or more soluble or cell-surface TNF family ligands. Herpesvirus- entry mediator (HVEM) binds both LIGHT and lymphotoxin- α (LT α), and LIGHT also binds LT β receptor (LT β R) and decoy receptor 3 (DCR3). LT α also binds TNFR1 and TNFR2. HVEM binds the immunoglobulin-domain- containing proteins B- and T-lymphocyte attenuator (BTLA) and herpes simplex virus type 1 glycoprotein D (HSV1 gD), whereas its viral homologue human cytomegalovirus (CMV) UL144 binds human BTLA.

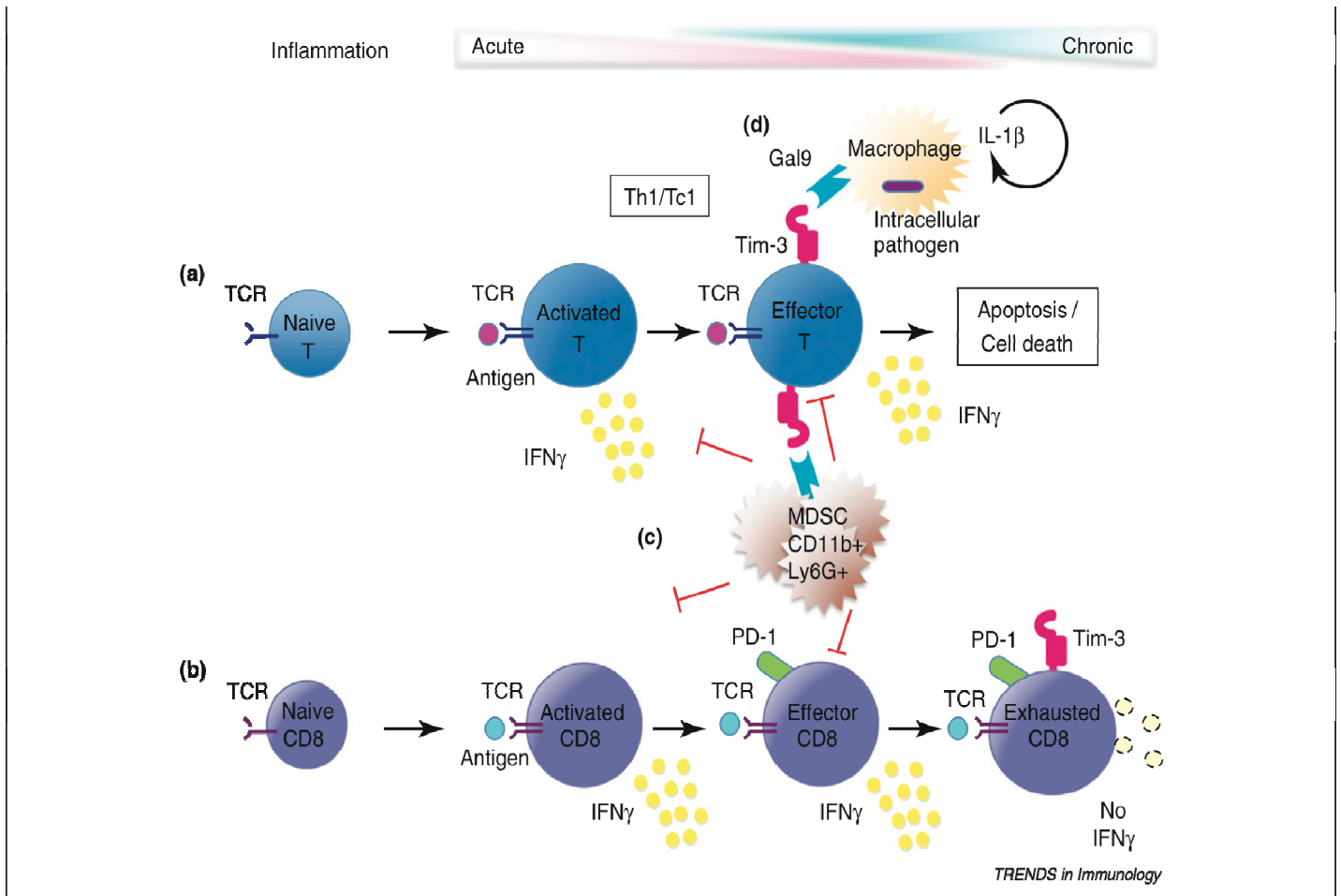


Figure 3. Model of Tim-3 function in the immune response. (a) In acute inflammation, Tim-3 is expressed on terminally differentiated IFN-g-producing CD4 $^{+}$ and CD8 $^{+}$ T cells. Upon recognition of its ligand, Gal-9, Tim-3-expressing T cells undergo apoptosis. (b) In chronic inflammation, Tim-3 is coexpressed with PD-1 on dysfunctional or exhausted CD8 $^{+}$ T cells. Combined targeting of the PD-1 \square PD-L1 and Tim-3 \square Tim-3L pathways successfully restores CD8 $^{+}$ T cell effector function and ameliorates chronic disease. (c) Tim-3 on T cells interacts

with Gal-9 on MDSC precursors to promote MDSC expansion, which in turn suppresses T cell responses. (d) Tim-3 on CD4+ T cells can also act to facilitate killing of intracellular pathogens in macrophages through interaction with Gal-9 and a mechanism involving IL-1b and caspase-1. Overall, Tim-3 on CD4+ and CD8+ T cells harnesses multiple mechanisms to regulate negatively effector T cell responses and terminate IFN-g-mediated inflammation while preserving or enhancing the ability of innate cells to kill intracellular pathogens.

PART-II

AN ANTI-INFLAMMATORY ROLE OF

VEGFR2/SRC KINASE INHIBITOR IN

HSV-1 INDUCED IMMUNOPATHOLOGY

Research described in this chapter is a modified version of an article published in 2011 in Journal of Virology by Shalini Sharma, Sachin Mulik, Naveen Kumar, Amol Suryawanshi, and Barry T Rouse.

Sharma S, Mulik S, Kumar N, Suryawanshi A and Rouse BT. An Anti-inflammatory Role of VEGFR2/Src Kinase Inhibitor in HSV-1 Induced Immunopathology J Virol: 2011 2011; 85: 5995-6007

Copyright © 2011, American Society for Microbiology.

In this chapter “our” and “we” refers to co-authors and me. My contribution in the paper includes (1) Selection of the topic (2) Compiling and interpretation of the literature (3) Designing experiments (4) understanding the literature and interpretation of the results (5) providing comprehensible structure to the paper (6) Preparation of graphs and figures (7) Writing and editing

Abstract

Corneal neovascularization represents a key step in the blinding inflammatory stromal keratitis (SK) lesion caused by ocular infection with Herpes simplex virus (HSV). In this report we describe a novel approach to limit the angiogenesis caused by HSV infection of the mouse eye. We show that topical or systemic administration of the src kinase inhibitor (TG100572) that inhibits downstream molecules involved in the VEGF signaling pathway, resulted in markedly diminished levels of HSV induced angiogenesis, and significantly

reduced the severity of SK lesions. Multiple mechanisms were involved in the inhibitory effects. These included blockade of IL-8/CXCL1 involved in inflammatory cells recruitment that are a source of VEGF, diminished cellular infiltration in the cornea, and reduced proliferation and migration of CD4⁺T cells into the corneas. As multiple angiogenic factors (VEGF, bFGF) play a role in promoting angiogenesis during SK and since src kinases are involved in signaling by many of them, the use of src kinase inhibition represents a promising way of limiting the severity of SK lesions the most common cause of infectious blindness in the Western world.

Introduction

Ocular Herpes Simplex virus (HSV) infection can result in blinding immuno-inflammatory lesions in the cornea termed stromal keratitis (SK) (3, 25). A critical step in the pathogenesis in SK is neovascularization of the normally avascular cornea, but such vessels are leaky and permit the escape of cells and inflammatory molecules into stromal tissues, events that impair vision. Preventing, or limiting, neovascularization was shown in animal models of SK to be a useful means to control the severity of lesions (16, 30, 31). Many molecules may participate in causing neovascularization in the HSV infected eye, but VEGF-A is the principal angiogenic factor involved (30). The VEGF-A can derive from multiple sources, that include endogenous production of VEGF-A whose angiogenic function is blocked by being bound to a soluble form of one of its receptors (2). HSV infection results in the breakdown of this inhibitory interaction

(26).Additional VEGF-A supplies come from newly synthesized protein by infected or cytokine stimulated cells, as well as from VEGF-A being transported to the eye by inflammatory cells (8). Whatever the source, VEGF-A mediates ocular angiogenesis by signaling mainly through the VEGFR2 receptor that in turn sets off a sequence of intracellular events that involve src kinases (6, 7, 29).

Recent studies have shown that src family of tyrosine kinases are responsible for VEGF mediated vascular permeability and angiogenesis in several systems (6, 11, 24). Accordingly, using inhibitors of src kinases represents a logical approach for therapy against pathological angiogenesis such as occurs in SK. Approaches tested to date to inhibit angiogenesis in the SK system have either targeted VEGF or one of its receptors, but inhibiting biochemical events set off by VEGF signaling such as src kinase activation has not been evaluated. This approach could have advantages over others since src kinase are also responsible for mediating vascular permeability and may also be involved in signaling by other angiogenic factors, such as fibroblast growth factors (24). The later are known to be involved in pathological angiogenesis caused by ocular HSV infection (10, 30).

Drugs have recently become available that effectively inhibit one or more src kinases and which can function to inhibit new blood vessel development and function (5, 19, 24). One such example is the drug TG100572, shown recently to be effective at inhibiting VEGF mediated events involved in a non infectious vascular disease of the retina (24). A compound of particular interest is the pro-drug src kinase inhibitor TG100801, since upon topical ocular administration to the eye it converts to the active src kinase inhibitor molecule TG100572 that inhibits

VEGF signaling (24). In the present report, we demonstrate that TG100801 given topically is an effective means of inhibiting neovascularization and the subsequent severity of SK in the HSV infected eye. The use of src kinase inhibitors could add to the arsenal of therapeutics useful for the clinical management of SK, an important cause of impaired vision in humans.

Materials and methods

Mice and virus

Female 5-6-week-old C57BL/6 mice and Balb/c mice were obtained from Harlan Sprague –Dawley (Indianapolis IN). The animals were housed in the animal facility at the University of Tennessee. All manipulations were done in a laminar flow hood. All experimental procedures were in complete agreement with the Association for Research in Vision and Ophthalmology resolution on the use of animals in research. HSV-1 RE was propagated and titrated on vero cells (American type culture collection CCL81) using standard protocols. The virus was stored in aliquots at -80°C until use.

Corneal HSV-1 infection and clinical observations

Corneal infections of C57BL/6 mice were conducted under deep anesthesia. Mice were scarified on their corneas with 27 gauge needles and a 3 µl drop containing the required viral dose (10^4 PFU of HSV RE) was applied to the eye. The eyes were examined on different time points post infection with a slit lamp biomicroscope (KOWA), and the clinical severity of keratitis and angiogenesis of individually scored mice was recorded. The scoring system was

as follows: 0, normal eye; 1, mild corneal haze; 2, moderate corneal opacity, iris visible; 3, severe corneal opacity, iris visible; 4, opaque cornea, ulcer formation; and 5, necrotizing SK. Similarly, the angiogenic scoring system was based on quantifying the degree of neovessel formation based on three primary parameters: 1) the circumferential extent of neovessels (as the angiogenic response is not uniformly circumferential in all cases). 2) The centripetal growth of the longest vessel in each quadrant of the circle; and 3) the longest neovessels in each quadrant was identified and graded between 0 (no neovessels) and 4) (neovessels in corneal centre) in increments of nearly 0.4mm (radius of the cornea is 1.5mm). According to this system, a grade of 4 for a given quadrant of the circle represents the centripetal growth of 1.5mm towards the corneal centre. The score of four quadrants of the eye were then be summed up to derive neovessel index (range, 0-16) for each eye at a given time point.

Antibodies and reagents

For flow cytometry measurement of the infiltrating cells, 6 corneas per group were collected at the indicated time points by dissecting the corneal buttons above the limbus by a scalpel. Corneas were digested in liberase (Roche diagnostics) for 45 minutes at 37⁰C. Single cell suspension was prepared as described elsewhere (30). The Fc receptors were blocked with unconjugated anti CD16/32 (BD pharminogen) for 30 min. Samples were incubated with CD4-APC (RM4-5), CD11b-PerCP (M1/70), F4/80-FITC (BM8), Gr1-PE (RB6-8C5), CD45-APC (LCA-Ly5, 30-F11), CD31-PE(MEC 13.3) ,CD49d (MFR4.B) CD8-PerCP, IFN γ -APC, CD44-FITC and CD62L-FITC purchased from BD pharmingen (San

Diego, CA) for 30 min. All samples were collected on a FACS scan (BD biosciences) and data were analyzed using Flowjo software.

Immunofluorescent staining for PECAM-1 in vascular endothelium was also performed on the corneal flat mounts. Corneas of Balb/c mice infected with 5×10^5 PFU of HSV-1 RE were dissected under stereomicroscope (Leica, Wetzlar, Germany) and corneal flat mounts were rinsed in PBS for 30 min and flattened on a glass slide under stereo microscope. Corneal flat mounts were dried and fixed in 100% acetone (Sigma St. Louis, MO) for 10 min at -20°C . Non specific binding was blocked with 10% goat serum (Sigma G 9023) for 24 hours at 4°C . Invitrogen). The PECAM-1 was detected by an antibody directly labeled with conjugate (PE anti mouse CD-31 MEC 13.3; BD pharmingen). Each step was followed by three washing with PBS. Stained corneal flat mounts were mounted with prolong gold antifade mounting reagent (invitrogen P36934) and visualized with Nikon Ti fluorescent microscope using the software Nikon elements.

TG100801 - a topically applied prodrug form of a src kinase inhibitor was obtained from Sanofi-Aventis (Paris)/Targegen Inc., San Diego, California. The active compound, TG100572 (also obtained from Targegen for in-vitro use and intra-peritoneal injections), is an ATP competitive multi targeted tyrosine kinase inhibitor whereas the prodrug TG100801 is devoid of kinase inhibitory activity.

Treatment of animals with Src kinase inhibitor TG100801/TG100572

Female 5-6-week-old C57 BL/6 mice were used. Corneal infections were conducted under deep anesthesia induced by i.p. injection of Avertin (Sigma Aldrich). The mice were scarified on their corneas with a 27 gauge needle and

infected with 10^4 PFU of HSV-1 RE per eye and divided randomly into groups. In some groups src kinase inhibitor TG100801 (0.6%, 0.3%; Targegen Inc.) was applied topically (5 μ l eye drop, twice daily) and in other group TG100572 (0.5, 1.5 and 5mg/kg body weight dissolved in DMSO was administered intra peritoneally) starting from either day 1 to day 14-post infection or day 6 to day 14 p.i. Animals in the control group received liposomal vehicle (25% phospholipon vehicle 90 G) in the case of topical drug administration and DMSO in the intra peritoneal treatment modality following the same regimen. Mice were observed for the development and the progression of HSK lesions and angiogenesis from day 6 until day 15 as described previously. Most of the experiments were repeated at least 3 times unless stated otherwise.

Treatment of animals with anti VEGF antibody, Bevacizumab(Avastin)

Anti VEGF antibody Avastin was obtained from Genentech. Female 5-6-wk-old C57 BL/6 mice were used. Corneal infection were conducted under deep anesthesia induced by i.p. injection of Avertin (Sigma Aldrich). The mice were scarified on their corneas with a 27 gauge needle and infected with 10^4 PFU of HSV-1 RE per eye and divided randomly into groups. In one group src kinase inhibitor TG100572 (5mg/kg, Targegen Inc.) was administered intra-peritoneally, daily and in the other group Avastin (5mg/kg body weight at day 3, 6, 9 and 12p.i.) was given intra-peritoneally. Animals in the control group received mock treatment. Mice were observed for the development and the progression of HSK lesions and angiogenesis from day 6 until day 15 as described previously in

materials and methods. Most of the experiments were repeated at least 3 times unless stated otherwise.

Virus specific CD8⁺ IFN γ staining

To determine the immune response generated in the controls and src kinase treated groups, intracellular cytokine staining was performed as previously described (13). Single cell suspension of infected DLN was prepared and 10^6 cells per well were cultured in 96 well U bottom plates. Cells were left untreated/stimulated with gB peptide (1 $\mu\text{g}/\text{ml}$) for 5 hrs at 37°C in 5% CO_2 . Brefeldin A (10 $\mu\text{g}/\text{ml}$) was added to the culture for the intracellular cytokine accumulation. Cell surface marker and intracellular cytokine staining for IFN- γ was performed using a cytofix /cytoperm kit (BD Pharmingen). All samples were collected with a FACSCAN and were analyzed by FLOWJO.

Thymidine incorporation assay

Lymphocytes from the draining cervical draining lymph nodes were obtained at day 15 p.i. and enriched for CD4⁺T cell population by Miltenyi biotech CD4⁺T cell isolation kit. The cells were plated at the density of 5×10^5 in 96 well round bottom tissue culture plate in a total volume of 200 μl of RPMI (GIBCO). The cells were stimulated with anti-CD3 (1 $\mu\text{g}/\text{well}$) anti-CD28 (1 $\mu\text{g}/\text{well}$). 16 hours before harvest, [^3H] thymidine (1mCi/well; 1Ci=37GBq) was added. The cells were harvested onto-UniFilter (PerKinElmer). [^3H] Thymidine incorporation was measured in a scintillation counter and the results were expressed as mean CPM from triplicate cultures.

Western blotting

For the detection of FAK phosphorylation, 3 corneas per group were dissected at the indicated time points in 300 ul of RIPA buffer containing protease inhibitor cocktail (aprotinin, PMSF and sodium orthovanadate), cell debris was removed by centrifugation and the samples stored at -80°C till used for SDS-PAGE. In brief, after 2 hrs of blocking with 3% nonfat milk in TBS, membranes were incubated with 1:1000 dilution of rabbit polyclonal phosphor-specific anti FAK⁸⁶¹ antibody and membranes were then incubated for 1 hr with secondary antibody coupled to horse raddish peroxidase. Specific bands were detected with Immobilon™ western; Millipore). Membranes were stripped and then reprobed to detect Total FAK and and β actin antibody.

Histopathology

For histopathological analysis, eye balls from different groups of mice were extirpated at the indicated time point post infection in 10% formalin. In brief, the samples were put overnight in tissue tek (Sakura), which virtually removes all the moisture content from the samples and embeds it in paraffin. Tissue tek was automatically programmed, that treated the samples sequentially with alcohol (100%), xylene (100%), and paraffin. 5µm sections were then cut using microtome and stained with hematoxylin and eosin.

Cytokine ELISA

Six corneas per group were collected at indicated time points. The corneas were sonicated and the levels of CXCL1/KC/mouse homologue of IL-8 were measured in the supernatants using Qantikine kit as per manufacturer's protocol. (R&D systems).

Quantitative PCR (QPCR)

Total mRNA was isolated from corneal cells using TRIzol LS reagent (Invitrogen). The cDNA prepared using 1 µg of RNA was used for subsequent analysis. QPCR was done using SYBR Green PCR Master Mix (Applied Biosystem, Foster City, CA) with iQ5 real-time PCR detection system. (Bio Rad, Hercules, CA). The expression levels of cytokines were normalized to β-actin with ΔCt method and relative quantification between control and infected mice was performed using the $2^{-\Delta\Delta C_t}$ formula. The primers used were as follows:

IL-1β Forward primer: CATCAACAAGAGCTTCAGGC
Reverse primer: CATCATCCCATGAGTCACAGAG

IL6 Forward primer: CCAGAGTCCTTCAGAGAGATAC;
Reverse primer: CTCCTTCTGTGACTCCAGCTTATC

IFN-γ Forward primer: GAACGCTACACACTGCATCT:
Reverse primer: CCAGTTCCTCCAGATATCCAAG

β-actin Forward primer: CCTTCTTGGGTATGGAATCCTG,
β-actin Reverse primer: GGCATAGAGGTCTTTACGGATG

Reverse Transcription Polymerase chain reaction (RT-PCR)

RT-PCR for the presence of CXCL1 transcripts was done according to the manufacturer's protocol (Promega, Madison, WI). The amplified products were resolved on 1% agarose gel. Primers for RT-PCR were as follows.

β-actin Forward primer: CCTTCTTGGGTATGGAATCCTG
β-actin Reverse primer: GGCATAGAGGTCTTTACGGATG
CXCL1 Forward primer: GGGATTCACCTCAAGAACATCC

CXCL1 Reverse primer: TCTGAACCAAGGGAGCTTCA

In vitro and in vivo virus (HSV-1) - drug interaction assay

The effect of src kinase inhibitor TG100572 on viral replication (if any) was confirmed by incubating cells with inhibitor either before (pretreatment) or after (post treatment) inoculation with the virus and then quantifying infectious HSV kos yield by the viral plaque assay. Vero cells were infected with MOI=1 and and were incubated with 100 nM (maximum below cytotoxicity levels) TG100572 or 0.1%DMSO either before (-1h) or after infection. The effect of the drug (TG100572) on production of HSV-1 was determined by titrating the virus in cell culture supernatant at different times following infection. For the in vivo assay, the virus (HSV-RE) was quantified in eye swabs following HSV-1 infection in TG100801 treated and control mice and titrated by viral plaque assay.

Statistical analysis

Most of the analyses for determining the level of significance were performed using either one way ANOVA (Dunnetts post hoc test) or two way ANOVA (Bonferroni test). Values of $p \leq 0.001$ (***), $p \leq 0.01$ (**), and $p \leq 0.05$ (*) were considered significant. Results are expressed as means \pm SD.

Results

Topical application of prodrug TG100801 inhibits angiogenesis and SK

The prodrug was shown by others to convert to an active inhibitor of the src kinase involved in VEGF signaling following topical application to the eye (5, 24). Using the same conditions shown by others to inhibit retinal angiogenesis

and vessel permeability, the effects on responses to ocular infection with HSV was evaluated. C57BL/6 animals infected with 10^4 PFU of HSV-1 and divided into 3 groups. One group served as infected and untreated control and the other groups were treated with TG100801 either 0.3% or 0.6%, topically. Drug treatment was administered twice daily with therapy begun 1 day after infection until experiments were terminated on day 14 p.i. Three separate experiments were performed and cumulated results are shown in Figs 2.1 a and b. As is evident, there was a significant inhibition of both angiogenesis and SK lesion severity with the higher dose of drug investigated compared to controls. The incidence of SK as recorded in three independent experiments was lower in TG100801 treated group (Fig 2.1c). Histological sections taken from sample animals from test and control groups revealed evident differences in ocular inflammatory responses (Figs.2.1 d, e &f).

In another experiment mice were infected with HSV-1 and divided into two groups, One group was treated with TG100801 (0.6%), a concentration that resulted in significant inhibition of both angiogenesis and SK lesion severity, and the non treated groups receiving liposomal vehicle served as an infected control. The corneas from these mice were collected at the indicated time points post infection and subjected to western blotting for the detection of FAK phosphorylation, an event known to be the biomarker of src kinase activity (6, 7, 29). Whereas phosphorylated FAK was undetectable in naïve corneal lysates, it could be demonstrated in infected corneas as early as day 1 post infection (Fig 2.2a). However there was a significant inhibition in FAK phosphorylation in

TG100801 treated corneal lysates at the time points tested within the periods of elevated FAK-p861 (Fig 2.2b) suggesting that an important step in VEGF signaling, i.e src kinase activation and FAK phosphorylation was efficiently blocked by the inhibitor (TG100801).

TG100572 controls the lesion severity independent of viral replication

Ocular swabs from control and TG100801 treated animals, from the above mentioned experiments were taken in the early time periods to determine if the drug was inhibitory to virus replication. The corneas were homogenized and centrifuged and the viral titers were determined in the supernatants of the infected control and TG100801 treated animals. No significant differences were observed in the viral titers recovered from the corneas in different groups (Fig 2.3 a). To measure if the src kinase inhibitors had any antiviral activity, we examined the effect of TG100572 on HSV infection in vitro. Vero cells were infected with 1 MOI of HSV kos and treated with maximum below cytotoxic levels (100nM) of TG100572 or 0.1% DMSO as control. Quantitation of viral titers in culture supernatants by plaque assay revealed no significant effect on viral titers as compared to DMSO treated controls (Fig 2.3 b). Accordingly, we conclude that TG100572 does not have anti viral activity.

Effect of active src kinase inhibitor given systemically on ocular HSV infection

Repeatedly administering drugs topically to the infected mouse eye can be problematic and requires a general anesthetic to facilitate the procedure. In consequence, experiments to measure the effects of drug treatment on cellular

and molecular events at different times after treatment were also done in infected animals given the active drug intra-peritoneally. Animals were ocularly infected with HSV and divided into different groups and treated with TG100572 (0.5, 1.5 or 5mg/kg body wt) once daily starting at 24 hours after infection. The pattern of angiogenic response, compared to sham treated controls, was recorded at day 15 p.i. Potent effects were obtained with a dose of 5mg/kg body weight (Fig 2.4a) with minimal effects on their general health. As shown in (Fig 2.4b&c), treatment started at day 1 p.i. (preventive) resulted in a major reduction in the extent of angiogenesis (which was >5 fold at day 12 post infection) and SK (3 fold at day 12 p.i.) along with a 6 fold reduction in CD11b⁺Gr1⁺ cells (at day 15 p.i) (Fig 2.4 g) compared to infected and untreated control (Fig 2.4f). Additionally, commencing treatment at day 6p.i (Fig 2.4d&e) also resulted in significant inhibition of angiogenesis, lesion scores and CD11b⁺Gr1⁺ infiltration (Fig 2.4h) measured at the termination of experiments at day 15 p.i. The visible angiogenesis and SK lesion severity was also significantly less in the treated mice (Fig 2.5a &b).

To compare our novel approach (TG100572) with a potential positive control bevacizumab (a monoclonal antibody that binds to VEGF with high specificity; thereby blocking VEGF mediated signaling pathways and thus angiogenesis) (22), experiments were done where mice were divided into three groups (n=6/group). One group received bevacizumab (Avastin) i/p (5 mg/kg body weight) at day 3, 6, 9 and 12 p.i and other was treated with TG100572 i/p (5mg/kg b wt) starting at day 3p.i until day 13p.i. The third group served as infected and

untreated control. As shown (Fig 2.4i) at day 9 p.i., bevacizumab (Avastin) resulted in significant inhibition of angiogenesis and SK severity ($p < 0.0201$) but this was less than observed in a group of animals that received TG100572 systemically. TG100572 treatment showed a highly significant inhibition of angiogenesis. At day 14p.i. (Fig 2.4j) there was around 1.6 fold and 2.9 fold reduction in angiogenesis following Bevacizumab (avastin) and TG100572 treatment respectively as compared to the control groups.

To evaluate whether the administration of the src kinase inhibitor could influence the expression of SK, animals were treated either with TG100572 starting from day 1 p.i till day 14 p.i. or day 6 to day 14 p.i and the extent of inflammatory ocular reactions were compared in the treated and control animals by sacrificing animals and recovering ocular cells from corneas following collagenase digestion. As is evident, there was a reduced infiltration of Gr1⁺CD11b⁺ cells (neutrophils) in treated mice at all indicated time points post infection (Fig 2.6a). The neutrophil infiltration peaked at day 2 and day 11 post infection in both the control and treated mice, however the control mice had 3 fold and 2.5 fold higher frequencies (Fig 2.6a) and absolute numbers (Fig 2.6e) of neutrophil infiltrates at day 2 and day 11p.i. respectively, as compared to the treated group.

A significant reduction in the infiltration of CD11b⁺ F4/80⁺ cells (macrophages) was also observed following src kinase inhibition when evaluated at the later time points post infection (in the clinical phase). There were both reduced frequencies (Fig 2.6b) and total numbers (Fig 2.6f) of F4/80 cells in treated compared to the infected and untreated controls. Strikingly, around 4 fold

decrease in the CD4⁺ T cells infiltration was evident in the src kinase inhibitor treated mice both in terms of percentages (Fig 2.6c) and absolute numbers (Fig 2.6g) at the clinical phase of the disease. Additionally, the frequencies and numbers of IFN γ ⁺ CD4⁺ T cells were reduced 7-8 fold as a consequence of TG100572 treatment along with a highly significant reduction in IFN γ and IL-2 producing CD4⁺ T cells upon stimulation with anti-CD3 anti-CD28 (Figs 2.7a, b, e & f) or uv inactivated HSV kos (Fig 2.7c, d, g & h). Corneal single cell suspension stained for CD45 (a pan leukocyte marker) revealed significantly reduced frequencies (Fig 2.6d) and absolute numbers (Fig 2.6h) of CD45⁺T cells (almost 2 fold) in the corneas of the treated mice at all indicated time points analyzed post infection. Taken together our data indicates that both topical and systemic administration of small molecule inhibitors of src kinases results in significant reduction in both the extent of neovascularization and severity of SK.

Inhibition of src activity blocks CXCL1 and proinflammatory cytokines

Our observation that src kinase inhibitors caused a reduction in neutrophil infiltration could mean that the drug inhibited the expression of molecules involved in neutrophil recruitment such as the chemokine CXCL1. In support of this CXCL1 mRNA was present in the infected eye at higher levels than the scarified controls. Fig 2.8a depicts the expression of CXCL1 in HSV-1 infected corneas as early as day 1 p.i. For the quantification of CXCL1 gene expression, mice were ocularly infected with HSV and 6 corneas from each group (control and treated) were collected, pooled and were analyzed by QPCR at indicated time points. Corneas from src kinase treated mice subjected to QPCR revealed a

decrease in CXCL1 levels at all time points tested with maximum reduction observed during the clinical phase of the disease (Fig 2.8b). In addition, the same situation was evident with the protein levels measured by ELISA. The corneal supernatants were assayed for CXCL1/IL-8 by ELISA as indicated in materials and methods. Fig 2.8c depicts the kinetics of CXCL1 protein expression levels in the control and src kinase inhibitor treated mice throughout the course of ocular infection. There was a significant reduction in the CXCL1 at day 2 and also during the clinical phase (around 8 fold reduction at day 11 p.i.) of the disease in the treated mice. Thus, our data could mean that Src kinases may regulate critical “downstream” signaling pathways that might contribute to expression of CXCL1, a pro-angiogenic and pro-inflammatory chemokine in murine cornea. Additionally treated mice represented diminished levels of proinflammatory cytokines notably IL-6, IFN- γ and IL-1 β as compared to infected and untreated controls (Fig 2.8d).

TG100572 may down regulate CD49d on CD4⁺T cells in lymphoid organs resulting in fewer cells to migrate to the ocular site

SK is well known to be orchestrated by CD4⁺T cells (25). The frequencies and absolute numbers of CD4⁺ T cells recovered by collagenase digestion of corneas were diminished in TG100572 treated animals at all time points tested after ocular HSV infection. To address the cause of reduced CD4⁺T cells in the treated mice, animals that were ocularly infected and begun TG100572 treatment i/p at day 1 p.i and continued daily were sacrificed and the phenotype of CD4⁺T cells isolated from the DLN as well as from corneal lesions after collagenase

digestion was evaluated at indicated time points (day 5, 7,9,11 post HSV-1 ocular infection). In these experiments, lesion severity was greater in the control animals as compared to the drug treated animals. FACS analysis revealed that whereas there was no difference in the expression of CD62L (data not shown) and a modest difference in the expression of CD44 (Fig 2.9b), interestingly CD49d on CD4⁺T cells in CLN (Fig 2.9a) and corneas (Fig 2.9c) was significantly down regulated at all time points in the src kinase inhibitor recipients. This observed down regulation of CD49d on CD4⁺T cells could be relevant since previous studies indicate that blocking CD49d reduces SK (27). Taken together, we interpret these observations to mean that src kinases are involved in controlling the expression of integrin molecules such as CD49d that are involved in migration of inflammatory cells to the ocular lesion site (10) which could explain the overall impaired infiltration of CD4⁺T cells in the cornea.

TG100572 inhibits CD4⁺T cell proliferation in vitro

Src knockout mice have shown marked reduction in inflammatory responses to a variety of physiological insults (11). Measurement of the absolute numbers of draining cervical lymph node (CLN) cells revealed diminished numbers of total lymph node cells (Fig 2.9d) and also CD4⁺T (Fig 2.9e) cells in the kinase inhibitor (TG100572 i.p) recipient mice at all the time points tested. This likely means that in addition to effects on VEGF, TG100572 may also interfere directly with CD4⁺T cell activation and proliferation. To explore this possibility, draining CLN cells from HSV infected mice at day 15 p.i were enriched for CD4⁺T cells and stimulated with anti-CD3 anti-CD28 (as described

in materials and methods). In some wells, different concentrations of TG100572 (non cytotoxic concentrations) were added and the effects on proliferation responses recorded. Whereas a minimal proliferation was observed with anti-CD3 alone, anti-CD3 anti-CD28 resulted in a significant CD4⁺T cell proliferation. TG100572 inhibited CD4⁺T cell proliferation in a dose dependent manner (Fig 2.9f) suggesting that by diminishing immune activation and CD4⁺T cell proliferation, TG100572 may additionally serve to limit the size of immunopathogenic CD4⁺T cells involved in lesion expression.

Discussion

Neovascularization of the otherwise avascular cornea represents a pathological hallmark of ocular HSV-1 infection. Present approaches for clinical management of corneal neovascularization rely on anti-virals, corticosteroids or anti VEGF antibody treatment. In this study we show that a small molecule inhibitor of src kinases, results in suppression of angiogenesis and lesion severity in a murine model of SK. Administered topically as a prodrug (TG100801) or the active form (TG100572) systemically, resulted in inhibition of several key events in the pathogenesis of SK. These included diminished cellular infiltration in the corneas, of CD4⁺T cells and neutrophils, the cells primarily involved in SK. There was also a reduction in levels of the chemokine CXCL1 and proinflammatory cytokines such as IFN γ , IL1B and IL-6. Importantly treatment resulted in inhibited FAK phosphorylation in the corneal tissues; an essential step in VEGF mediated angiogenesis (1). Additionally TG100572

administered systemically resulted in down regulation of CD49d on CD4⁺T cells in the DLN and cornea. However, the src kinase inhibitor had no demonstrable proinflammatory effect and failed to express antiviral activity.

The current anti-angiogenic approach shows effective control of newly proliferating vascular endothelial cells and since the phosphorylation of FAK and src activation appears to be very early events post infection, src blockade by the inhibitors early during the course of infection could be advantageous for significant and complete anti angiogenic effects. Additionally achieving efficacious drug concentration in the corneal tissues following the topical delivery route (TG100801) is generally considered a technical challenge. However recent clinical trials with these drugs have shown that TG100801, while lacking anti kinase activity of its own, quickly generated active TG100572 within the eye upon topical delivery, however neither compound was detectable in plasma, indicating that delivery to the eye occurs by local penetration and not systemic absorption (5).

Systemic treatment with the src kinase inhibitors also significantly reduced angiogenesis and cellular infiltration, particularly of neutrophils, one plausible explanation being that by inhibition of FAK phosphorylation, src kinase inhibitors preserves the junctional integrity of the endothelial cells (14) and thus inhibited the paracellular transport of neutrophils. However, src kinases were also shown to modulate the expression of the pro angiogenic neutrophil attracting chemokine CXCL1/mouse KC/homologue of IL8 (28) and that src kinase activation correlates with the amount of IL-8 produced (14, 17, 28). Consistent

with this, src kinase inhibitors resulted in inhibition of CXCL1 expression. Thus it is possible that significant reduction in the neutrophils in the treated group may be a consequence of reduced chemokine levels, which is the prominent regulator of neutrophil infiltration into the inflamed cornea (23).

In humans, SK may lead to permanent loss of vision and the current treatment modalities that are used for the clinical management of SK includes anti VEGF antibody treatment such as bevacizumab (4, 23), antivirals and corticosteroids but none of them are considered ideal. Antiviral compounds that block virus entry or reduce viral replication can be prophylactic and may not be efficacious against SK. As a result, small-molecule inhibitors targeting cellular responses that contribute to disease may have a substantial advantage over antiviral approaches. Corticosteroid therapy, on the other hand when continued for a longer duration might exhibit several side effects (15), and anti VEGF antibody (bevacizumab) although shown to reduce VEGF induced neovascularization (22, 23), however abnormal vascular permeability is frequently associated with neovascularization (24). Thus, an antivascular permeability compound that is also antiangiogenic such as src kinase inhibitor should have added therapeutic benefit. Endothelial cell barrier functions are disrupted by a number of viruses and a very recent study suggests that VEGFR2 and SFK inhibitors may be of therapeutic utility in stabilizing vasculature during viral infections(9) .Additionally both VEGF and FGF growth factors have been shown to be potent proangiogenic factors in HSV-1 induced corneal neovascularization. The binding of angiogenic growth factors (VEGF, bFGF) to

their receptors is known to result in activation of non receptor tyrosine kinases (src kinases) which in turn regulates endothelial cell proliferation, migration and survival (by inhibiting apoptosis of endothelial cells) (6). A compound that inhibits redundant pathways of angiogenesis has the potential of being therapeutically advantageous (24). In support of this our results clearly indicate that bevacizumab (avastin), a VEGF antagonist, inhibit HSV-1 induced corneal neovascularization, but the levels of inhibition achieved were less than that caused by TG100572. Although we do not preclude the possibility that the observed lesser reduction in angiogenesis in the avastin treated mice could be due to a weaker binding affinity of avastin to mouse VEGF-A (4, 23). Our findings therefore rationalize testing of these kinase inhibitors for additional indications and clinical application in reducing HSV induced immunopathology. The fact that VEGFR2 and SFK inhibitors are already FDA approved for use in humans, they could be immediately rationalized for use in clinical cases of HSK.

A significant anti-angiogenic and anti-inflammatory effect was also observed following systemic treatment with TG100572. This mode of treatment also produced additional effects such as CD49d expression (on CD4⁺T cells) and attenuation of T cell function. It may be argued that these effects might be due to the limited specificity of the src kinase inhibitors (20). However the drug was well tolerated systemically with no adverse effects on the general health except for some reduction in the body weight of the animals. Our observations that systemically administered TG100572 influences the severity of SK lesions is supported by the observation of significantly less CD4⁺T cell infiltration in the

cornea in the clinical phase suggesting that TG100572 (src kinase inhibitor, i/p) could control the lesion development by limiting the migration of pathogenic T cells to the extra lymphoid inflammatory site. The SK model represents a situation where normally immunoprotective CD4⁺T cells exert an immunopathological function in the cornea of the eye(18). The Integrin CD49d (VLA-4) is known to be involved in the migration of pathogenic CD4⁺Tcells to the ocular site and that in SK 70–80% of corneal T cells in disease expresses CD49d (VLA-4) early in lesion development (27). Thus, it was intriguing to observe that the CD49d integrin was expressed on a significantly lower percentage of lymphoid CD4⁺ T cells in the src kinase inhibitor treated mice compared to controls. The down regulation of CD49d in src kinase inhibitor treated mice was not unexpected since there is mounting evidence that α4 integrins use the src family kinases to transduce intracellular signals (21). Our observations could shed light on the relative merits of various cellular targets as candidates for therapeutic intervention during an ongoing immune-inflammatory reaction such as is SK. Src kinase inhibition also resulted in a less activated phenotype of CD4⁺T cells as shown by decreased CD44 expression on cells in the draining cervical lymph nodes. Additionally src kinase inhibitors resulted in diminished levels of inflammatory cytokines which is in accordance with findings that the reduction in proinflammatory cytokines resulted in impairment of Th1 differentiation(12).

In conclusion, we demonstrated that the blockade of Src kinase activation (which is an essential step in VEGF signaling) with VEGFR2/src kinase inhibitor

resulted in reduced SK lesion severity and diminished cellular infiltration, probably by inhibition of vascular leak and removal of a corneal chemokine gradient. In the present approach, which is novel for infectious ocular angiogenesis, we did achieve highly significant but not complete anti angiogenesis. We advocate that combining src kinase inhibitor with additional therapeutic approaches could be valuable for use in the clinic to manage herpetic ocular lesions.

LIST OF REFERENCES

1. **Abu-Ghazaleh, R., J. Kabir, H. Jia, M. Lobo, and I. Zachary.** 2001. Src mediates stimulation by vascular endothelial growth factor of the phosphorylation of focal adhesion kinase at tyrosine 861, and migration and anti-apoptosis in endothelial cells. *Biochem. J.* **360**:255-264.
2. **Ambati, B. K., M. Nozaki, N. Singh, A. Takeda, P. D. Jani, T. Suthar, R. J. C. Albuquerque, E. Richter, E. Sakurai, M. T. Newcomb, M. E. Kleinman, R. B. Caldwell, Q. Lin, Y. Ogura, A. Orecchia, D. A. Samuelson, D. W. Agnew, J. St Leger, W. R. Green, P. J. Mahasreshti, D. T. Curiel, D. Kwan, H. Marsh, S. Ikeda, L. J. Leiper, J. M. Collinson, S. Bogdanovich, T. S. Khurana, M. Shibuya, M. E. Baldwin, N. Ferrara, H. P. Gerber, S. De Falco, J. Witta, J. Z. Baffi, B. J. Raisler, and J. Ambati.** 2006. Corneal avascularity is due to soluble VEGF receptor-1. *Nature* **443**:993-997.
3. **Biswas, P. S., and B. T. Rouse.** 2005. Early events in HSV keratitis - setting the stage for a blinding disease. *Microbes Infect.* **7**:799-810.
4. **Bock, F., J. Onderka, T. Dietrich, B. Bachmann, F. E. Kruse, M. Paschke, G. Zahn, and C. Cursiefen.** 2007. Bevacizumab as a potent inhibitor of inflammatory corneal angiogenesis and lymphangiogenesis. *Invest. Ophthalmol. Vis. Sci.* **48**:2545-2552.
5. **Doukas, J., S. Mahesh, N. Umeda, S. Kachi, H. Akiyama, K. Yokoi, J. Cao, Z. Chen, L. Dellamary, B. Tam, A. Racanelli-Layton, J. Hood, M. Martin, G. Noronha, R. Soll, and P. A. Campochiaro.** 2008. Topical administration of a multi-targeted kinase inhibitor suppresses choroidal neovascularization and retinal edema. *J. Cell. Physiol.* **216**:29-37.
6. **Eliceiri, B. P., R. Paul, P. L. Schwartzberg, J. D. Hood, J. Leng, and D. A. Cheresh.** 1999. Selective requirement for Src kinases during VEGF-induced angiogenesis and vascular permeability. *Mol. Cell.* **4**:915-924.
7. **Eliceiri, B. P., X. S. Puente, J. D. Hood, D. G. Stupack, D. D. Schlaepfer, X. Z. Z. Huang, D. Sheppard, and D. A. Cheresh.** 2002. Src-mediated coupling of focal adhesion kinase to integrin alpha v beta 5 in vascular endothelial growth factor signaling. *J. Cell Biol.* **157**:149-159.
8. **Gong, Y., and D. R. Koh.** 2010. Neutrophils promote inflammatory angiogenesis via release of preformed VEGF in an in vivo corneal model. *Cell and Tissue Research* **339**:437-448.
9. **Gorbunova, E. E., I. N. Gavrilovskaya, T. Pepini, and E. R. Mackow.** 2011. VEGFR2 and Src kinase inhibitors suppress Andes virus-induced endothelial cell permeability. *J Virol* **85**:2296-2303.
10. **Kim, B., Q. Q. Tang, P. S. Biswas, J. Xu, R. M. Schiffelers, F. Y. Xie, A. M. Ansari, P. V. Scaria, M. C. Woodle, P. Lu, and B. T. Rouse.** 2004. Inhibition of ocular angiogenesis by siRNA targeting vascular endothelial growth factor pathway genes - Therapeutic strategy for herpetic stromal keratitis. *American Journal of Pathology* **165**:2177-2185.
11. **Kim, M. P., S. I. Park, S. Kopetz, and G. E. Gallick.** 2009. Src family kinases as mediators of endothelial permeability: effects on inflammation and metastasis. *Cell Tissue Res.* **335**:249-259.

12. **Kuka, M., R. Baronio, S. Valentini, E. Monaci, A. Muzzi, S. Aprea, E. De Gregorio, and U. D'Oro.** 2010. Src kinases are required for a balanced production of IL-12/IL-23 in human dendritic cells activated by Toll-like receptor agonists. *PLoS One* **5**:e11491.
13. **Kumaraguru, U., and B. T. Rouse.** 2000. Application of the intracellular gamma interferon assay to recalculate the potency of CD8(+) T-cell responses to herpes simplex virus. *J. Virol.* **74**:5709-5711.
14. **Kvietys, P. R., and M. Sandig.** 2001. Neutrophil diapedesis: Paracellular or transcellular? *News Physiol. Sci.* **16**:15-19.
15. **McGhee, C. N. J., S. Dean, and H. Danesh-Meyer.** 2002. Locally administered ocular corticosteroids - Benefits and risks. *Drug Saf.* **25**:33-55.
16. **Nagy, J. A., A. M. Dvorak, and H. F. Dvorak.** 2007. VEGF-A and the induction of pathological angiogenesis. *Annu. Rev. Pathol.-Mech. Dis.* **2**:251-275.
17. **Natarajan, K., M. S. Rajala, and J. Chodosh.** 2003. Corneal IL-8 expression following adenovirus infection is mediated by c-Src activation in human corneal fibroblasts. *J. Immunol.* **170**:6234-6243.
18. **Newell, C. K., S. Martin, D. Sendele, C. M. Mercadal, and B. T. Rouse.** 1989. Herpes simplex virus-induced stromal keratitis: role of T-lymphocyte subsets in immunopathology. *J Virol* **63**:769-775.
19. **Noronha, G., K. Barrett, A. Boccia, T. Brodhag, J. G. Cao, C. P. Chow, E. Dneprovskaja, J. Doukas, R. Fine, X. C. Gong, C. Gritzen, H. Gu, E. Hanna, J. D. Hood, S. Hu, X. S. Kang, J. Key, B. Klebansky, A. Kousba, G. Li, D. Lohse, C. C. Mak, A. McPherson, M. S. S. Palanki, V. P. Pathak, J. Renick, F. Shi, R. Soll, U. Splittgerber, S. Stoughton, S. H. Tang, S. Y. Yee, B. Q. Zeng, N. N. Zhao, and H. Zhu.** 2007. Discovery of 7-(2,6-dichlorophenyl)-5-methylbenzo 1,2,4 triazin-3-yl - 4-(2-pyrrolidin-1-ylethoxy)phenyl amine - a potent, orally active Src kinase inhibitor with anti-tumor activity in preclinical assays. *Bioorg. Med. Chem. Lett.* **17**:602-608.
20. **Okutani, D., M. Lodyga, B. Han, and M. Y. Liu.** 2006. Src protein tyrosine kinase family and acute inflammatory responses. *Am. J. Physiol.-Lung Cell. Mol. Physiol.* **291**:L129-L141.
21. **Pereira, S., M. Zhon, A. Mocsai, and C. Lowell.** 2001. Resting murine neutrophils express functional alpha(4) integrins that signal through Src family kinases. *J. Immunol.* **166**:4115-4123.
22. **Perez-Santonja, J. J., E. Campos-Mollo, M. Lledo-Riquelme, J. Javaloy, and J. L. Alio.** 2010. Inhibition of Corneal Neovascularization by Topical Bevacizumab (Anti-VEGF) and Sunitinib (Anti-VEGF and Anti-PDGF) in an Animal Model. *Am. J. Ophthalmol.* **150**:519-528.
23. **Saravia, M., G. Zapata, P. Ferraiolo, L. Racca, and A. Berra.** 2009. Anti-VEGF monoclonal antibody-induced regression of corneal neovascularization and inflammation in a rabbit model of herpetic stromal keratitis. *Graefes Arch. Clin. Exp. Ophthalmol.* **247**:1409-1416.
24. **Schepcke, L., E. Aguilar, R. F. Gariano, R. Jacobson, J. Hood, J. Doukas, J. Cao, G. Noronha, S. Yee, S. Weis, M. B. Martin, R. Soll, D. A. Cheresch, and M. Friedlander.** 2008. Retinal vascular permeability suppression by topical

- application of a novel VEGFR2/Src kinase inhibitor in mice and rabbits. *J. Clin. Invest.* **118**:2337-2346.
25. **Streilein, J. W., M. R. Dana, and B. R. Ksander.** 1997. Immunity causing blindness: five different paths to herpes stromal keratitis. *Immunology Today* **18**:443-449.
 26. **Suryawanshi, A., S. Mulik, S. Sharma, P. B. Reddy, S. Sehrawat, and B. T. Rouse.** 2011. Ocular neovascularization caused by herpes simplex virus type 1 infection results from breakdown of binding between vascular endothelial growth factor A and its soluble receptor. *J Immunol* **186**:3653-3665.
 27. **Suvas, S., A. K. Azkur, B. S. Kim, U. Kumaraguru, and B. T. Rouse.** 2004. CD4(+) CD25(+) regulatory T cells control the severity of viral immunoinflammatory lesions. *J. Immunol.* **172**:4123-4132.
 28. **Trevino, J. G., J. M. Summy, M. J. Gray, M. B. Nilsson, D. P. Lesslie, C. H. Baker, and G. E. Gallick.** 2005. Expression and activity of Src regulate interleukin-8 expression in pancreatic adenocarcinoma cells: Implications for angiogenesis. *Cancer Res.* **65**:7214-7222.
 29. **Weis, S. M., and D. A. Cheresh.** 2005. Pathophysiological consequences of VEGF-induced vascular permeability. *Nature* **437**:497-504.
 30. **Zheng, M., S. Deshpande, S. Lee, N. Ferrara, and B. T. Rouse.** 2001. Contribution of vascular endothelial growth factor in the neovascularization process during the pathogenesis of herpetic stromal keratitis. *J. Virol.* **75**:9828-9835.
 31. **Zheng, M., M. A. Schwarz, S. J. Lee, U. Kumaraguru, and B. T. Rouse.** 2001. Control of stromal keratitis by inhibition of neovascularization. *Am. J. Pathol.* **159**:1021-1029.

APPENDIX

Figure 2.1 Effect of topical administration of src kinase inhibitor (TG100801) on the severity of SK

C57BL/6 animals infected with 10^4 PFU of HSV-1 were treated with TG100801 (0.3%, 0.6%, topically). TG100801 was applied topically starting at day 1 till day 14 post infection (p.i.). (a,b) Cumulative data of angiogenesis (a) and HSK scores (b) at day 12 p.i as measured by slit lamp biomicroscopy, of three independent experiments. The level of significance was determined by one-way ANOVA using Dunnett's post hoc setting. (c) The bar diagram demonstrates the percentage severity of each group of mice infected with 10^4 PFU of HSV-1 RE at day 15 p.i. in three independent experiments. The SK scores of three or greater than three were counted as SK incidence (black bars= infected control; white bars represents TG100801 treated). (d-f) H&E staining of the corneal sections of naïve (d) control (e) and TG100801-treated animals (f).

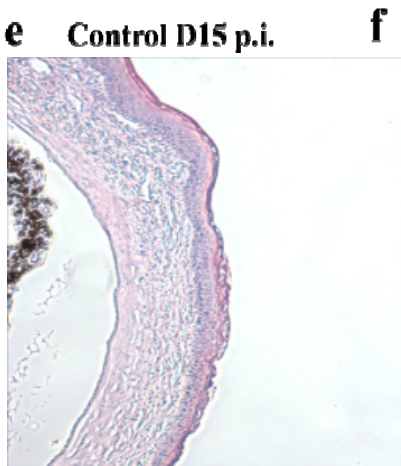
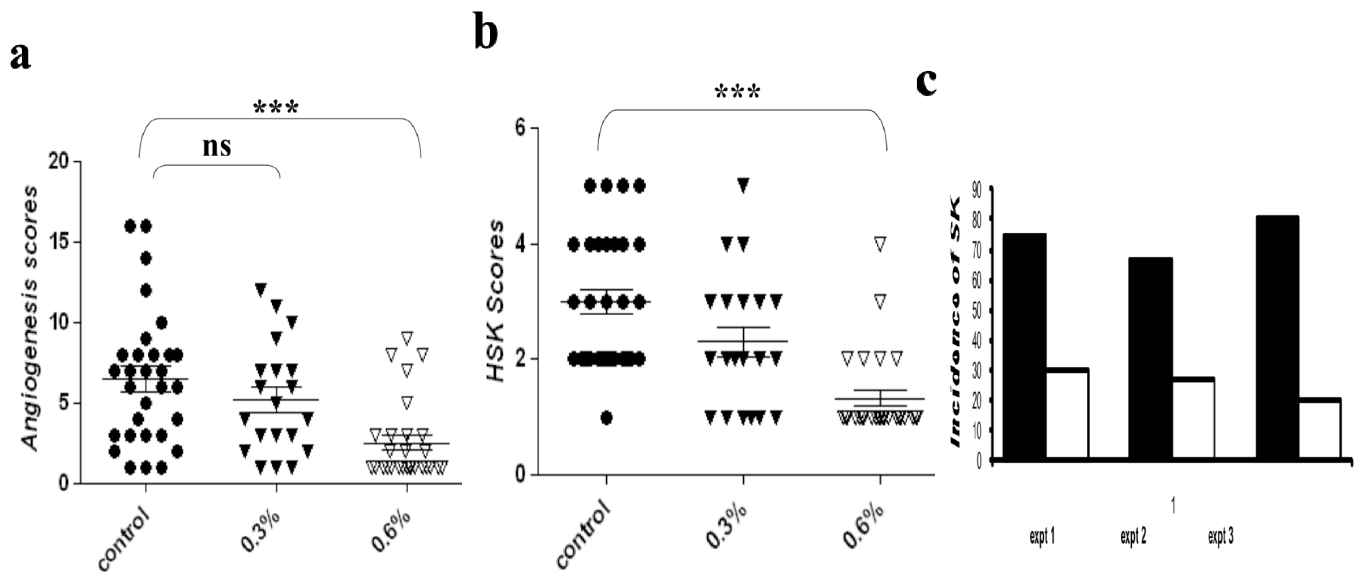


Figure 2.2 TG100801 inhibits FAK-y861 phosphorylation in the murine cornea

(a) Western blot analysis for phosphorylated FAK⁸⁶¹ in corneal cell lysate at different time points following HSV-1 infection. **(b)** Inhibition of FAK phosphorylation: Mice were infected with 10⁴ pfu of HSV-1 RE. Twenty four hrs following infection, one group was treated topically (cornea) with a 5µl drop of 0.6% TG100801, twice daily till 14 dpi. Second group received the vehicle control in the same way. Corneal cell lysate was used to detect level of phosphorylated FAK^{Y861} by anti-rabbit FAK antibody in Western blot. Drug treated mice showed inhibition of FAK phosphorhylation at all time points tested within the periods of elevated phoshorylated FAK. (N=naïve;C=control;T=treated).

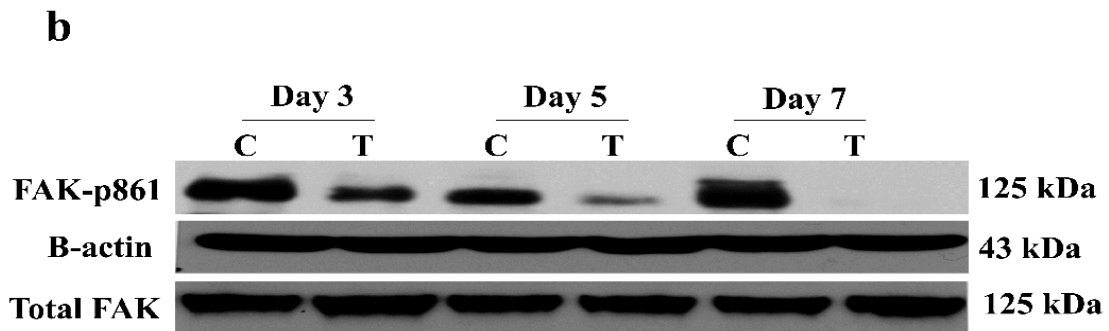
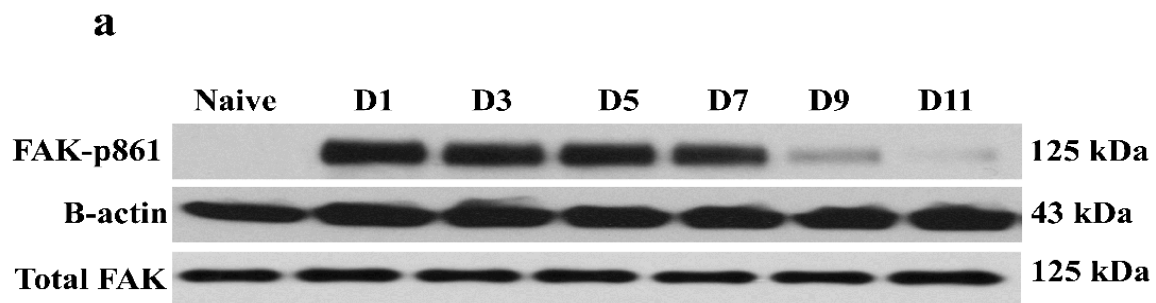
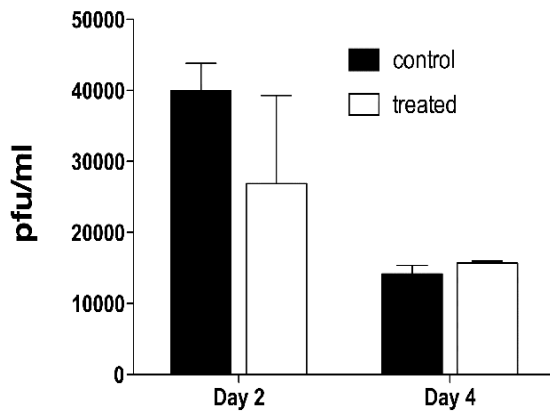


Figure 2.3 TG100572 controls SK lesion severity independent of viral replication

(a) Viral titers in corneal swabs in control and TG100801 treated mice at day 2 and 4p.i. is shown. (b) Vero cells were infected with MOI=1 and incubated with 100 nM of TG100572 (maximum below cytotoxicity level) after infection or 0.1%DMSO. The effect of the drug (TG100572) on production of HSV-1 was determined by titrating the virus in cell culture supernatant at different times following infection.

a



b

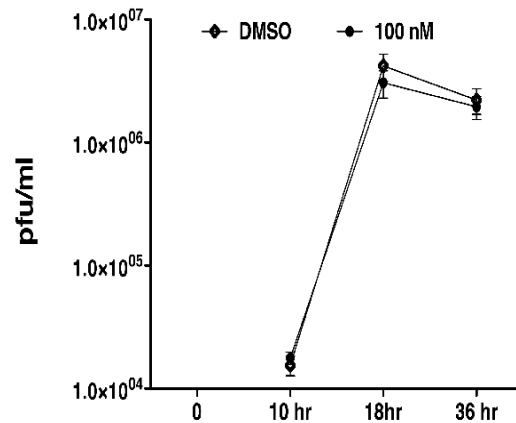


Figure 2.4 Effect of systemic administration of src kinase inhibitor (TG100572) on angiogenesis and SK lesion severity

(a) C57BL/6 animals infected with 10^4 PFU of HSV were treated with different concentrations of TG100572 (0.5, 1.5 and 5 mg/kg body weight), intraperitoneally daily starting from either 24 hrs post infection (preventive) or day 6 p.i. (therapeutic manipulation) until day 14. The comparative angiogenesis scores of HSV infected animals at day 14, treated with indicated concentrations of TG100572. The statistical significance was determined using one way ANOVA.

(b-e) Kinetics of angiogenesis and lesion expression in control and TG100572 treated animals at 9-15 dpi is shown. Disease progression in control and TG100572 treated mice following infection with 10^4 pfu of HSV-1 to C57Bl/6 animals under preventive **(b & c)** and therapeutic **(d & e)** mode of treatment. The level of significance was calculated by two way ANOVA. **(i & j)** Comparative angiogenesis scores in bevacizumab and TG100572 treated mice compared to infected but untreated controls at day 9p.i **(i)** and day 14 p.i **(j)**. The statistical significance was determined by student's t test. **(f-h)** Infiltration of CD11b⁺Gr1⁺ polymorph nuclear neutrophils in the corneas of control **(f)**, following preventive **(g)** and therapeutic **(h)** treatment at day 15 p.i. All experiments were repeated at least three times.

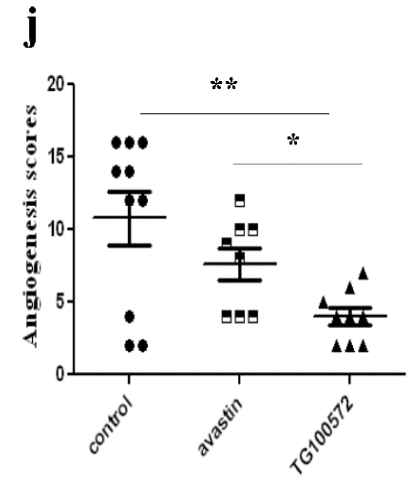
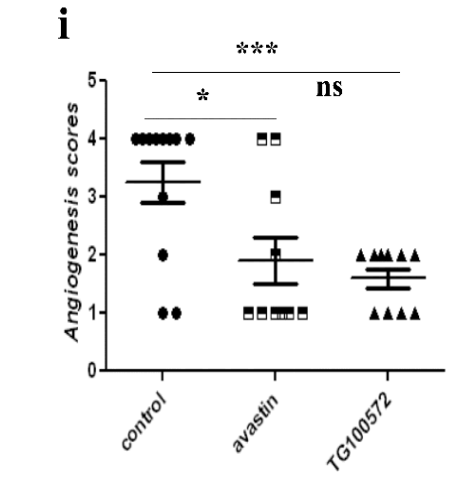
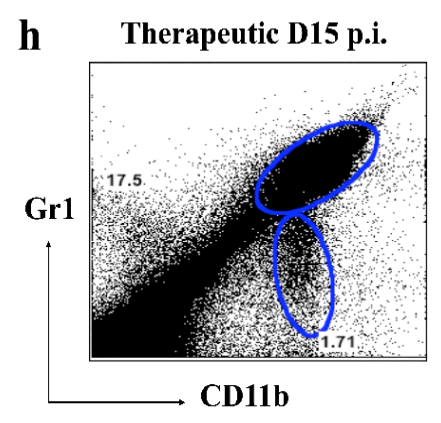
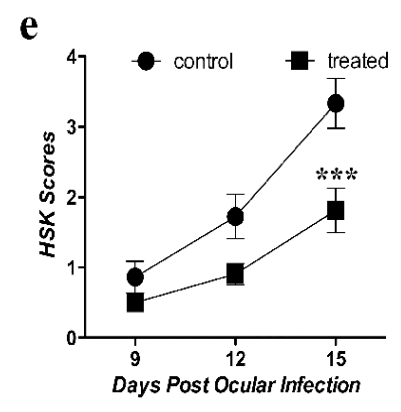
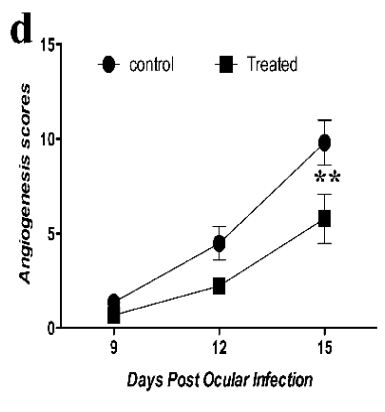
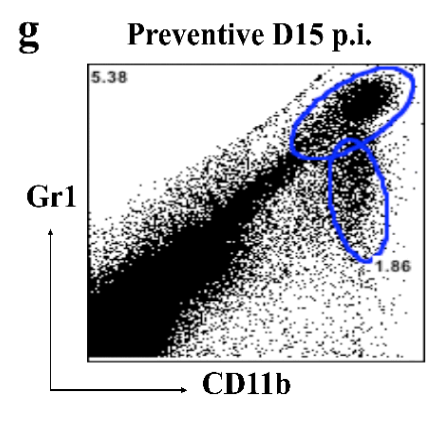
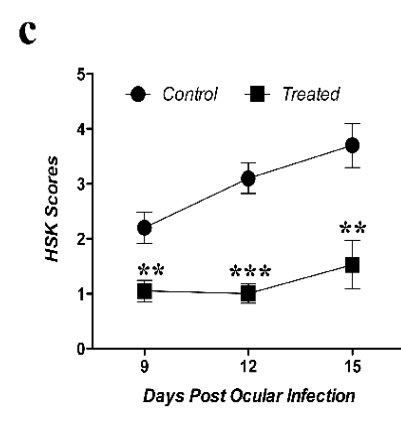
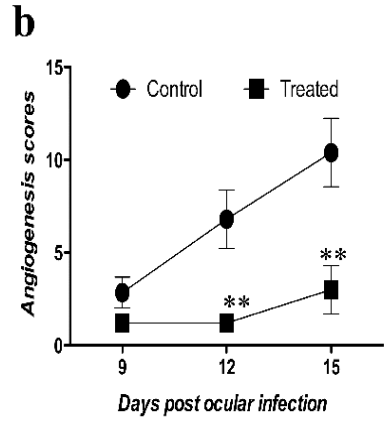
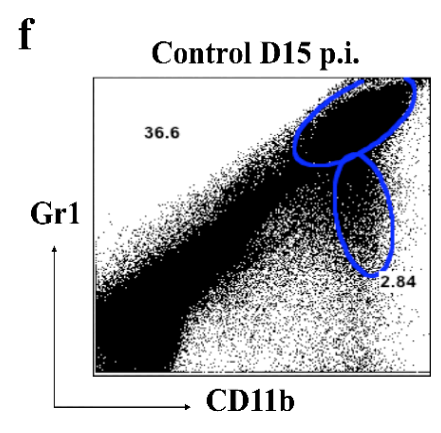
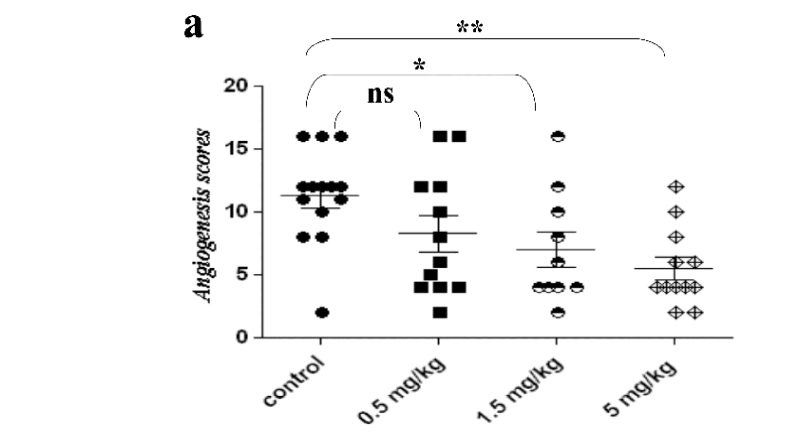
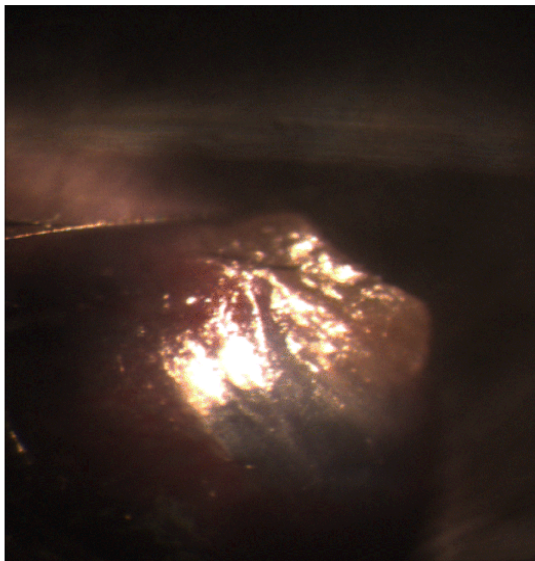


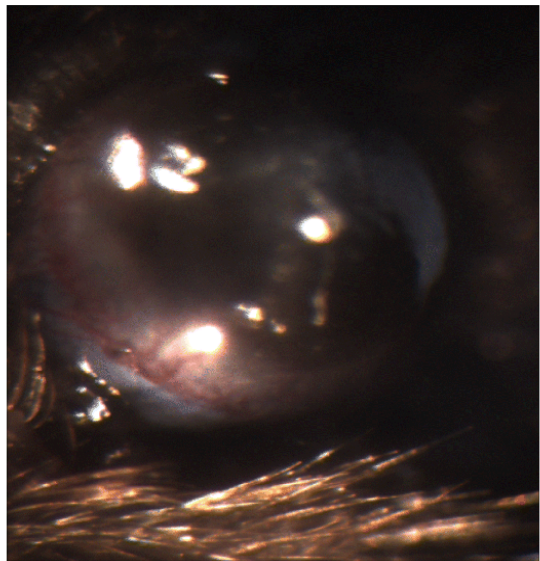
Figure 2.5 Representative eye photograph (at day 15 p.i.) of control (a) and TG100572 treated (b) mice.

a



Control

b



Treated

Figure 2.6 Kinetics of Cellular infiltration in the corneas of control and TG100572 treated mice.

Effects of TG100572 treatment on kinetics of cellular infiltration in corneas of HSV infected animals analyzed by flow cytometry. C57BL/6 infected with 10^4 PFU of HSV were either treated with TG100572 5 mg/kg body weight i/p daily starting from 24 hr p.i. until day 14p.i. or untreated controls. Single cell suspension of the infected corneas were prepared from pooled 6 corneas (n=3) at indicated time points from each group (TG100572 treated or control) of mice. The cells were labeled for: **(a, e)** Gr1⁺CD11b⁺ (polymorph nuclear cells), **(b, f)** CD11b⁺F4/80⁺ (macrophage), **(c, g)** CD4⁺ and **(d, h)** CD45⁺ (leucocyte common antigen; pan leucocyte marker). The numbers on the dot plots indicates the percentage of the cells expressing the particular markers in control and kinase inhibitor treated mice at indicated time points p.i. The experiment was repeated three times and data are representative of a single experiment.

Figure 3

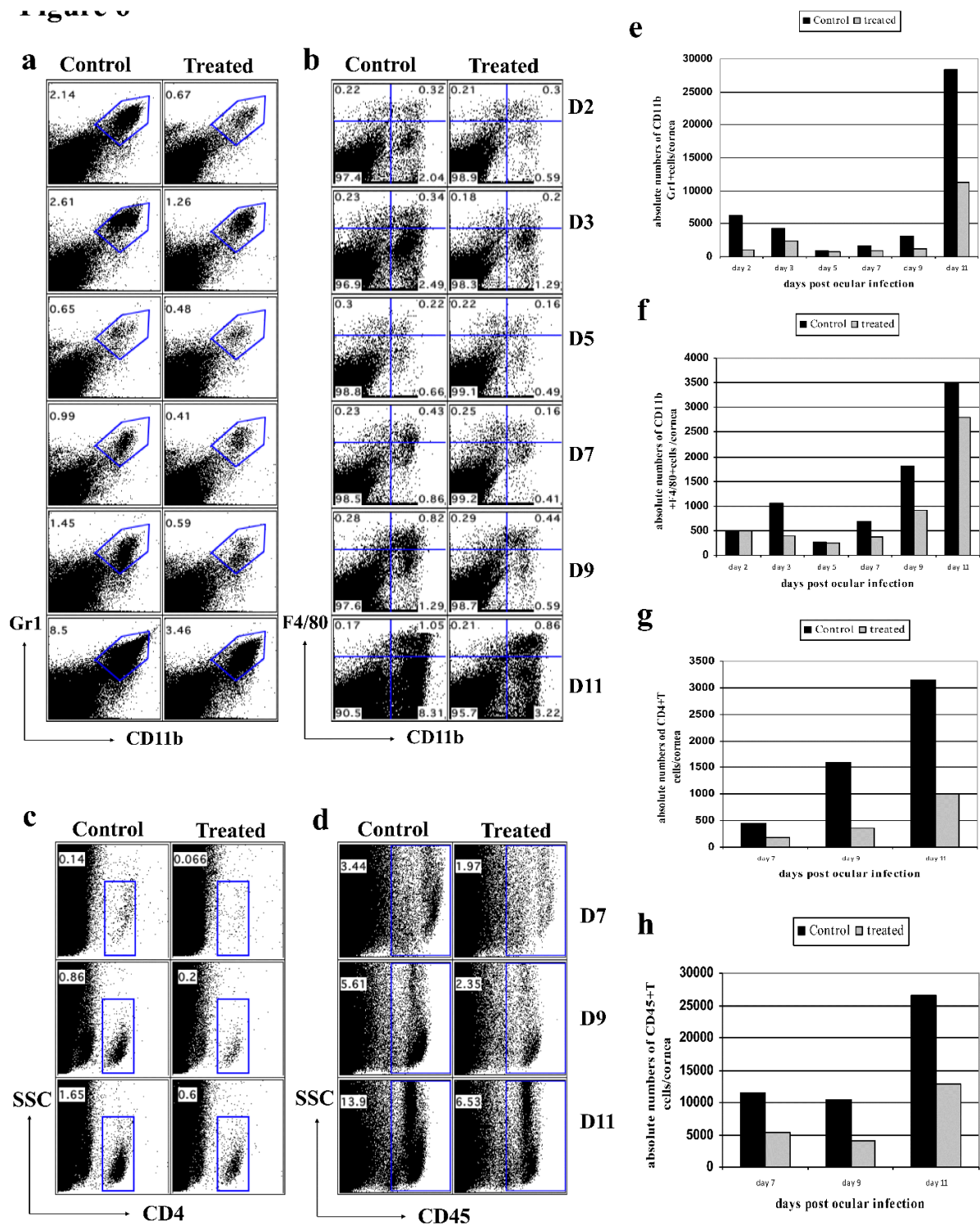


Figure 2.7 TG100572 treatment diminishes the infiltration of pathogenic Th1 cells in the cornea.

C57BL/6 infected with 10^4 PFU of HSV-1 was treated with TG100572 (5 mg/kg body weight) i/p daily starting from 24 hr p.i. until the termination of the experiments. Single cell suspension of the infected corneas were prepared from pooled 6 corneas at day 15 p.i. from each group (control and treated) of mice. The cells were stimulated with either anti-CD3 anti-CD28 or UV inactivated HSV Kos and stained for CD4⁺T cells producing IFN γ and IL-2. Frequencies (**a & b**) and absolute numbers (per cornea) (**e & f**) of IFN γ ⁺ and IL2⁺ T cells respectively in control and treated group was observed following stimulation by anti-CD3 anti-CD28. The frequencies (**c & d**) and absolute numbers (**g & h**) of IFN γ ⁺ and IL2⁺ T cells respectively in control and treated group following stimulation by UV inactivated HSV Kos is shown. The experiment was repeated three times and data are representative of a single experiment.

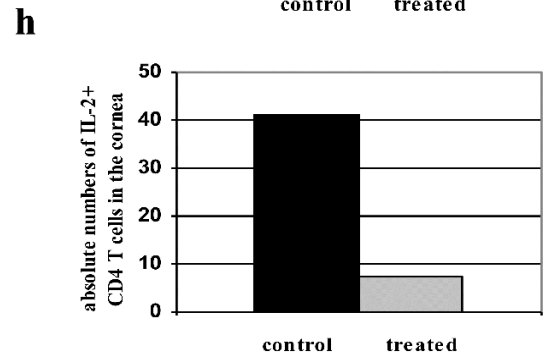
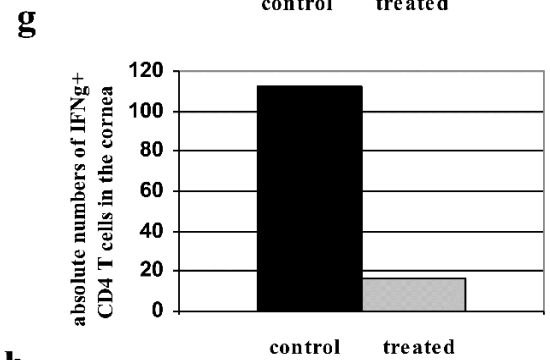
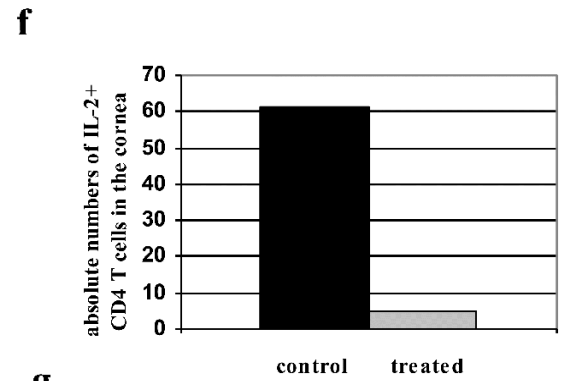
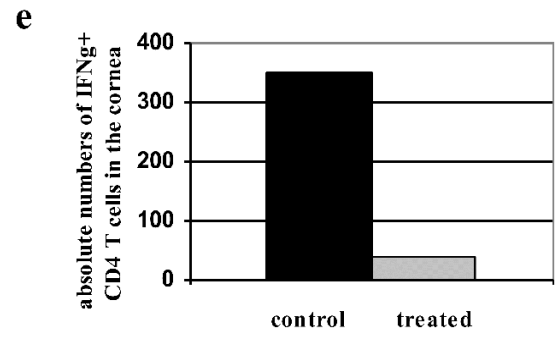
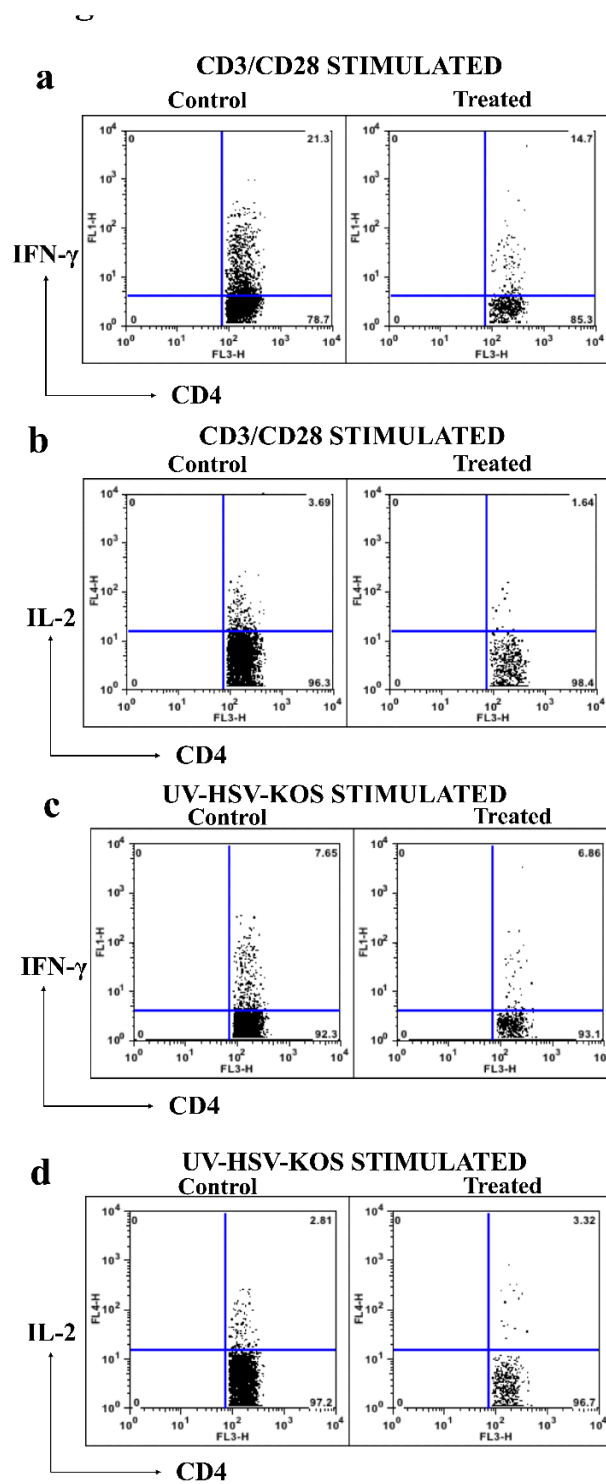


Figure 2.8 TG100572 treatment results in the blockade of CXCL1 in the cornea.

(a) Agarose gel analysis for CXCL1 (132bp) (Lane 4) transcripts from infected corneas is shown. Lane M is Marker; lane 2 is beta actin (92bp). Lane 1 and lane 3 are RT negative control for beta actin and CXCL1 respectively. Lane 5 is negative control (water) (b) Kinetic analysis for the expression of CXCL1 mRNA by QPCR at different time p.i after src kinase inhibitor or mock treatment is shown. WT mice were infected with HSV and treated with mock or TG100572. 6 Corneas were harvested from respective groups at an indicated time points, pooled and subjected to quantification by QPCR for CXCL1 mRNA. (c) Quantification of CXCL1 protein in HSV-1 infected corneas by ELISA after mock or TG100572 treatment is shown. At each time point, 6 corneas were harvested from HSV infected mice treated with mock or TG100572 and levels of CXCL1 protein were determined by ELISA. The level of significance was determined using two way ANOVA with Bonferroni post test. (d) Reduction in IL6, IFN- γ and IL-1 β after TG100572 treatment is shown. The mice infected with HSV were treated with mock or TG100572 and corneas collected from respective groups at an indicated time points were subjected to QPCR for IL-6, IFN- γ and IL-1 β mRNAs. The values are represented as fold change m RNA compared to infected control. The above experiments were repeated three times.

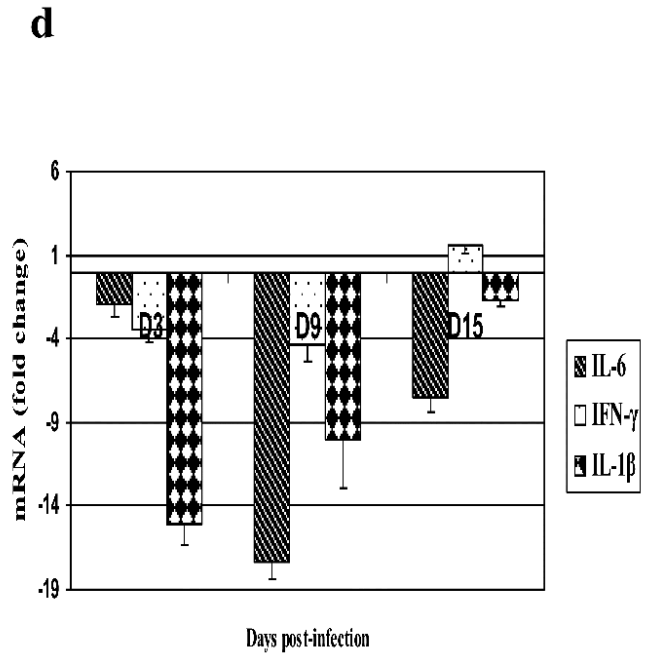
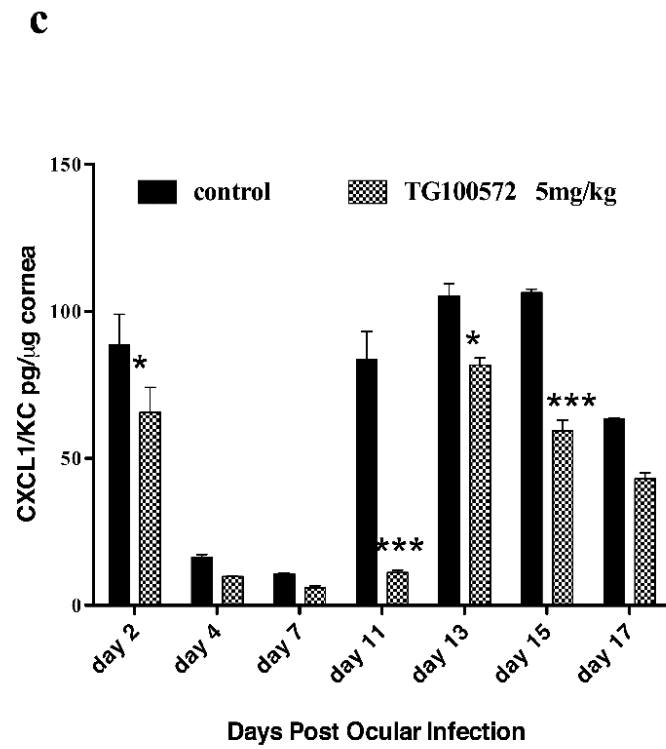
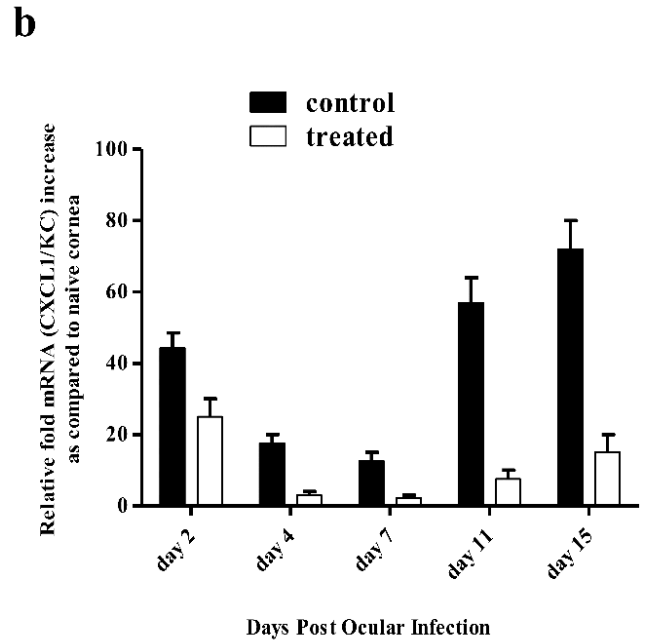
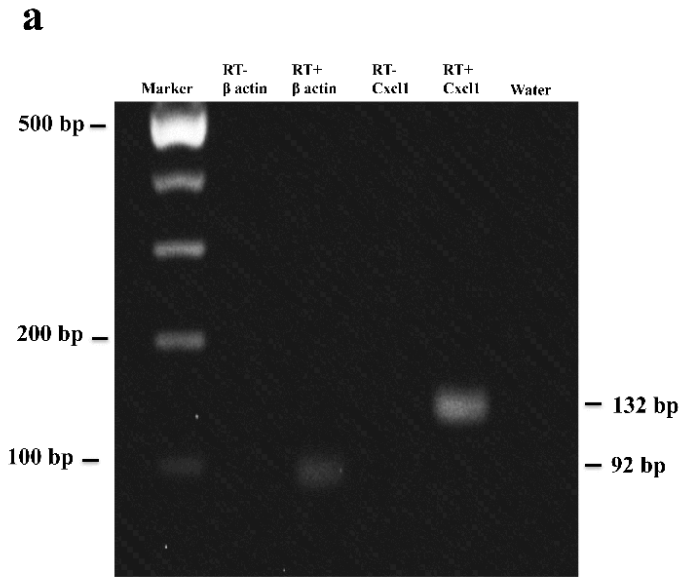
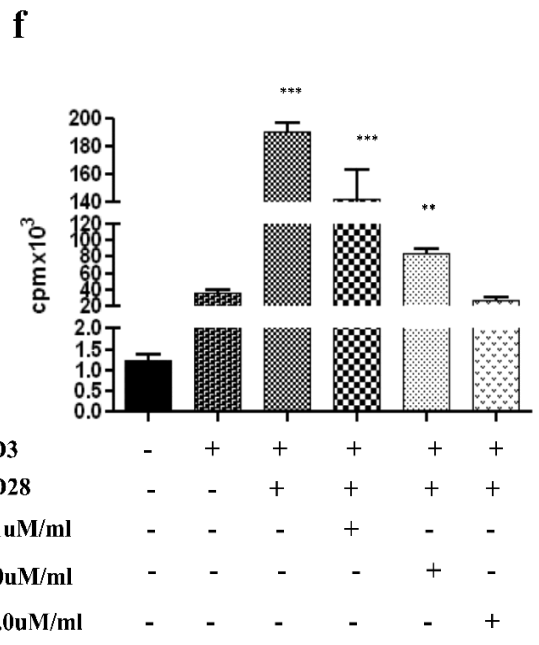
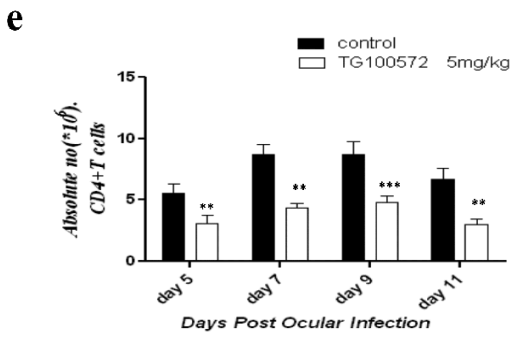
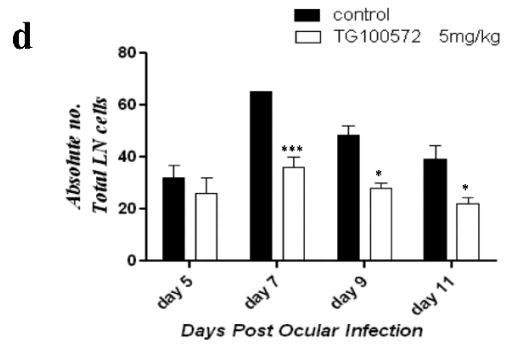
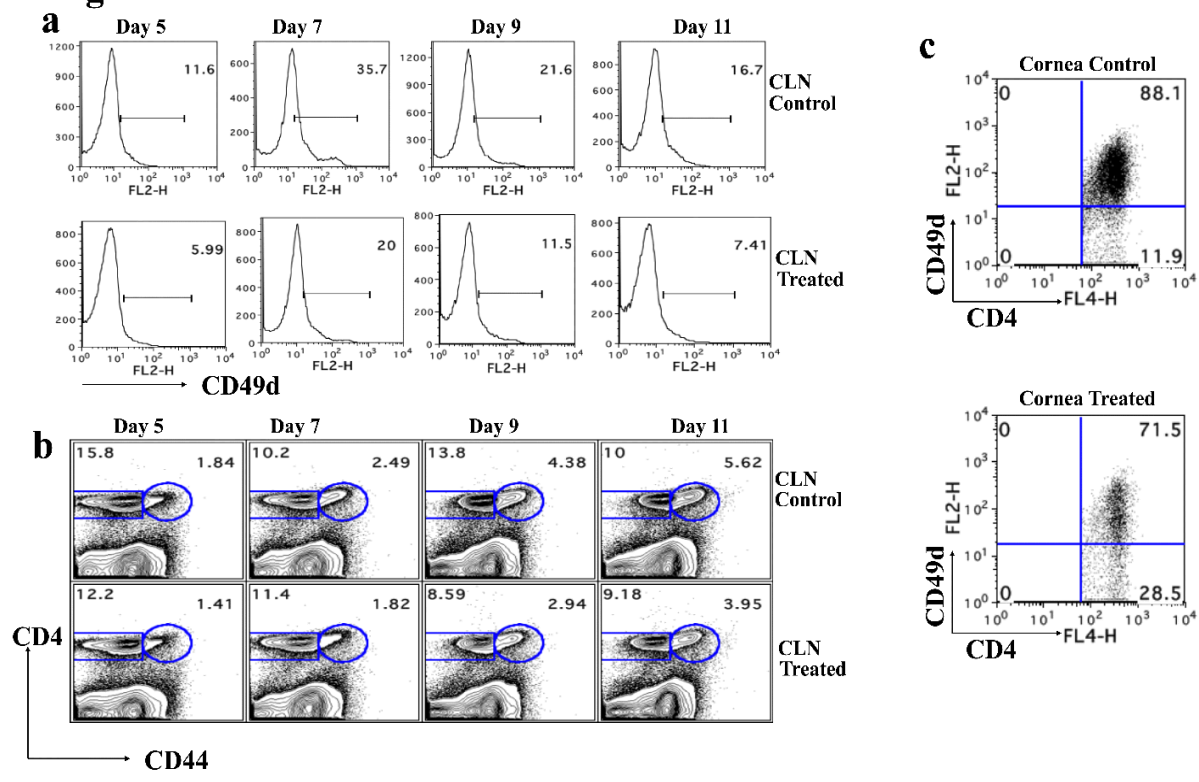


Figure 2.9 Src kinase inhibition may result in the attenuation of T cell function

(a) Kinetic analysis of CD49d expression on the CD4⁺T cells in the control and treated animals after ocular HSV-1 infection. C57BL/6 mice were infected with 10⁴ PFU of HSV. Mice (n=3) were sacrificed at each indicated time points and their draining cervical lymph nodes and corneas were analyzed for surface expression of CD4 and CD49d by flow cytometry. **(a)** Histograms representing the percentage of CD49d expression on CD4⁺T cells in draining cervical lymph node at the indicated time points post infection. Data are shown from one representative experiment. **(b)** Reduced expression of CD44 on CD4⁺T cells in draining CLN of TG100572 treated mice. **(c)** FACS plots showing the percentage of CD4⁺ CD49d⁺ T cells in the corneas in control and TG100572 treated animals at day 11-post infection. All kinetic experiments were repeated at least twice. **(d, e)** Absolute numbers (x10⁶) of the total lymph node cells and **(d)** and CD4⁺T cells **(e)** in control and treated animals is shown at indicated time points p.i. The level of significance was determined using two way ANOVA with Bonferroni post test. **(f)** DLN cells were enriched for CD4⁺Tcells and stimulated with anti-CD3 anti-CD28 in the presence or absence of drug at the indicated concentrations. Cell proliferation results are expressed as mean CPM from triplicate cultures.



PART-III

TIM-3/GALECTIN-9 INTERACTION

REGULATES INFLUENZA A VIRUS

SPECIFIC HUMORAL AND CD8 T CELL

RESPONSES

Research described in this chapter is a modified version of an article published in 2011 in *Proc. Natl. Acad. Sci. USA*. by Shalini Sharma, Aarthi Sundararajan, Amol Suryawanshi, Naveen Kumar, Tamara Veiga Parga, Vijay K Kuchroo, Paul G Thomas, Mark Y Sangster and Barry T Rouse.

Shalini Sharma, Aarthi Sundararajan, Amol Suryawanshi, Naveen Kumar, Tamara Veiga Parga, Vijay K Kuchroo, Paul G Thomas, Mark Y Sangster and Barry T Rouse. Tim-3/Galectin-9 interaction regulates influenza A virus specific humoral and CD8 T cell responses. *pnas.org/cgi/doi/10.1073/pnas.1107087108*.

In this chapter “our” and “we” refers to co-authors and me. My contribution in the paper includes (1) Selection of the topic (2) Compiling and interpretation of the literature (3) Designing experiments (4) understanding the literature and interpretation of the results (5) providing comprehensible structure to the paper (6) Preparation of graphs and figures (7) Writing and editing.

Abstract

Reactions to pathogens are usually tuned to effect immunity and limit tissue damage. Several host counter inflammatory mechanisms inhibit tissue damage but these may also act to constrain the effectiveness of immunity to acute infections, as we demonstrate in mice acutely infected with influenza A virus (IAV). We show that compared to wild type (WT), galectin-9 knockout (G9KO) mice mounted a more robust acute phase virus-specific CD8 T cell

response as well as higher and more rapid virus specific serum IgM, IgG and IgA responses, and also cleared virus more rapidly than did WT mice. Blocking galectin-9 signals to Tim-3 expressing cells using a Tim-3 fusion protein resulted in improved immune responses in WT mice. When IAV immune mice were challenged with a heterologous IAV, the secondary IAV-specific CD8 T cell responses were 4-5 fold higher in G9KO compared with WT mice. Our results indicate that manipulating galectin signals may represent a convenient approach to improve immune responses to some vaccines.

Introduction

The host immune response to pathogens needs precise regulation to minimize tissue damage whilst still achieving defense (24, 39). Some bystander tissue damage usually happens since several host defenses can destroy cells or orchestrate inflammatory reactions. With chronic infections, for example, immune mediated tissue damage would be more severe were it not for several cellular and chemical host components that inhibit inflammatory reactions (24). However, the activity of some of these counter inflammatory mechanisms could act to constrain the efficiency of protective immune components (27). For instance, regulatory T cells (Treg) can inhibit inflammatory reactions associated with chronic virus infections (1), but the same Treg response can also limit the magnitude of protective immunity to a virus or induced by a vaccine (32, 34). Other host components may also function to limit and help resolve inflammatory reactions. These include some cytokines (31), groups of molecules derived from

omega-3 polyunsaturated fatty acids (29), as well as some of the carbohydrate binding proteins of the galectin family (22). Galectin-9 (Gal-9), for example, upon binding to Tim-3 on T cells acts to limit the extent of immuno-pathological lesions in autoimmunity (14) as well as in some chronic infections (7, 9, 28). In the present study, we investigated whether the inhibitory effects of Gal-9 on Tim-3 expressing cells could influence the outcome of acute infection with IAV. We demonstrate that animals lacking the regulatory effects of Gal-9/Tim-3 triggering mount superior CD8 T cell and humoral immune responses and were more refractory to IAV. Moreover, IAV immune G9KO mice challenged with a heterologous IAV strain generated better virus-specific memory CD8 T cell responses than WT animals. Our results indicate that manipulating galectin signaling may represent a convenient approach to improve responses to some vaccines.

Materials and Methods

Mice and virus infections

Female 6-8-wk-old C57BL/6 were purchased from Harlan Sprague-Dawley and housed in the animal facilities at the University of Tennessee, Knoxville. G9KO were kindly provided by Gal Pharma Co. Ltd, Japan. Stocks of IAV strains HK/x31 (H3N2)(x31) and A/Puerto Rico/8/34 (H1N1)(PR8) for mice infections were grown and titrated as described previously (11). Mice were infected intranasally with 5000 EID₅₀ of IAV HKx31 in 30- μ l volume. To assess

secondary CD8T cell responses, mice were infected with x31 and challenged intranasally at least 4 weeks later with 8000 EID₅₀ of PR8. The Animal Care and Use Committee of the University of Tennessee approved all animal procedures.

Tissue sampling

Spleen, BAL fluid, plasma and lung samples were recovered from mice at acute phases of the primary and secondary infections. BAL samples were obtained from individual mice as described previously (20). Cells in the BAL were collected by centrifugation and the supernatants were stored at -80 °C for ELISA. BAL associated cells were pooled from three mice in each group and single cell suspensions were prepared from individual spleens. IAV x31 titers in lungs were determined by plaque assay using MDCK cells (15).

Flow cytometry

The antibodies to CD8 (53-6.7), CD4 (RM4-5), CD62 ligand (CD62L) (MEL-14), CD44 (IM7), IFN γ , TNF α , IL-2, and CD103 (2E7) were purchased from BD Bioscience. PE and APC conjugated Tim-3 antibodies were purchased from R&D Systems. Intra-nuclear FoxP3 staining was performed using a kit from E-Bioscience according to the instructions. Cell suspensions were blocked with anti-mouse CD16/32 and then incubated with specific antibodies or isotypes for 30 min at 4 °C. The antibody-stained cells were acquired with a FACS Calibur (BD Biosciences) and the data were analyzed using the FlowJo software (Tree Star, OR).

Tetramer and phenotypic staining of CD8 T cells

Influenza A peptide NP₃₆₆₋₃₇₄ (ASNENMETM), NP₃₁₁₋₃₂₅ (QVYSLIRPNENPAHK) were kindly provided by the Trudeau Institute and Dr. John Altman respectively. The experiments utilized the H-2D^b MHC class I glycoprotein complexed with the influenza virus nucleoprotein (NP) ASNENMETM peptide (NP) and being designated NPtet and staining was done as described previously (17). H-2D^b-NP₃₆₆₋₃₇₄ is an immuno-dominant CD8 T cell response to IAV in H-2b mice (35). IFN γ and TNF α producing T cells were enumerated by ICCS as previously described (16). In brief, 10⁶ freshly isolated splenocytes were cultured in U bottom 96-well plates. Cells were left untreated or stimulated with NP₃₆₆₋₃₇₄ ASNENMETM peptide (0.1 μ g/ml or 0.02 μ g/well), NP₃₁₁₋₃₂₅ QVYSLIRPNENPAHK (10 μ g/ml or 2 μ g/well), and incubated for 5 h at 37°C in 5% CO₂. Brefeldin A (10 μ g/ml) was added for the duration of the culture period to facilitate intracellular cytokine accumulation. After this period, cell surface staining was performed, followed by intracellular cytokine staining using a Cytofix/Cytoperm kit (BD PharMingen) as per the manufacturer's recommendations. The fixed cells were re-suspended in FACS buffer (PBS with 3% heat inactivated serum) and analyzed flow cytometrically.

Ex vivo apoptosis assay

Spleen single cell suspension isolated 10 days pi from IAV infected animals were incubated for 5 hrs with varying concentrations of Gal-9 in the absence or the presence of α lactose in 96-well flat-bottom plates in humidified incubators in the presence of 5% CO₂. After the incubation period was over, cells were stained for annexin V using a kit from BD Biosciences. Additionally, cells

were also co-stained for CD8, Tim-3, D^bNPTet. Stained cells were analyzed immediately by flow cytometry.

ELISA

Virus-specific antibodies levels in plasma and BAL were determined by ELISA using plates coated with purified, detergent disrupted virus (25). The antibody titer is expressed as the reciprocal of the highest dilution giving an absorbance value more than twice that for simultaneously titrated samples from naive mice.

Quantification of IAV in infected lung tissue

The quantification of IAV (HKx31) in lung tissue was done as previously reported (15). Briefly, Lungs were removed from infected mice on days 2,4,7,8, 9 and 10 days after infection and snap-frozen in serum free minimal essential medium (MEM) supplemented with 0.2% bovine serum albumin, 20 mmol/L HEPES, 100 U/ml penicillin, and 100 mg/ml streptomycin. Snap-frozen lungs were stored at -80°C until further processing. Tissues were disrupted by chopping with scissors, homogenized and centrifuged at 10,000 rpm for 15 minutes. The resulting supernatant was used to titrate the virus on MDCK cells as follows: Serial 10-fold dilution (in MEM) of the virus was incubated on 90-100% confluent MDCK cells for 1 hr. Thereafter, the infection medium was replaced with 2 ml of agar-overlay medium containing equal volume of 2X L-15 medium (Invitrogen) and 2% agar (Becton Dickinson). The plates were further incubated at 37°C. The plaques were visible at 3 days post-infection which were counted following staining with 0.2% crystal violet. The 2X L-15 medium contained 27.4g L-15

powder (2 bags), 0.25% Bovine serum albumin, 2X L-glutamine (Invitrogen), 2X Penicillin and streptomycin (Invitrogen), 2X HEPES (Invitrogen), 2X nonessential amino acids (NEAA) (Invitrogen) 0.15% sodium bicarbonate and 2 mg/ml TPCK treated trypsin (Life Technologies, Inc., Grand Island, NY).

Immunoblotting for the detection of galectin-9 expression and quantification

Mediastinal Lymph node (MLN) and lung homogenate samples (10 mg/lane) were resolved on 15% SDS-PAGE and transferred electrophoretically on to a PVDF membrane (Bio-Rad). The membrane was blocked overnight with 5% BSA and washed 5 times with TBS containing 0.05% Tween-20 (TBST) and incubated with biotinylated anti- galectin antibody (R&D Systems) at a concentration of 0.5 mg/ml diluted in TBST for 1 hr at room temperature. The membrane was washed 5 times with TBST and incubated with streptavidin- HRP antibody (Pierce) at a dilution of 1:10000 for 1 hr at room temperature. The membrane was developed with chemiluminescent substrate (Immobilon western chemiluminescent HRP substrate, Millipore) and the image was taken on CL-XPosure X-ray film (Thermo scientific).

Ninety-six-well microplates were coated with capture antibody at a concentration of 3000 ng/ml (100 ml/well, anti-galectin-9, GalPharma Co. Ltd, Japan). After incubation overnight at 4°C, the wells were washed three times with PBST (PBS containing 0.05% Tween-20) and blocked with 5% BSA for 2 h at RT. The wells were washed three times with PBST and Lymph node, spleen homogenate samples (100 ml) were added to the wells and incubated at RT for 2

h and aspirated. The wells were then washed with wash buffer. Biotinylated anti galectin detection antibody (1;10000, R&D Systems) diluted in reagent diluent (R&D Systems, PBS, 5% Tween 20, 2% goat serum) was added to each well and incubated at RT for 1 h. The wells were then washed three times and 100 µl of streptavidin–horseradish peroxidase (1:10000 dilution) added and incubated for 1 hr at room temperature. The plate was washed thrice and developed with TMB (R&D systems) substrate and the absorbance of each sample was determined at 450 nm. A standard curve ranging from 5 mg to 156.25 ng of recombinant galectin-9 (Gal Pharma, Japan) was generated to calculate the galectin-9 concentration in the unknown samples.

In vivo blockade with Tim-3 fusion protein

For blockade of Tim-3 pathway, 100 µg Tim-3 Ig fusion protein were injected intra peritoneally on alternate days starting from day 1 until the time of sampling on day 10 p.i.

Adoptive transfers

Splenocytes from WT or G9KO (both Thy1.2) x31 immune mice were enriched (miltenyi biotech kit) for CD8 T cells and then titrated for 10^4 NPtet⁺ CD8 T cells and transferred into Thy1.1 C57BL/6 animals. Alternatively 10^4 NPtet⁺ CD8 T from B6Thy1.1 (x31 immune) mice were transferred into Thy1.2 C57BL/6 WT or G9KO animals. 24 hrs post transfer, recipient animals were infected with 8000 EID₅₀ PFU of IAV PR8. 8 days post challenge CD8 T cell analysis was performed.

Statistical analysis

Data were analyzed using Prism 5.0 software (Graph pad). Experiments were repeated two to three times. The data presenting the differences between the groups were assessed using two-tailed unpaired student's t tests or by two way ANOVA with Bonferroni post hoc settings. Values of $p < 0.001$ (***), $p < 0.01$ (**), and $p < 0.05$ (*) were considered significant. $P < 0.05$ indicates that the value of the test sample was significantly different from that of relevant controls.

Results

Virus-specific CD8 T cells up regulate Tim-3 expression after IAV infection

Both BAL and spleens were isolated at different times from IAV infected WT animals and analyzed by FACS for CD8 T cells that expressed Tim-3. The highest levels in the BAL were observed at day 8, with 30-40% of total CD8 T cells expressing Tim-3 (Fig 3.1A). In addition, most of these Tim-3⁺ cells were also CD44^{hi} and CD62L^{lo} (Fig 3.1D, upper panel) indicative of activated or effector phenotype. Peak frequencies of Tim-3⁺ CD8 T cells were also present on day 10 p.i. in the spleen (Fig 3.3J). Using tetramers and the ICCS assay to detect D^bNP₃₆₆₋₃₇₄ (ASNENMETM) specific CD8 T cells, up to 75% IAV NP tetramer-specific cells were Tim-3⁺ (Fig 3.1 A and C) as well as CD44^{hi} and CD62L^{lo} (Fig 3.1D, lower panel). Furthermore, after NP peptide stimulation the majority (around 75%) of IFN γ ⁺ CD8 T cells were Tim-3⁺ (Fig 3.1B). Endogenous levels of Gal-9 in the lung extracts of IAV infected animals were also quantified by both western blotting (Fig 3.1E) and ELISA (Fig 3.1F). Basal levels of Gal-9 were

detectable in control lung extracts and these were moderately increased after IAV infection. A significant increase (2-2.5 fold) was observed at around 7 days p.i.

We could also show at day 10p.i. that around 20-22% of total CD4 T cells (Fig 3.1G) were Tim-3⁺ in the BAL samples of the WT animals. Moreover, using the ICCS assay to detect NP311–325 (QVYSLIRPNENPAHK) peptide- specific CD4 T cells, up to 65-70% (on average) of virus specific IFN γ ⁺ CD4 T cells were Tim-3⁺ (Fig 3.1H). Tim-3 expression was not detected on CD3⁻B220⁺CD19⁺ B cells.

Gal-9 induces apoptosis of IAV NPtet⁺CD8 T cells ex-vivo

The results of previous in vitro studies revealed that Gal-9 binding to Tim-3 receptors on some, although not all, T cell subsets causes them to undergo apoptosis (28, 38). To test the fate of the CD8⁺Tim-3⁺ population following IAV infection to Gal-9 exposure, spleen cells were collected at day 10 pi and exposed in vitro for 5 hrs to a range of concentrations of Gal-9. Subsequently, the cells were analyzed by FACS for changes in the expression levels of Tim-3 and annexin V, the latter indicative of apoptosis (12). As shown in Fig (3.2A), approximately 16-17% of CD8⁺T cells were Tim-3⁺ at the onset of culture and this percentage did not change significantly in the absence of Gal-9 (Fig 3.2A). However, Gal-9 addition (at 1.0 μ M) caused a loss of almost all cells that were Tim-3⁺ (Fig 3.2A). Baseline levels of annexin V⁺ cells also did not change significantly in the absence of Gal-9 (or in the presence of Gal-3, data not shown). However, when optimal amounts of Gal-9 were present, annexin V⁺ cells

increased 15-20% beyond baseline numbers (Fig 3.2A lower right quadrant). This number roughly correlated with the fraction of Tim-3⁺CD8⁺T cells that disappeared upon Gal-9 exposure.

In additional experiments, we measured the effects of Gal-9 addition on the fate of NPtet⁺CD8⁺T cells, the majority of which, as described previously, were Tim-3⁺. As shown in Fig 3.2B, the great majority of NPtet⁺ CD8⁺T cells were lost after Gal-9 exposure and there was a notable increase in annexin V⁺T cells (Fig 3.2B lower right quadrant). In other experiments with Gal-9 treated cultures, we investigated the effects of adding an excess of α-lactose, the sugar that binds to the carbohydrate binding domain of Gal-9 and reduces Gal-9 binding to Tim-3 (3, 38). In such experiments, lactose addition served to prevent the disappearance of most Tim-3⁺ (Fig 3.2A) as well as NPtet⁺CD8⁺T (Fig 3.2B) cells and also reduced the increase in annexin V⁺ cells. Taken together, our results imply that Gal-9 binding to Tim-3⁺ effectors can cause them to die by apoptosis.

The major effect of Gal-9 was observed in Tim-3⁺ cells and was dose dependent. However there was a low level of apoptosis of Tim-3⁻ cells consistent with recent reports that Gal-9 could regulate T cell function independently of Tim-3 (30). Our *ex-vivo* results indicate that Gal-9 binding to Tim-3⁺ effectors causes them to die by apoptosis *in-vitro*, an effect that might similarly occur *in vivo*.

Animals unable to produce Gal-9 mount better acute phase virus-specific CD8 T cell responses

We reasoned that if the presence of endogenous Gal-9 acts to limit the magnitude of CD8 T cell responses in the WT animals, then mice unable to

produce Gal-9 due to gene knockout (G9KO), should respond better than WT animals to IAV. To analyze this possibility, WT and G9KO animals were infected intranasally with 5000 EID₅₀ of IAV (x31) and the magnitude of CD8 T cell responses were compared 6, 8 and 10 days later. As shown, the responses of virus-specific CD8 T cells in both BAL and spleen, as measured by tetramers (3.3A-E) and ICCS (3.3H-J) were significantly higher at multiple time points in the G9KO mice. In both WT and G9KO animals up to 70-73% IFN γ ⁺ CD8 T cells were Tim-3⁺ (3.3I). However, a higher proportion of Tim-3⁺ and NPtet⁺ T cells in G9KO were CD44^{hi} (3.3K and L) and CD62L^{lo} (3.3M and N) indicating that more virus specific CD8 T cells in G9KO animals expressed the activation phenotype. We also evaluated and compared the mean fluorescence intensity (MFI) of IFN γ and co-expression of multiple cytokines, both indicative of high quality T cells (26). G9KO animals expressed significantly higher MFI of IFN γ as compared to WT animals (3.3F). Collectively our data indicates that G9KO animals have a 2.5-3.5 fold augmented IAV specific CD8 T cell responses that have a higher proportion of CD8 T cells with properties of high quality.

ICCS was also performed on the BAL fluid cells using NP₃₁₁₋₃₂₅ peptide stimulation (to detect IAV specific CD4 T cells) at day 10p.i. G9KO mice had 2-3 fold higher frequencies of IFN γ ⁺CD4 T (IAV specific CD4 T) cells in the BAL as compared to the WT (3.3H). Additionally, around 39-40% of CD4 T cells were Tim-3⁺ at day 10 p.i. in the BAL of G9KO (3.3G) compared to only 18-20% in the WT mice. It is conceivable that better CD4 T cell responses of G9KO mice play a

role in maintaining higher CD8 T cell responses and also provides help for antibody (Ab) responses (33). Additionally, compared to WT mice, G9KO animals had fewer Tregs both in the BAL (Fig3.10 A, B and C) and spleen (Fig3.10 D) particularly that were CD103⁺ and Tim-3⁺ (Fig3.10 E and F).

Gal-9 knockout mice generate a more rapid IAV-specific humoral response

WT and G9KO mice were also compared for their serum virus-specific Ab responses. Serum levels of virus-specific IgM and IgG were substantially higher in G9KO compared with WT mice on day 7 (Fig 3.4 A and B), indicating a markedly more rapid Ab response in the G9KO mice. IgG levels remained significantly higher in G9KO mice for at least 2 wk after infection. The strong early Ab response in G9KO mice reflected enhanced production of both the IgG1 and IgG2c isotypes, but by day 14 only IgG2c remained significantly higher in G9KO mice (Fig 3.4 C and D). To gain further insights into the B cell response, Ab-secreting cells (Fig 3.4 J and K) and germinal center B cells (Fig 3.4 L and M) in the draining lymph node on day 8 after infection were identified by flow cytometry. The proportion of cells with the B220^{int} CD138⁺ phenotype of Ab-secreting cells was significantly higher in G9KO mice, consistent with the higher level of circulating virus-specific Ab early in the response. Interestingly, the proportion of PNA⁺ FAS⁺ germinal center B cells was significantly higher in WT mice, raising the possibility that strong early Ab-secreting cell formation in G9KO mice was at the expense of entry of activated B cells into germinal center reactions.

Virus-specific Ab levels were measured in the BAL to evaluate the IgA response as well as Ab-mediated antiviral activity at the site of viral replication. There was a trend towards higher BAL levels of IgG and IgA in G9KO compared with WT mice on day 10, but differences were not quite significant (Fig 3.4 E and F). An analysis of virus-specific serum Ab levels in G9KO and WT mice on day 8 after IAV PR8 infection demonstrated a much earlier response in the G9KO mice (Fig 3.4 G and H), consistent with the result after x31 infection.

Diminished viral titers and enhanced viral clearance in Gal-9 knockout mice

To evaluate if G9KO and WT mice differed in their effectiveness at clearing viral infection, animals were infected with 5000 EID₅₀ of IAV (x31) intranasally and the lungs from the infected WT and G9KO mice (n=3 per group at each time point) were collected at days 2,4,7,8 and 9 p.i. to quantify IAV. Viral levels were similar in early lung homogenate samples but by day 7p.i. levels in G9KO mice were significantly ($p<0.05$) decreased compared to WT (Fig 3.4 I). G9KO mice cleared virus by day 8 p.i., but WT animals still possessed virus 9 days p.i. The results of viral clearance experiments clearly indicated that G9KO animals had more effective protective immunity to IAV. Susceptibility of G9KO mice to IAV HKx31 was also compared with WT mice by three different approaches: body weight loss (Fig 3.7), neutrophil infiltration (Fig 3.8), and lung histopathology (Fig 3.9). Our data indicate that G9KO showed greater weight loss and significantly increased CD11b⁺Ly6G⁺ neutrophil infiltration at day 3p.i in the BAL following IAV infection. By histopathology no differences were observed at the lower viral doses, but at 5×10^7 EID₅₀ multifocal type II pneumocytic

hyperplasia was observable in at least 50% of the G9KO mice.

Gal-9 knockout mice develop more robust recall responses to IAV infection

To compare recall response to IAV, animals were primed with x31 then challenged intranasally 41 days later with the heterologous IAV strain PR8. The NPtet⁺ CD8 T cell responses were around 4-5 fold higher in the G9KO as compared to WT animals in the BAL (Fig 3.5 A and D) and spleen (Fig 3.5 E, H and I). Additionally G9KO mice had a 4 fold greater proportion of NPtet⁺ cells that were Tim-3⁺ in the BAL (Fig 3.5C) and spleen (Fig 3.5G). More interestingly, when primary and secondary responses were compared, WT mice expressed 2-3 fold higher frequencies of NPtet⁺ CD8 T cells compared to the primary response, while in G9KO mice the NPtet⁺ T cell frequencies were enhanced 8 fold. Furthermore a significantly higher proportion of NPtet⁺ CD8 T cells were CD62L^{lo} (5 fold higher) in BAL (Fig 3.5B) and (9 fold higher) in the spleens (Fig 3.5F) of G9KO animals. Using the ICCS assay IFN γ ⁺TNF α ⁺ CD8 T cells in BAL (3.5 J and K) and spleen (Fig 3.5L) in G9KO mice were increased over WT indicative of larger and higher quality responses. The significantly higher proportion of CD62L^{lo} and Tim-3⁺ IAV NP tetramer specific CD8 T cells in the G9KO mice that followed secondary infection suggests that a greater proportion of these cells were in an activated state in G9KO mice during recall responses. In an attempt to address the issue of whether G9KO CD8 T cells were intrinsically more responsive or being less inhibited in G9KO environment, adoptive transfer experiments were conducted (Fig 3.11A). The accumulation of WT D^bNPtet⁺ donor Thy1.1⁺ CD8 T cells was significantly greater in G9KO than WT recipient

animals (Fig 3.11 G and H) indicating that Gal9/Tim-3 signaling is responsible for the observed T cell phenotype. The reverse experiment, where WT or G9KO cells were transferred to WT animals resulted in no observed differences in expansion. Taken together our results suggest that the Tim-3/Gal-9 interaction acts in normal animals to limit the magnitude and efficiency of recall CD8 T cell responses.

In vivo blockade of Tim-3 pathway results in augmented primary IAV specific CD8 T cell responses

Our results indicated that Gal-9 may be playing a role *in vivo* to limit the extent of anti-viral CD8 T cell responses. To further evaluate the regulatory effect of Tim-3/Gal-9 interaction, this pathway was inhibited *in vivo* with a Tim-3 fusion protein (Tim-3 Ig). Using tetramers and the ICCS assay to record virus specific CD8 T cell responses in the BAL and spleen, Tim-3 blockade resulted in approximately 1.6 to 2 fold higher frequencies and 4 fold higher absolute numbers of NPtet⁺ and IFN γ ⁺TNF α ⁺ CD8 T cells in BAL (Fig 3.6 A and B) and spleen (Fig 3.6E) at day 10 p.i. The blockade also resulted in better viral control (Fig 3.6C). Additionally a higher proportion of virus specific CD8 T cells were CD62L^{lo} both in the BAL (Fig 3.6D) and spleen of Tim-3Ig treated mice (Fig 3.6F). A similar phenotype was observed when the Tim-3 fusion protein administration was begun at day 4p.i. (data not shown).

Discussion

The host response to pathogens is usually tuned to effect immunity and to minimize any bystander tissue damage resulting from the immune reaction to the invader (24). Tissue damage is limited by several counter inflammatory events that act to functionally inhibit or destroy damaging cells as occurs when Gal-9 binds to one of its receptors, Tim-3 (38). Counter inflammatory event benefit the host in some chronic inflammatory processes (13, 14), autoimmunity and some viral immunopathological lesions (28, 38) but, as we demonstrate in this report, Tim-3/Gal-9 interactions can also act to limit the effectiveness of immunity to acute infectious agents, such as influenza virus. Accordingly, we show that mice lacking the ability to produce Gal-9 because of gene knockout generate more robust anti-viral T cell responses, more rapid antibody responses and control intranasal infection more effectively than WT animals. The more effective responses to IAV by G9KO animals was explained by the observation that virus specific CD8 and CD4 T cells up regulate Tim-3 early after infection, making them susceptible to apoptosis upon binding to Gal-9, as we demonstrated in *ex vivo* studies. G9KO animals also developed better recall responses to IAV and generated superior CD8 T cell responses compared to WT upon heterologous IAV infection. Our results could mean that manipulating signals that are usually provided by Gal-9 could result in improved responses to influenza vaccines.

Our data indicate that decreased cellular responses observed in WT animals were likely the consequence of the elevated endogenous production of Gal-9 that occurred after infection, along with the fact that most of the responder T cells, both CD8 and CD4, up-regulated the Tim-3 receptor. This scenario would

set the scene for T cell apoptosis as demonstrated by our ex-vivo studies. However, alternative events might also explain the better responses of G9KO animals compared to WT. For example, G9KO animals have lower numbers of FoxP3 Tregs compared to WT. Such cells could be responsible for suppressing the magnitude of influenza specific T cell responses as some have reported (8), at least as a minor effect. In addition to the observance of 2-3 fold higher responses in G9KO animals, on the basis of multi-cytokine production and the levels of cytokine produced by antigen stimulated CD8 T cells (26), the responses in G9KO mice were also of higher quality than were those in WT mice. This may mean that the levels of Tim-3 differ between responding T cells accounting for differential susceptibility to Gal-9 mediated killing or inhibition. However, such effects were not formally investigated.

Whereas a number of previous studies reported the modulating effects of Tim-3/Gal-9 on T cell-mediated lesions and immunity, few if any have analyzed the influence on Ab responses. We show that the early production of virus-specific antibody responses to influenza infection was strikingly enhanced in the absence of Gal-9. Since we could not demonstrate Tim-3 expression on B cells, their destruction as a consequence by Gal-9 binding would seem an unlikely mechanism. A better explanation may be that the enhanced responses of G9KO animals reflected the absence of modulating effects of Gal-9 on Tim-3 expressing helper CD4 T cells. Antibody responses to influenza virus are largely T cell dependent (25). Thus, accelerated B cell help due to an increase in the availability or effectiveness of CD4 T cells could explain the stronger early

antibody responses observed in G9KO mice (18, 19). We did not evaluate CD4 T cell activation in lymph nodes draining the respiratory tract where cognate help for early B cell responses is delivered. However, Gal-9 deficiency resulted in higher frequencies of virus-specific CD4 T cells in the airways after influenza infection, consistent with a more vigorous CD4 T cell response in the draining lymph nodes. The rapidity of the B cell response in G9KO mice suggests an increase in antibody-secreting cell generation via the extrafollicular pathway of B cell differentiation, an arm of the B cell response that is enhanced by increased availability of T cell help (23). The expression of Tim-3 by activated Th1, but not Th2, cells suggests that the Th1 response may be preferentially enhanced in G9KO mice. This could fit with the pattern of isotype expression in the antibody response of G9KO mice, since enhanced IgG2c production (driven by Th1-type cytokines) was sustained for longer than was IgG1 production (driven by Th2-type cytokines). We also observed that the frequency of germinal center B cells was significantly lower in G9KO than in WT mice likely reflecting differentiation of activated B cells via the extrafollicular pathway at the expense of germinal center formation in G9KO mice. At this time, we cannot exclude other mechanisms that may also contribute to the enhanced Ab response in G9KO mice. For instance Gal-9 deficiency may limit other mechanisms of suppression (5), resulting in increased levels of factors that act directly on B cells to promote their activation (4).

Antiviral antibody production in response to influenza infection contributes in large part to viral control (37). We analyzed virus-specific antibody levels in the

airways as a measure of antibody-mediated antiviral activity at the site of viral replication. This strategy also permitted an evaluation of the effect of Gal-9 deficiency on the virus-specific IgA response, since IgA-secreting cells generated in lymphoid tissues rapidly home to the respiratory tract submucosa and secrete IgA that is transported to the airway lumen (10, 25). IgG that is recovered from the airways is thought to be primarily derived from circulating antibody by transudation (21). The levels of virus-specific IgG and IgA recovered from the airways on day 10 after infection were generally higher in G9KO compared with WT mice, but differences were not quite statistically significant. However, the overall kinetic pattern suggested earlier production of both IgG and IgA in G9KO mice and a contribution of these antibodies to antiviral activity in the lung during the phase of viral clearance. A strong IgA response in G9KO mice, as for the IgG response, may reflect a more vigorous and sustained CD4 T cell response (25). However, this mechanism must be weighed against evidence that strong Th1 responses and IFN γ production, as might be expected in G9KO mice, are antagonistic to IgA production (2, 6, 36). Further studies are required to clarify this situation.

LIST OF REFERENCES

1. **Belkaid, Y., and B. T. Rouse.** 2005. Natural regulatory T cells in infectious disease. *Nat Immunol* **6**:353-360.
2. **Cerutti, A.** 2008. The regulation of IgA class switching. *Nat Rev Immunol* **8**:421-434.
3. **Chabot, S., Y. Kashio, M. Seki, Y. Shirato, K. Nakamura, N. Nishi, T. Nakamura, R. Matsumoto, and M. Hirashima.** 2002. Regulation of galectin-9 expression and release in Jurkat T cell line cells. *Glycobiology* **12**:111-118.
4. **Chang, W. L., E. S. Coro, F. C. Rau, Y. Xiao, D. J. Erle, and N. Baumgarth.** 2007. Influenza virus infection causes global respiratory tract B cell response modulation via innate immune signals. *J Immunol* **178**:1457-1467.
5. **Dardalhon, V., A. C. Anderson, J. Karman, L. Apetoh, R. Chandwaskar, D. H. Lee, M. Cornejo, N. Nishi, A. Yamauchi, F. J. Quintana, R. A. Sobel, M. Hirashima, and V. K. Kuchroo.** 2010. Tim-3/galectin-9 pathway: regulation of Th1 immunity through promotion of CD11b+Ly-6G+ myeloid cells. *J Immunol* **185**:1383-1392.
6. **Gajewski, T. F., and F. W. Fitch.** 1988. Anti-proliferative effect of IFN-gamma in immune regulation. I. IFN-gamma inhibits the proliferation of Th2 but not Th1 murine helper T lymphocyte clones. *J Immunol* **140**:4245-4252.
7. **Golden-Mason, L., B. E. Palmer, N. Kassam, L. Townshend-Bulson, S. Livingston, B. J. McMahon, N. Castelblanco, V. Kuchroo, D. R. Gretch, and H. R. Rosen.** 2009. Negative immune regulator Tim-3 is overexpressed on T cells in hepatitis C virus infection and its blockade rescues dysfunctional CD4+ and CD8+ T cells. *J Virol* **83**:9122-9130.
8. **Haeryfar, S. M., R. J. DiPaolo, D. C. Tschärke, J. R. Bennink, and J. W. Yewdell.** 2005. Regulatory T cells suppress CD8+ T cell responses induced by direct priming and cross-priming and moderate immunodominance disparities. *J Immunol* **174**:3344-3351.
9. **Jones, R. B., L. C. Ndhlovu, J. D. Barbour, P. M. Sheth, A. R. Jha, B. R. Long, J. C. Wong, M. Satkunarajah, M. Schwenker, J. M. Chapman, G. Gyenes, B. Vali, M. D. Hycza, F. Y. Yue, C. Kovacs, A. Sassi, M. Loutfy, R. Halpenny, D. Persad, G. Spotts, F. M. Hecht, T. W. Chun, J. M. McCune, R. Kaul, J. M. Rini, D. F. Nixon, and M. A. Ostrowski.** 2008. Tim-3 expression defines a novel population of dysfunctional T cells with highly elevated frequencies in progressive HIV-1 infection. *J Exp Med* **205**:2763-2779.
10. **Joo, H. M., Y. He, and M. Y. Sangster.** 2008. Broad dispersion and lung localization of virus-specific memory B cells induced by influenza pneumonia. *Proc Natl Acad Sci U S A* **105**:3485-3490.
11. **Joo, H. M., Y. He, A. Sundararajan, L. Huan, and M. Y. Sangster.** 2010. Quantitative analysis of influenza virus-specific B cell memory generated by different routes of inactivated virus vaccination. *Vaccine* **28**:2186-2194.
12. **Koopman, G., C. P. Reutelingsperger, G. A. Kuijten, R. M. Keehnen, S. T. Pals, and M. H. van Oers.** 1994. Annexin V for flow cytometric detection of

- phosphatidylserine expression on B cells undergoing apoptosis. *Blood* **84**:1415-1420.
13. **Kuchroo, V. K., V. Dardalhon, S. Xiao, and A. C. Anderson.** 2008. New roles for TIM family members in immune regulation. *Nat Rev Immunol* **8**:577-580.
 14. **Kuchroo, V. K., J. H. Meyers, D. T. Umetsu, and R. H. DeKruyff.** 2006. TIM family of genes in immunity and tolerance. *Adv Immunol* **91**:227-249.
 15. **Kumar, N., Z. T. Xin, Y. Liang, and H. Ly.** 2008. NF-kappaB signaling differentially regulates influenza virus RNA synthesis. *J Virol* **82**:9880-9889.
 16. **Kumaraguru, U., and B. T. Rouse.** 2000. Application of the intracellular gamma interferon assay to recalculate the potency of CD8(+) T-cell responses to herpes simplex virus. *J Virol* **74**:5709-5711.
 17. **La Gruta, N. L., W. T. Rothwell, T. Cukalac, N. G. Swan, S. A. Valkenburg, K. Kedzierska, P. G. Thomas, P. C. Doherty, and S. J. Turner.** 2010. Primary CTL response magnitude in mice is determined by the extent of naive T cell recruitment and subsequent clonal expansion. *J Clin Invest* **120**:1885-1894.
 18. **MacLeod, M. K., A. David, A. S. McKee, F. Crawford, J. W. Kappler, and P. Marrack.** 2011. Memory CD4 T cells that express CXCR5 provide accelerated help to B cells. *J Immunol* **186**:2889-2896.
 19. **Marshall, D., R. Sealy, M. Sangster, and C. Coleclough.** 1999. TH cells primed during influenza virus infection provide help for qualitatively distinct antibody responses to subsequent immunization. *J Immunol* **163**:4673-4682.
 20. **Nedrud, J. G., X. P. Liang, N. Hague, and M. E. Lamm.** 1987. Combined oral/nasal immunization protects mice from Sendai virus infection. *J Immunol* **139**:3484-3492.
 21. **Persson, C. G., J. S. Erjefält, L. Greiff, I. Erjefält, M. Korsgren, M. Linden, F. Sundler, M. Andersson, and C. Svensson.** 1998. Contribution of plasma-derived molecules to mucosal immune defence, disease and repair in the airways. *Scand J Immunol* **47**:302-313.
 22. **Rabinovich, G. A., and M. A. Toscano.** 2009. Turning 'sweet' on immunity: galectin-glycan interactions in immune tolerance and inflammation. *Nat Rev Immunol* **9**:338-352.
 23. **Rothaeusler, K., and N. Baumgarth.** 2010. B-cell fate decisions following influenza virus infection. *Eur J Immunol* **40**:366-377.
 24. **Rouse, B. T., and S. Sehrawat.** 2010. Immunity and immunopathology to viruses: what decides the outcome? *Nat Rev Immunol* **10**:514-526.
 25. **Sangster, M. Y., J. M. Riberdy, M. Gonzalez, D. J. Topham, N. Baumgarth, and P. C. Doherty.** 2003. An early CD4+ T cell-dependent immunoglobulin A response to influenza infection in the absence of key cognate T-B interactions. *J Exp Med* **198**:1011-1021.
 26. **Seder, R. A., P. A. Darrah, and M. Roederer.** 2008. T-cell quality in memory and protection: implications for vaccine design. *Nat Rev Immunol* **8**:247-258.
 27. **Sehrawat, S., P. B. Reddy, N. Rajasagi, A. Suryawanshi, M. Hirashima, and B. T. Rouse.** 2010. Galectin-9/TIM-3 interaction regulates virus-specific primary and memory CD8 T cell response. *PLoS Pathog* **6**:e1000882.

28. **Sehrawat, S., A. Suryawanshi, M. Hirashima, and B. T. Rouse.** 2009. Role of Tim-3/galectin-9 inhibitory interaction in viral-induced immunopathology: shifting the balance toward regulators. *J Immunol* **182**:3191-3201.
29. **Serhan, C. N., S. Krishnamoorthy, A. Recchiuti, and N. Chiang.** 2011. Novel anti-inflammatory - pro-resolving mediators and their receptors. *Curr Top Med Chem* **11**:629-647.
30. **Su, E. W., S. Bi, and L. P. Kane.** 2010. Galectin-9 Regulates T Helper Cell Function Independently of Tim-3. *Glycobiology*.
31. **Sun, J., R. Madan, C. L. Karp, and T. J. Braciale.** 2009. Effector T cells control lung inflammation during acute influenza virus infection by producing IL-10. *Nat Med* **15**:277-284.
32. **Suvas, S., U. Kumaraguru, C. D. Pack, S. Lee, and B. T. Rouse.** 2003. CD4+CD25+ T cells regulate virus-specific primary and memory CD8+ T cell responses. *J Exp Med* **198**:889-901.
33. **Swain, S. L., R. W. Dutton, and D. L. Woodland.** 2004. T cell responses to influenza virus infection: effector and memory cells. *Viral Immunol* **17**:197-209.
34. **Toka, F. N., S. Suvas, and B. T. Rouse.** 2004. CD4+ CD25+ T cells regulate vaccine-generated primary and memory CD8+ T-cell responses against herpes simplex virus type 1. *J Virol* **78**:13082-13089.
35. **Townsend, A. R., J. Bastin, K. Gould, and G. G. Brownlee.** 1986. Cytotoxic T lymphocytes recognize influenza haemagglutinin that lacks a signal sequence. *Nature* **324**:575-577.
36. **Ulloa, L., J. Doody, and J. Massagué.** 1999. Inhibition of transforming growth factor-beta/SMAD signalling by the interferon-gamma/STAT pathway. *Nature* **397**:710-713.
37. **Waffarn, E. E., and N. Baumgarth.** 2011. Protective B cell responses to flu--no fluke! *J Immunol* **186**:3823-3829.
38. **Zhu, C., A. C. Anderson, A. Schubart, H. Xiong, J. Imitola, S. J. Khoury, X. X. Zheng, T. B. Strom, and V. K. Kuchroo.** 2005. The Tim-3 ligand galectin-9 negatively regulates T helper type 1 immunity. *Nat Immunol* **6**:1245-1252.
39. **Zinkernagel, R. M.** 1996. Immunology taught by viruses. *Science* **271**:173-178.

APPENDIX

Figure 3.1 Tim-3 expression is up regulated on virus-specific CD8 T cells after IAV infection:

At different time points after infection, BAL and spleen cells (n=3) isolated at each time point were analyzed flow cytometrically for Tim-3 expression on IAV specific CD8 T cells. BAL samples from 3 mice were pooled. (A) Percentage of total CD8 T cells and NPtet⁺ CD8 T cells expressing Tim-3 in BAL is shown. (B) FACS plots showing Tim-3⁺IFN γ ⁺ CD8 T cells at day 10 p.i in the BAL fluid of WT animals. (C) Frequencies of Tim-3⁺ NPtet⁺ CD8 T cells in the BAL of IAV infected animals. (D) Co-expression of Tim-3 (upper panel) and D^bNPtet⁺ (lower panel) with CD44 and CD62L in BAL of WT mice at day 8 p.i. is shown by representative FACS plots. (E) Immunoblots showing Gal-9 expression in the lung homogenates from naïve and IAV infected mice at different time points post infection. (F) Gal-9 concentrations as measured by sandwich ELISA using anti-Gal-9 mAb in the lung homogenates is shown. (G) Histograms depict Tim-3 expression on CD4 T cells in WT and G9KO animals at day 10 p.i. in the BAL. (H) Representative FACS plots showing IFN γ ⁺ Tim-3⁺ CD4 T cells in BAL of WT and G9KO animals upon NP311–325 peptide stimulation. Numbers in the quadrants indicate percent of each subset. Data are representative of three independent experiments.

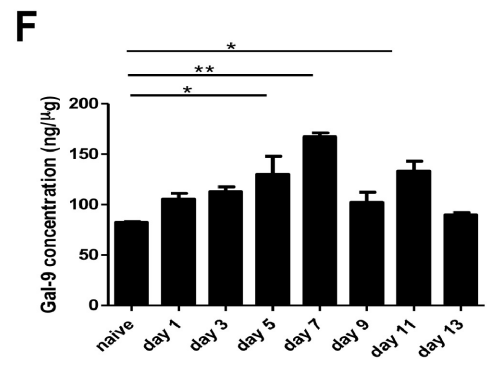
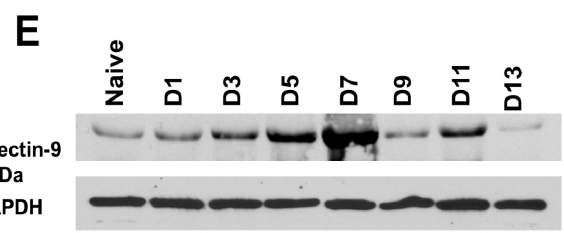
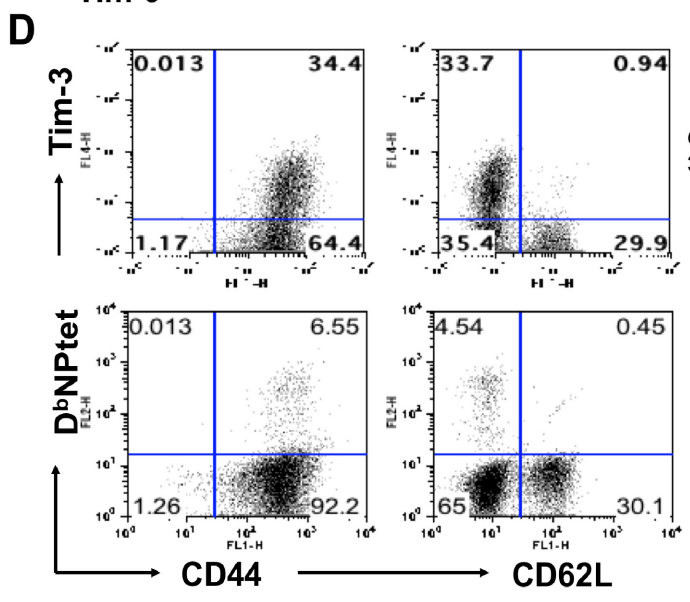
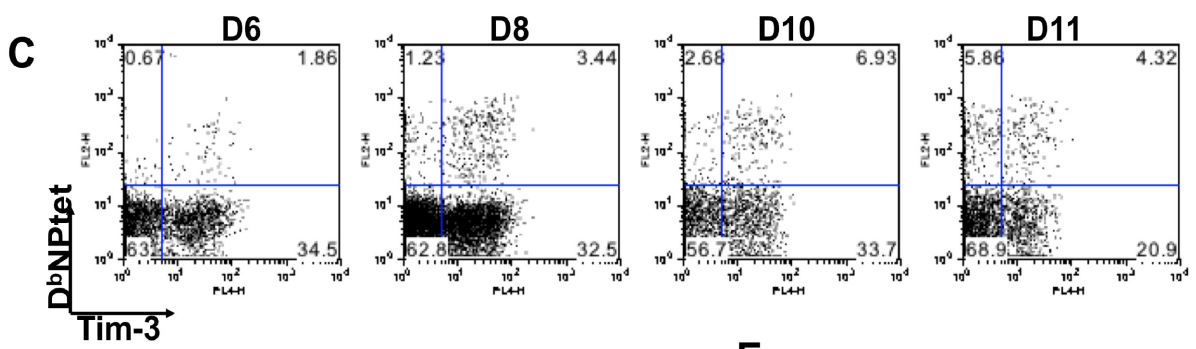
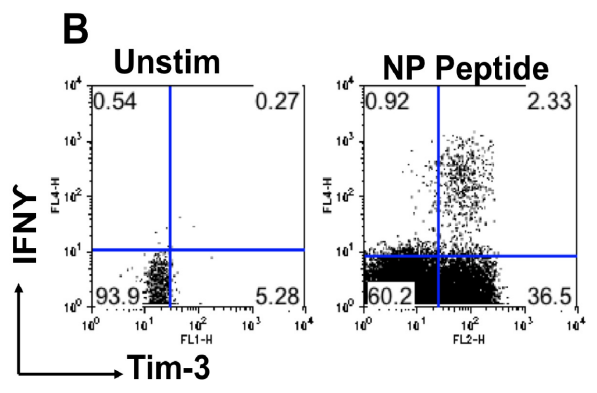
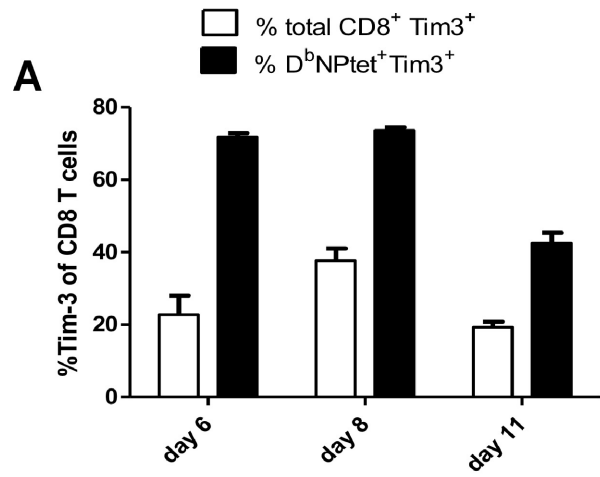
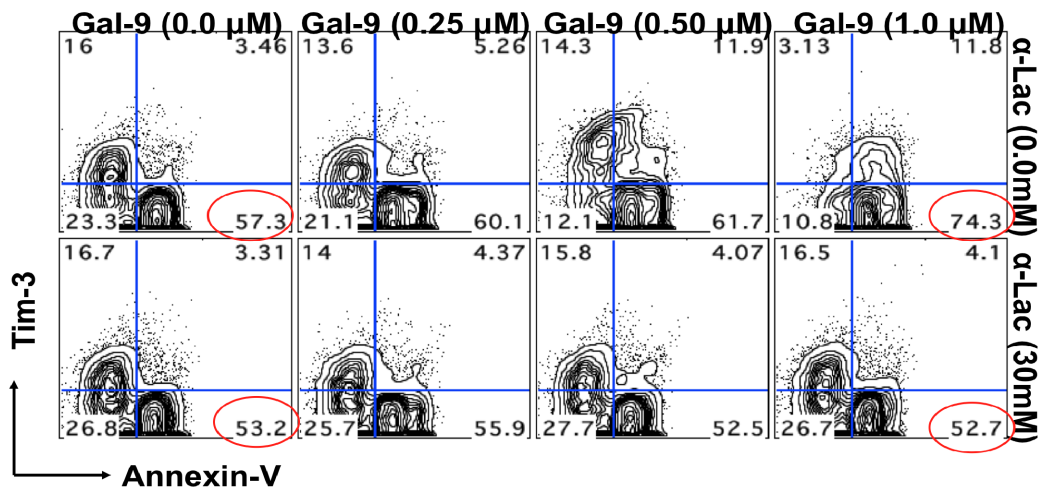


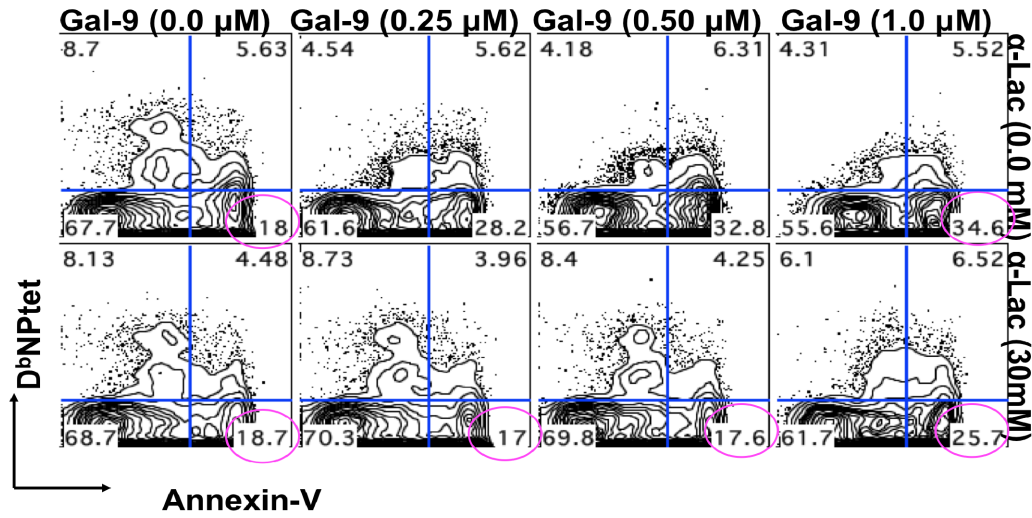
Figure 3.2 Galectin 9 induces apoptosis of IAV NP tetramer specific and Tim-3⁺ CD8 T cells in vitro:

Ex Vivo apoptosis assay was performed with Splenocytes isolated at 10 dpi from IAV infected animals as described previously (3). Briefly splenocytes were incubated for 5 hours with varying concentrations of galectin-9 in the absence or the presence of α -lactose. The experiments were repeated multiple times with similar results. (A) Representative FACS plots showing the expression of Tim-3 and annexin-V on gated CD8 T cells under indicated incubation conditions. (B) Representative FACS plots showing the expression of NPtet and annexin-V on gated CD8 T cells under indicated incubation conditions. (C) The bar diagram shows the percent of Tim-3⁺ CD8 T cells as calculated from A (with three triplicate wells). (D) The bar diagram shows the percentage of NPtet⁺ CD8 T cells as calculated from B. Statistical analysis was done by 2 way ANOVA with Bonferroni post hoc settings.

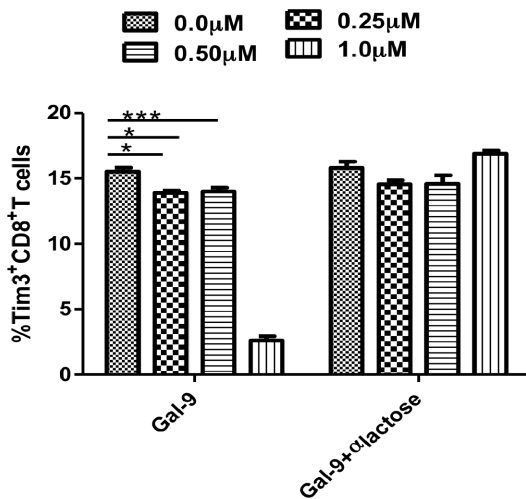
A



B



C



D

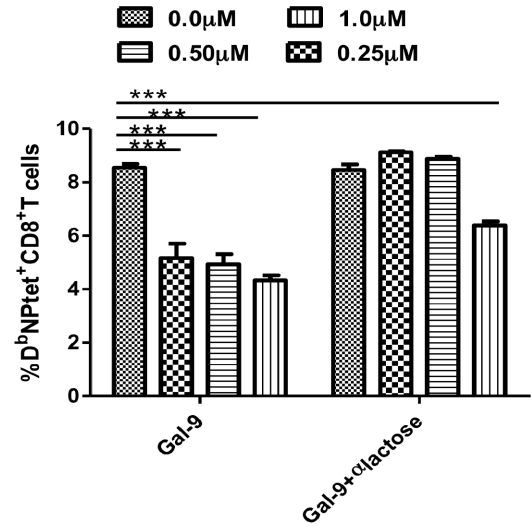


Figure 3.3 Gal-9 knockout animals mount stronger virus-specific CD8 T cell responses in the acute phase:

Virus-specific CD8 T cell responses were compared among age and gender matched IAV infected WT and G9KO animals at indicated time points post infection. Representative FACS plots showing NPtet⁺CD8 T cells from WT and G9KO animals in the BAL (A) and spleen (B). (C) Absolute numbers of NPtet⁺ and IFN γ ⁺TNF α ⁺ CD8 T cells at day 10 p.i. in BAL. Bar diagram shows the frequencies (D) and absolute numbers (E) of NPtet⁺ CD8 T cells in spleen. (F) The MFI of cytokine IFN γ produced by CD8 T cells in BAL. (G) Histograms showing Tim-3 expression on total BAL CD8 T cells in WT (light line) and G9KO mice (darker line) at day 10p.i. Representative FACS plots show the frequencies of Influenza A peptide NP₃₆₆₋₃₇₄ (ASNENMETM) stimulated polyfunctional (IFN γ ⁺TNF α ⁺) CD8 T cells isolated from the BAL (H, upper panel) and spleen (H, lower panel) at day 10 p.i. of WT and G9KO animals. (I) Tim-3 expression by IFN γ ⁺CD8 T cells in WT and G9KO animals at day 10 p.i following stimulation with NP₃₆₆₋₃₇₄ peptide. (J) Absolute numbers of Tim-3⁺, IFN γ ⁺, IFN γ ⁺TNF α ⁺ CD8 T cells in the spleen at indicated time points p.i. Co-expression of Tim-3 and NPtet⁺ with CD44 in BAL (K), spleen (L) and with CD62L in BAL (M) and spleen (N) at day 8 p.i. is shown in WT and G9KO animals by representative FACS plots. Data are representative of three independent experiments with 3 mice per group in each experiment. Error bars represent SEM.

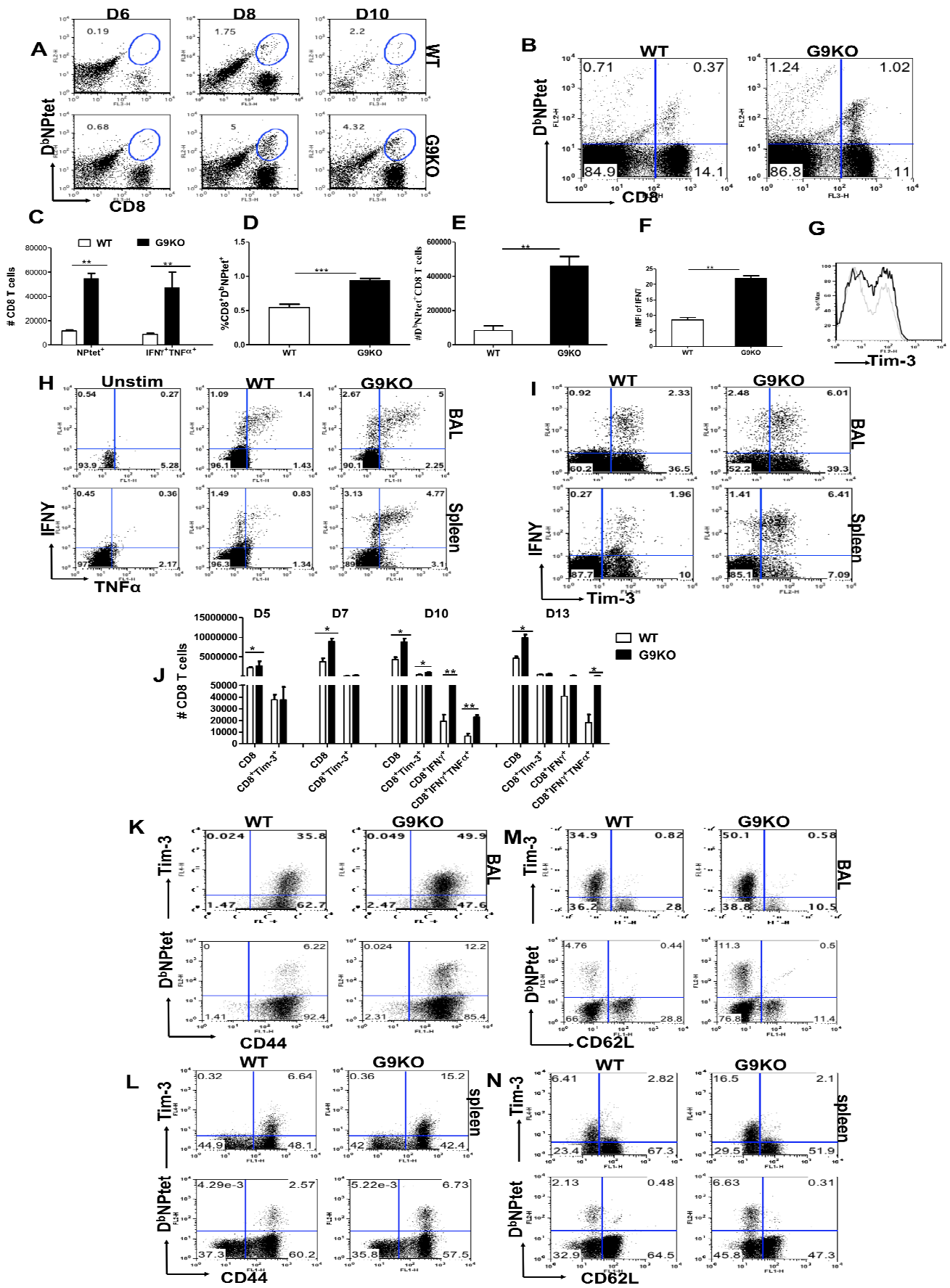


Figure 3.4 Enhanced virus-specific antibody production in G9KO mice after influenza infection.

(A-F) WT and G9KO mice were sampled on the indicated days after intranasal infection with influenza X31. Plasma levels of virus-specific IgM (A), IgG (B), IgG1 (C), and IgG2c (D), and BAL levels of virus-specific IgG (E) and IgA (F) were measured by ELISA. Titers are expressed as the reciprocal of the endpoint dilution and are shown as mean + SE for 6-8 individual mice in each group. (G, H) Plasma levels of virus-specific IgM (G) and IgG (H) on day 8 after intranasal infection with influenza PR8. The mean + SE is shown for 6-8 individual mice in each group. Arrows indicate values below the level of assay sensitivity. (I) On indicated days post infection, lungs from WT and G9KO mice were collected and assayed for influenza viral titer by viral plaque assay. Representative FACS plots (J) and bar graphs (K) depicting the frequencies of CD3⁻B220⁺CD138⁺ B cells in the MLN of WT and G9KO mice at D8 p.i. Representative FACS plots (L, upper panel= naïve; lower panel= day 8p.i) and bar graphs (M) showing CD3⁻B220⁺PNA⁺FAS⁺ germinal center B cells in the MLN of WT and G9KO mice.

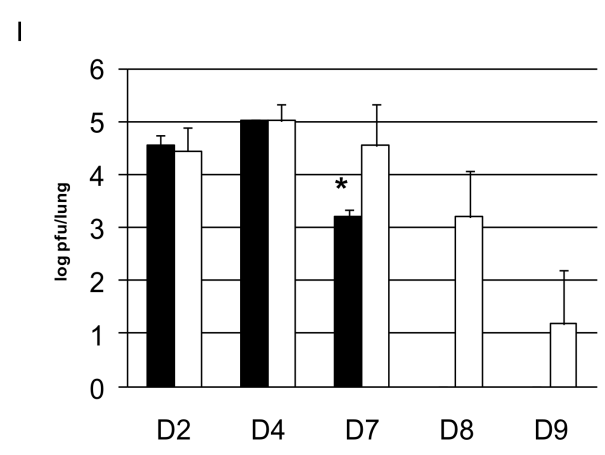
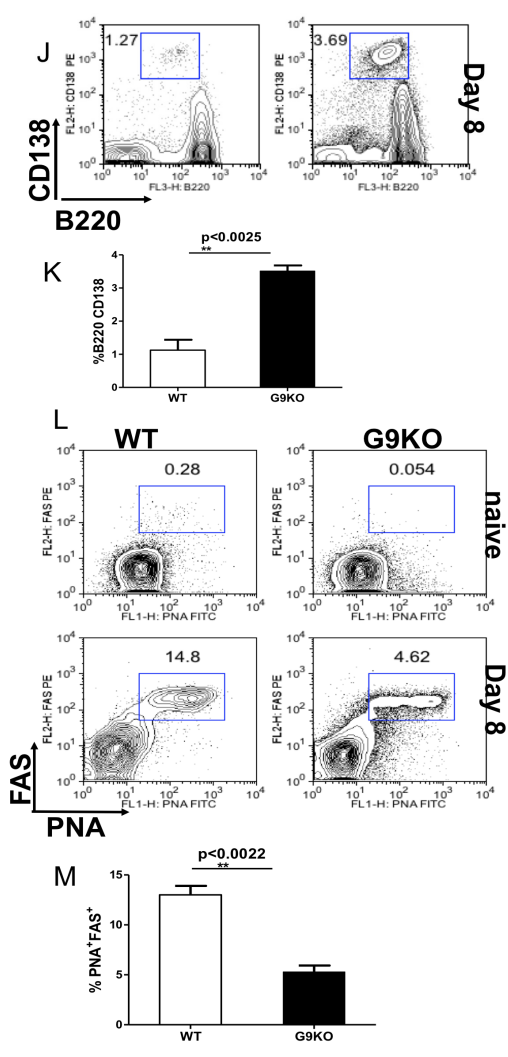
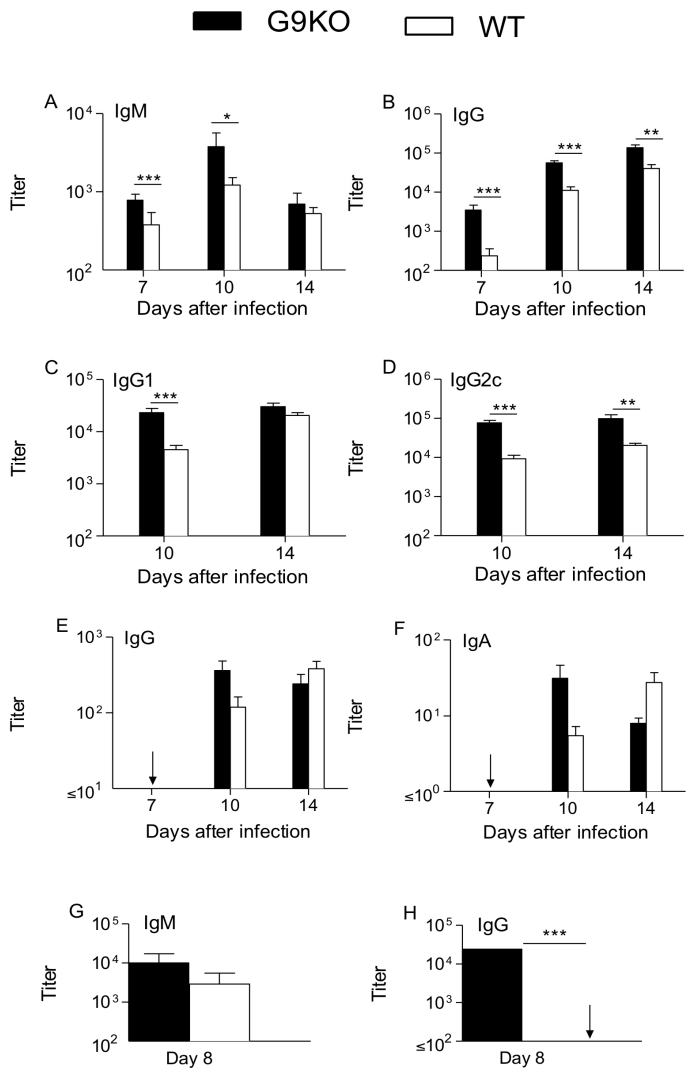


Figure 3.5 Gal-9 knockout mice develop more robust recall responses to influenza A virus upon heterologous challenge:

Both WT and Gal-9 KO animals primed 41 days previously with x31 were challenged intranasally with 8000 EID₅₀ of heterologous IAV (PR8) and the response in the BAL and spleen measured at day 8-post challenge by tetramers and ICCS assays. Representative FACS plots showing the frequencies of NPtet⁺ CD8 T cells in the x31 immune WT and G9KO animals in BAL (A) and spleen (E and H) respectively. Absolute numbers of NPtet⁺ CD8 T cells in BAL (D) and spleen (I). Co-expression of NPtet and CD62L in BAL (B) and spleen (F). Tim-3 expression on NPtet⁺ CD8 T cells isolated from BAL fluid (C) and spleen (G) of WT and G9KO animals. Representative FACS plots showing the frequencies (J) and absolute numbers (K) of IFN γ ⁺TNF α ⁺ CD8 T cells at day 8 post challenge in the BAL of x31 immune WT and G9KO animals. (L) Absolute numbers of IFN γ ⁺TNF α ⁺ CD8 T cells in the spleen of x31 immune WT and G9KO animals. Data are representative of three independent experiments. Error bars represent SEM.

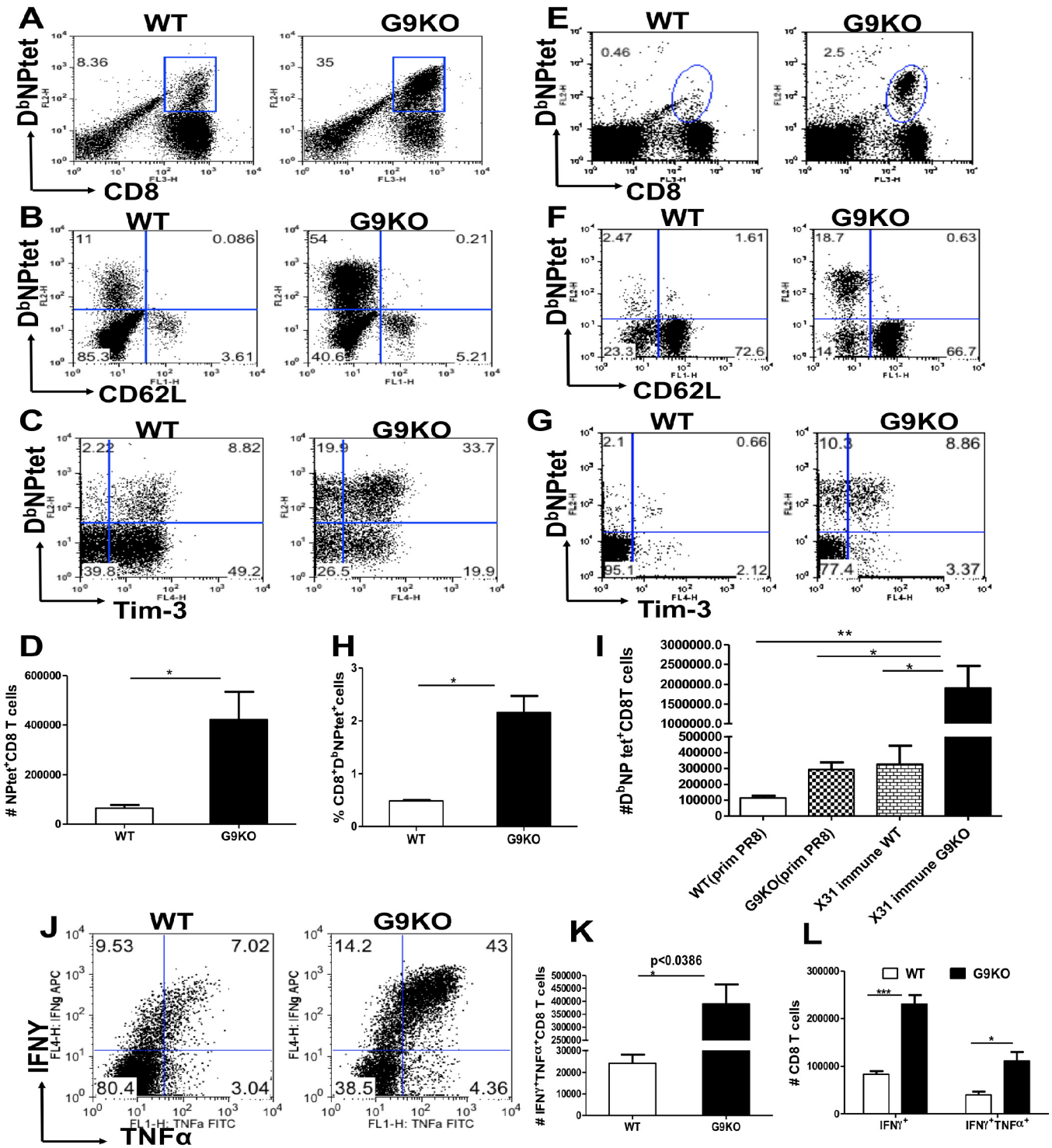
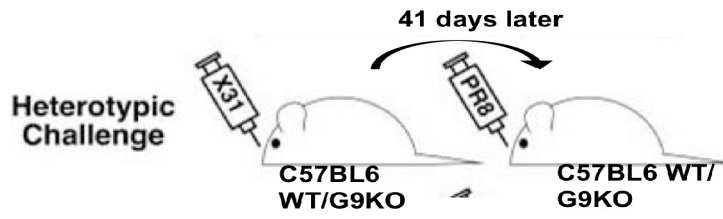


Figure 3.6 Administration of Tim-3 fusion protein in mice after IAV infection enhances the magnitude and quality of IAV-specific CD8 T cells responses.

IAV infected C57BL/6 animals were treated with 100 μ g of Tim-3 fusion protein per mice from day 1 post infection at alternate days until day 9 p.i. and those in the other group were given control Ig and animals were sacrificed at day 10 p.i. Percentages (A) and absolute numbers (B) of NPtet⁺ and IFN γ ⁺ TNF α ⁺ CD8 T cells isolated from the BAL of Tim-3 fusion protein treated and control animals are shown. (C) Viral titers in the lungs of control and Tim-3 Ig treated mice. (D and F) Co-expression of NPtet and CD62L on CD8 T cells in BAL and spleen respectively is shown. (E) Absolute numbers of NPtet⁺ CD8 T cells isolated from the spleen at day 10 p.i. Data are representative of three independent experiments with three to four mice per group. Error bars represent SEM.

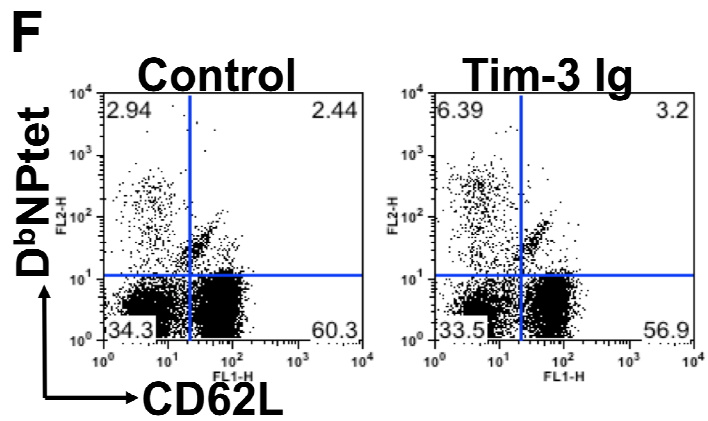
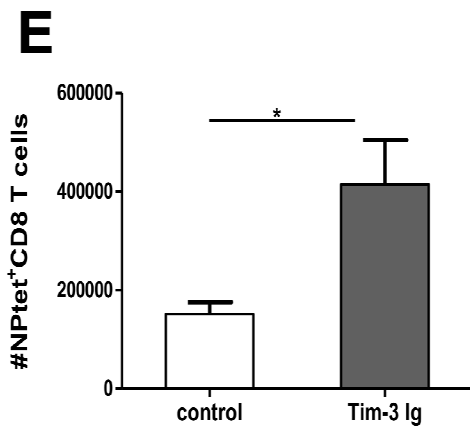
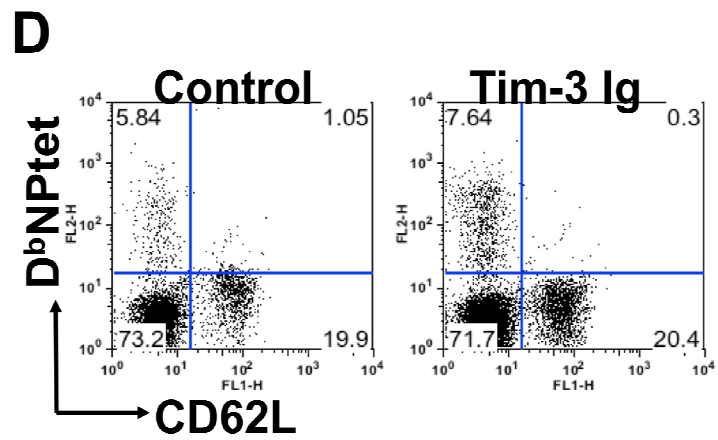
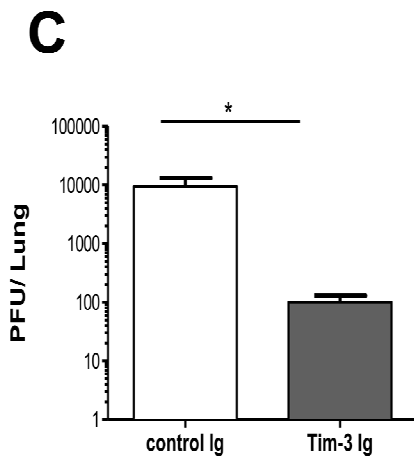
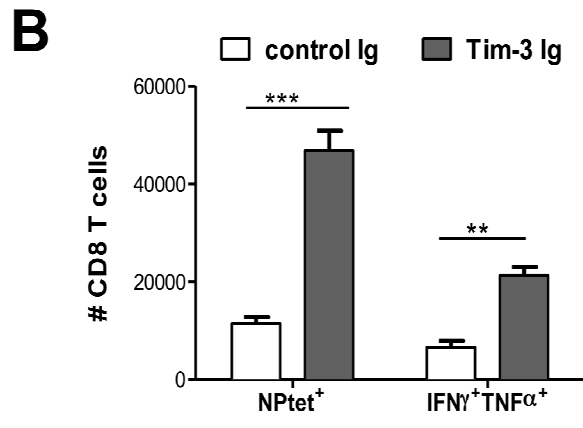
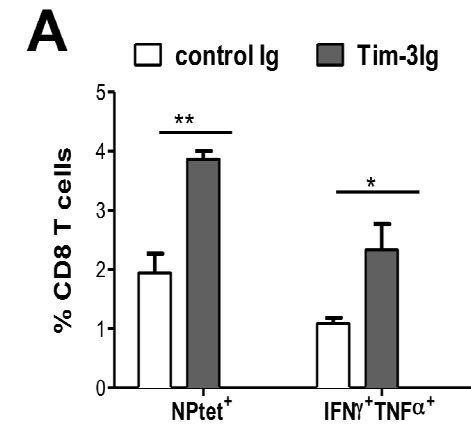


Figure 3. 7 Outcome of infection with IAV HKx31:

WT mice were inoculated with IAV HKx31 (10^8 , 10^7 , 10^6 , 10^5 , 10^4 EID₅₀ or PBS). (A) Body weight of WT mice after infection was determined daily and expressed as the percentage of the body weight lost following infection. (B) % body weight loss comparison between the WT and G9KO mice infected with 5000 EID₅₀ i/n. over a period of 10 days is shown. (C) % body weight loss comparison between the WT and G9KO mice infected with 5×10^7 EID₅₀ i/n. over a period of 10 days is shown. The data are representative of 5-6 mice per group.

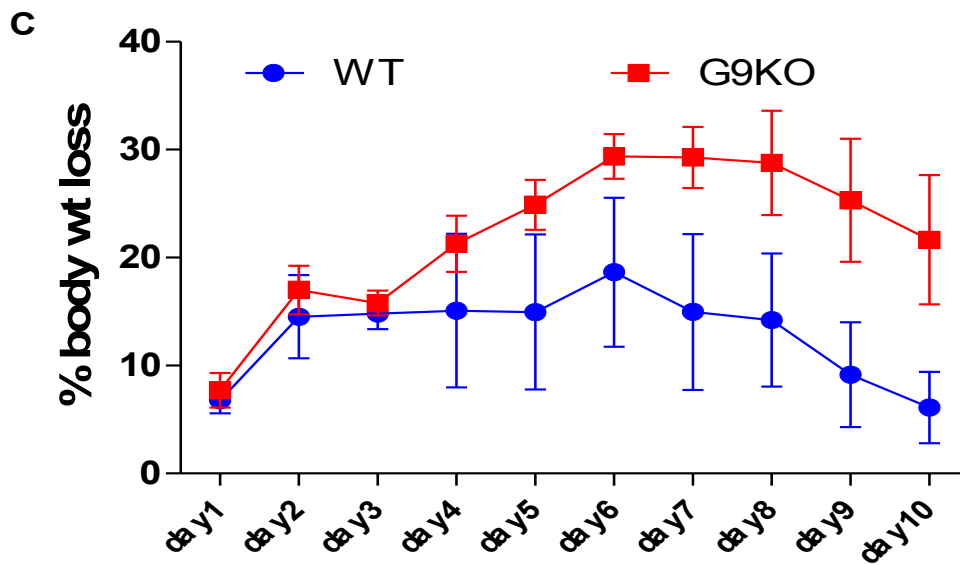
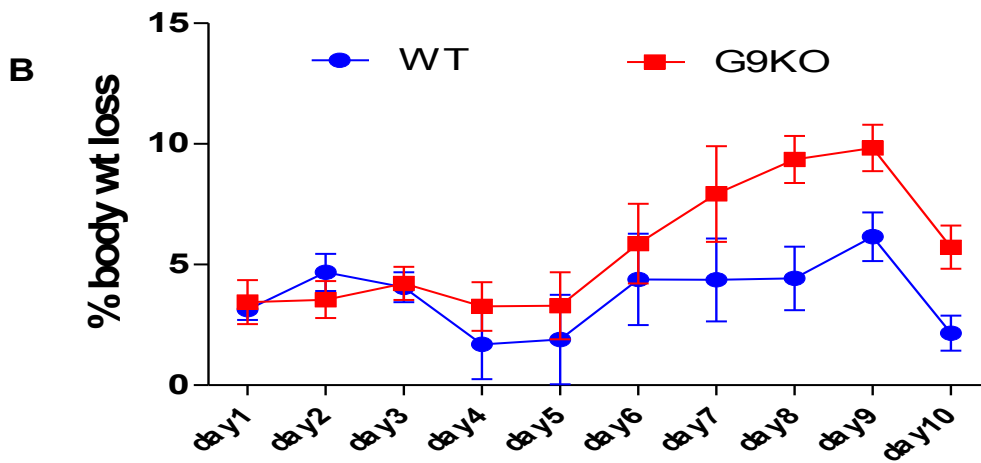
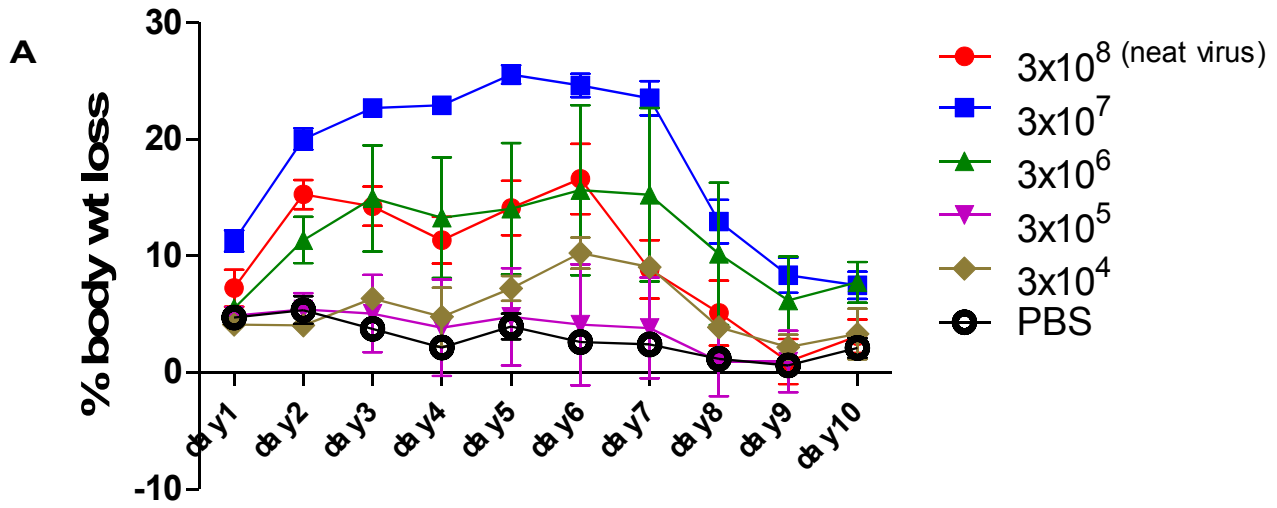


Figure 3.8 Cells obtained from broncho-alveolar lavage (BAL) were stained for CD45⁺ (pan leukocyte marker) and CD45⁺CD11b⁺Ly6G⁺ (neutrophils) and FACS analysis performed at day 3 (A and B) and day 7 (D and E) in WT and G9KO mice. Bar graphs representing % CD45⁺CD11b⁺Ly6G⁺ (neutrophils) at day 3p.i (C) and day 7p.i. (F) is shown. The experiments were repeated multiple times and the data are representative of pooled BAL samples from 3 mice. Statistical analysis was done by student's t test and the Error bars represent SEM.

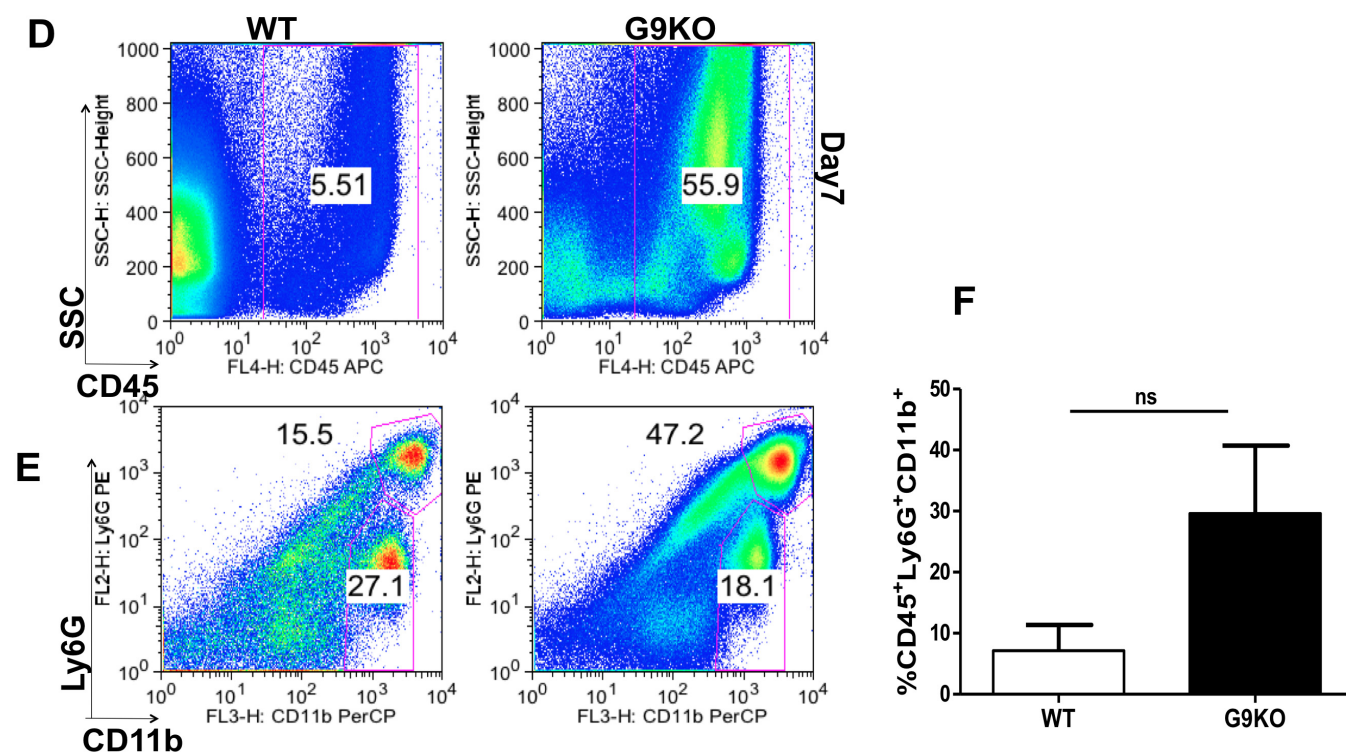
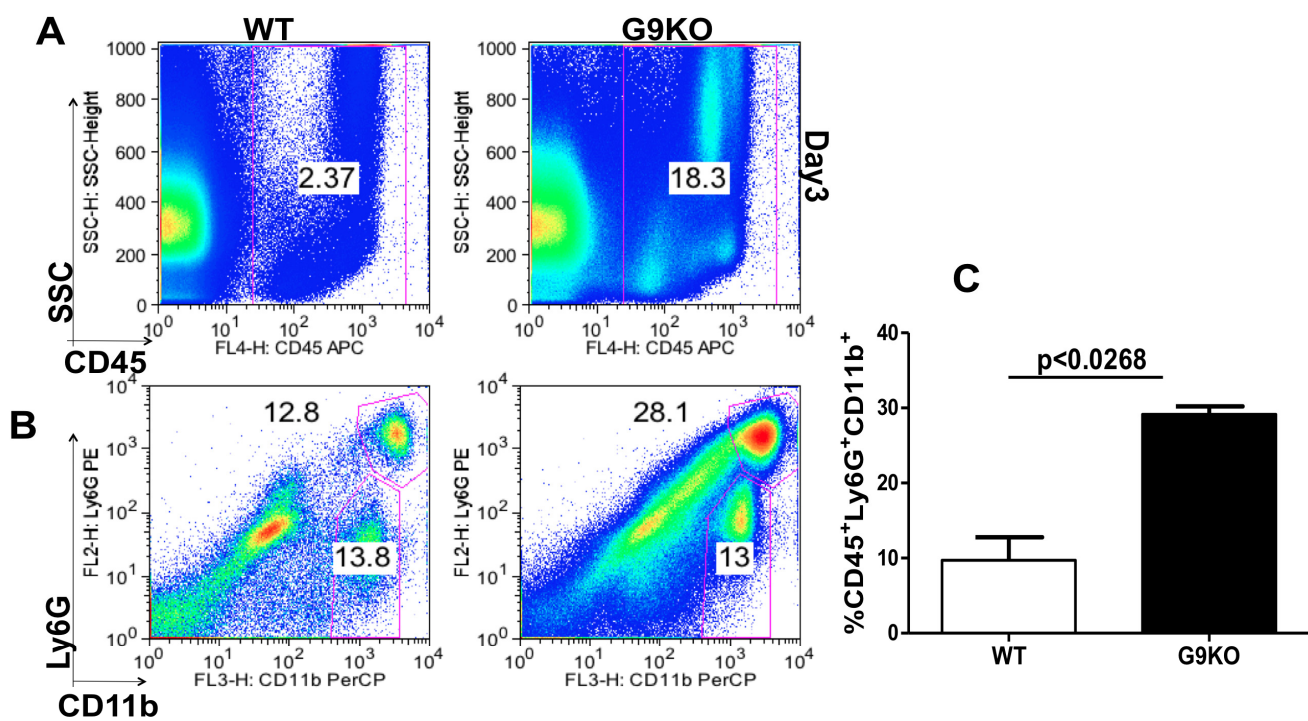
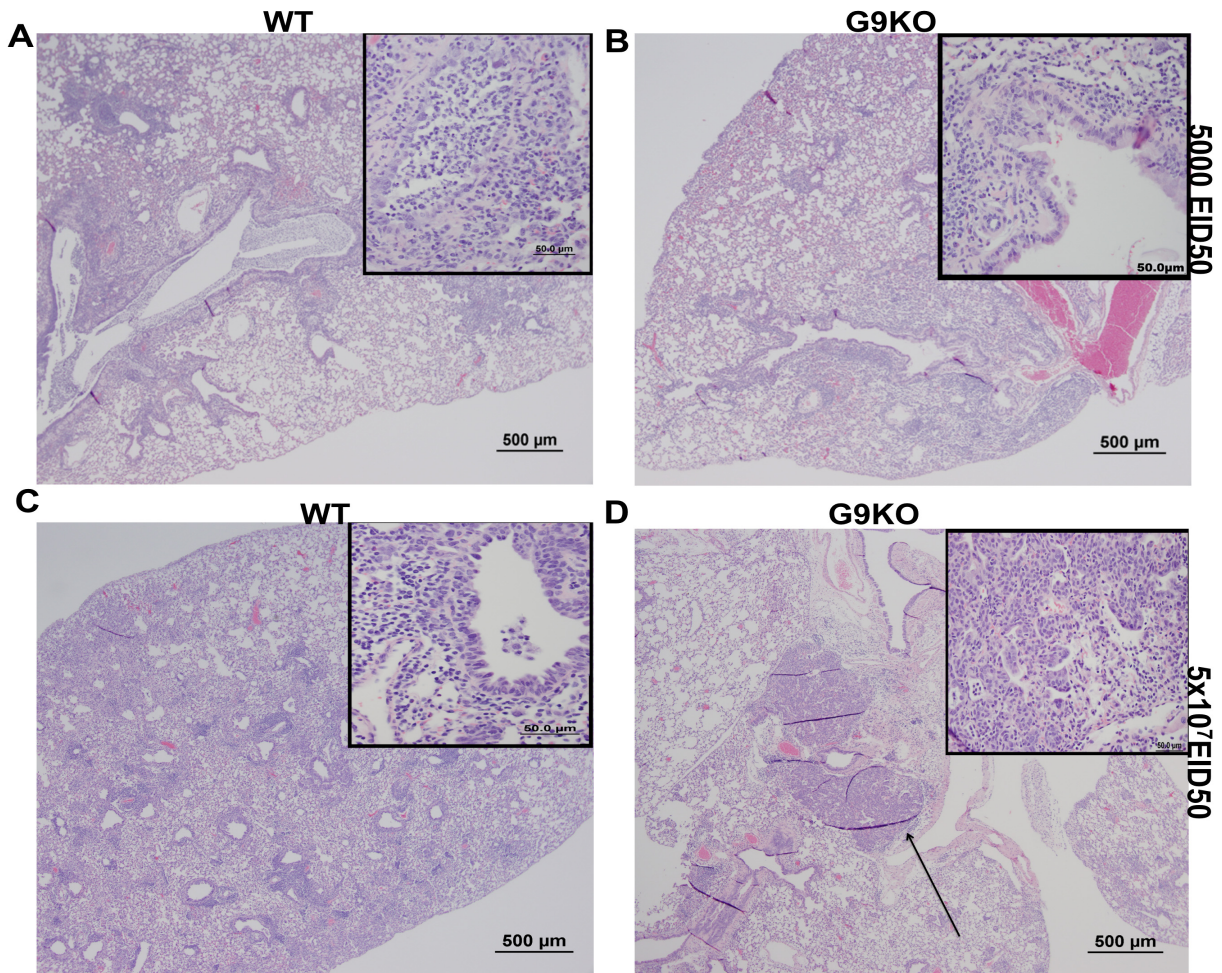


Figure 3.9 Lung histopathology: The lungs of mice infected with 5000 EID₅₀ of virus were harvested at indicated time points post infection, washed in PBS, fixed in 10% neutral buffered formalin and embedded in paraffin wax. Sections (5 mm) were stained with haematoxylin and eosin and microscopically reviewed. H&E sections from WT (A) and G9KO (B) animals infected with 5000EID₅₀ of IAV x31 at day 9 p.i is shown. Representative H&E sections from WT (C) and G9KO (D) animals infected with 5x10⁷EID₅₀ of IAV x31 at day 10 p.i is shown. The section blocks in the upper right corner represent the 40X magnification. The overall lung readouts (n=3 mice at each time points/group infected with x31 5000 EID₅₀) is indicated as table E.



E

		%Parenchyma involved	PMN# (Average/40x field)	Remarks
WT	Day 3	0%	0	Normal lung, no recognizable pathological changes
	Day 7	1-4	2-4	Mild multifocal broncho-interstitial pneumonia
	Day 9	21-30%	4-30	Moderate to marked multifocal broncho-interstitial pneumonia, primarily mononuclear lymphocytic infiltrates with lesser number of macrophages, scattered parenchymal/infiltrative individual cell necrosis and degeneration
G9KO	Day 3	4%	0-5	Mild, regionally limited, multifocal broncho-interstitial pneumonia
	Day 7	4-5%	5-7	Mild multifocal broncho-interstitial pneumonia
	Day 9	10-20%	2-50	Moderate multifocal broncho-interstitial pneumonia, primarily mononuclear lymphocytic infiltrates with lesser numbers of macrophages, occasional foci of intense neutrophilic infiltrates, moderate scattered parenchymal/infiltrative individual cell necrosis/apoptosis

Figure 3.10 Characterization of CD4⁺FoxP3⁺ regulatory T cells from WT and the G9KO mice:

C57BL/6 and G9KO animals were infected intra-nasally with 5000 EID₅₀. BAL samples from 3 mice were pooled and spleens from individual mice were stained for FoxP3. Representative FACS plots show the frequencies of FoxP3⁺ Tregs in the BAL (A) and spleens (D) of WT and G9KO animals at day 10 p.i. The kinetics of Treg frequencies at indicated time points p.i. (B) and their absolute numbers at day 10 p.i (C) in the BAL fluid of WT and G9KO is shown. Histograms showing the expression of Tim-3 (E) CD103 (F) and CD44 (WT-light line) and (G9KO-dark line) (G) on FoxP3⁺ Tregs isolated from the Spleens of WT and G9KO animals at day 10 p.i.

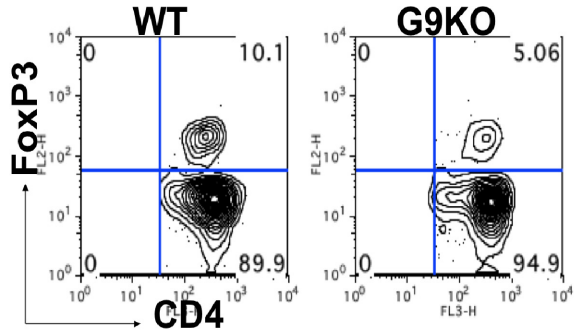
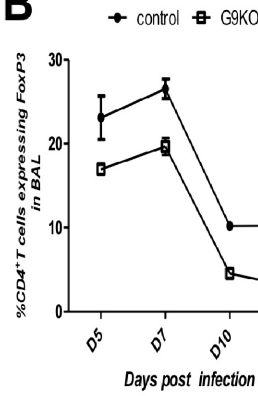
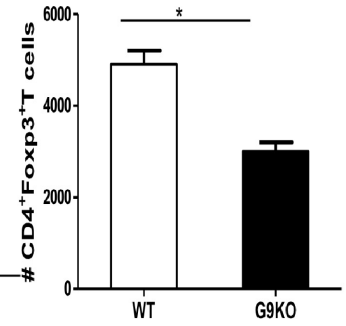
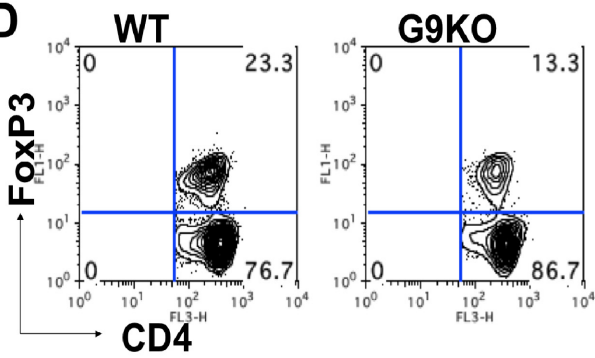
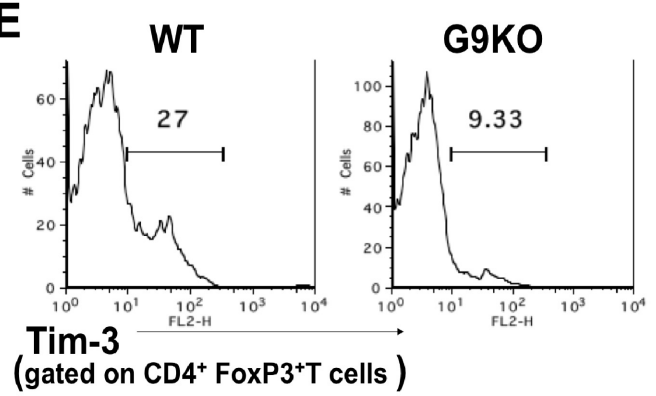
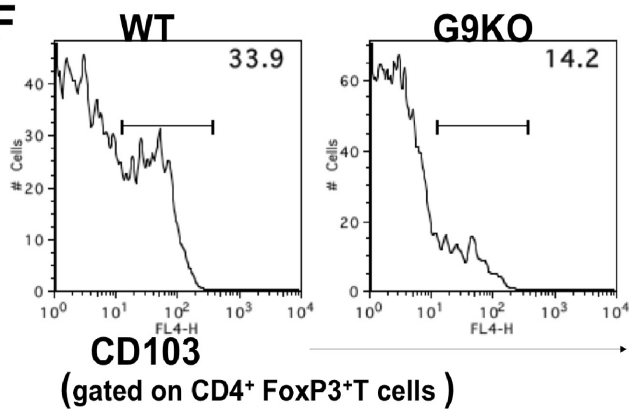
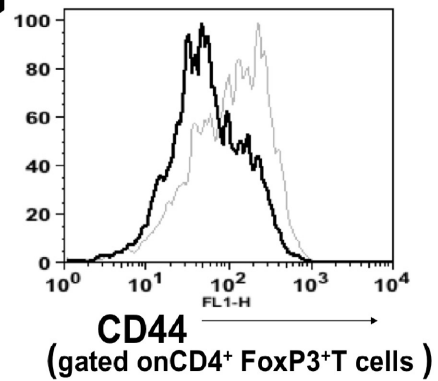
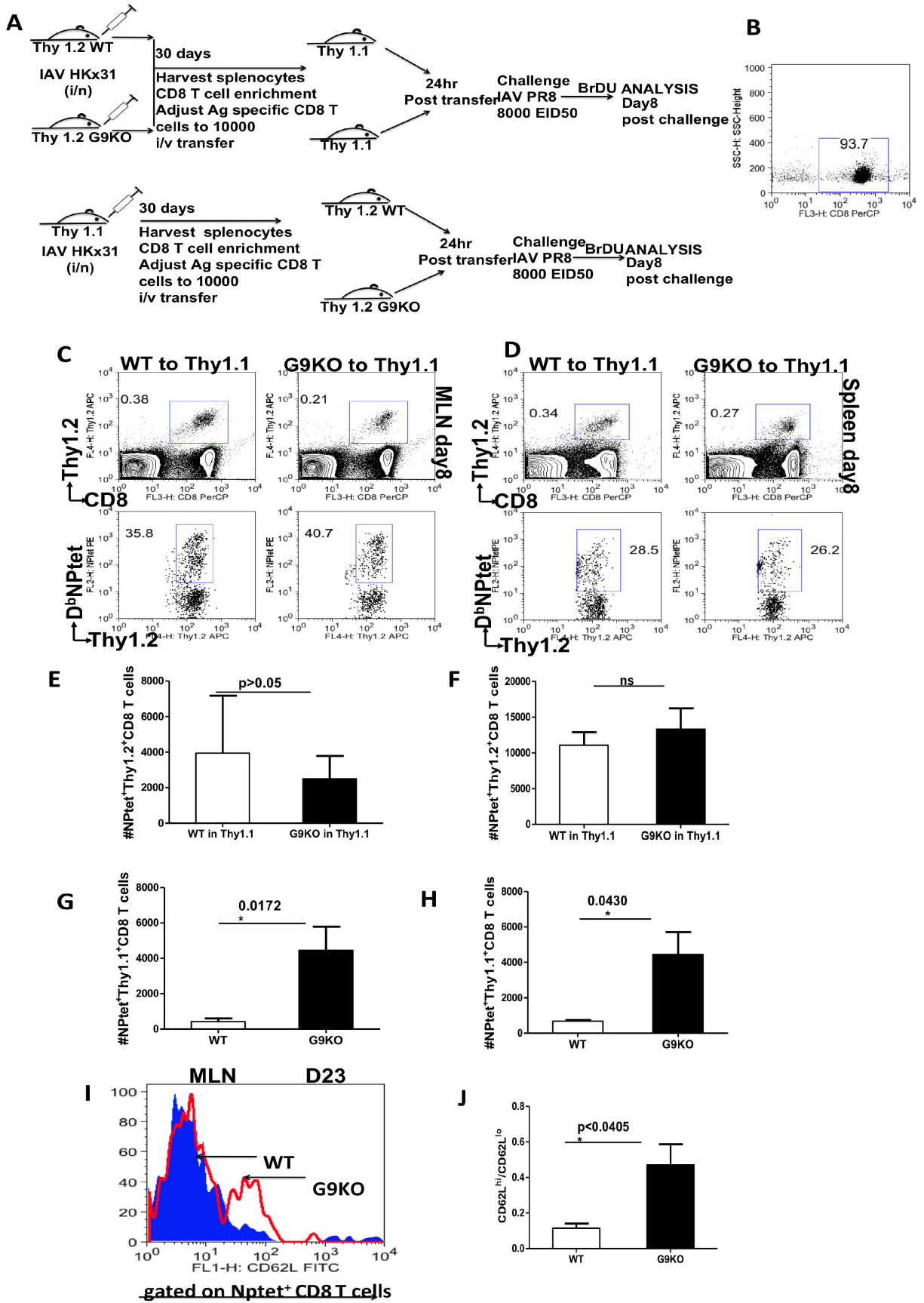
A**B****C****D****E****F****G**

Figure 3.11 Adoptive transfer of memory CD8 T cells: Splenocytes from either WT or G9KO (both Thy 1.2) HKx31 immune mice (mice were held for at least one month following infection with IAV HKx31 i/n) were enriched for CD8T cells using miltenyi biotech (CD8T cell isolation) kit. Around 93-94% pure CD8T cells were obtained in the enriched CD8T cell population. The enriched CD8T cells were then titrated for equal number of NP tetramer specific CD8T cells and 1×10^4 antigen specific CD8T cells were transferred in B6 Thy1.1 mice (n=4). Alternatively splenocytes from B6 thy1.1 HKx31 immune mice (mice were held for at least one month following infection with IAV HKx31 i/n) were enriched for CD8T, and equal number of NP tetramer specific CD8T cells (1×10^4) cells were transferred in WT or G9KO mice (n=4). 24 hrs post transfer, the recipients were challenged with 8000EID₅₀ of heterologous IAV (PR8). (A) Diagrammatic depiction of the scheme for adoptive transfer experiments. (B) Representative FACS plots for enriched CD8T cell population is shown. FACS plots show the frequencies of donor Thy1.2⁺CD8⁺ (C, upper panel) and NPtet⁺ Thy1.2⁺ CD8⁺ (C, lower panel) WT or the G9KO cells in the MLN (C), and spleen (D) of Thy1.1 animals at 8dpi. Absolute numbers of the donor NPtet⁺thy1.2⁺CD8⁺T cells WT or the G9KO cells in the MLN (E) and spleens (F) of the recipients. Absolute numbers of the donor NPtet⁺Thy1.1⁺CD8⁺T WT or the G9KO cells in the MLN (G) and spleens (H) of the recipients are shown. The experiments were repeated two times. Statistical analysis was done by student's t test and the Error bars represent SEM. (I) Representative histograms showing CD62L expression by

NPtet⁺ CD8 T cells in the MLN's of WT and G9KO animals at day 23 p.i. (J) Bar graphs represents the ratios of CD62L^{hi}/CD62L^{lo} of NPtet⁺ CD8 T cells in the MLN of WT and G9KO animals at day 23 p.i.



PART-IV

REGULATORY T CELL EXPRESSION OF

HERPES VIRUS ENTRY MEDIATOR

(HVEM) FOLLOWING HSV-1 INFECTION

AND ITS FUNCTIONAL SIGNIFICANCE

Research described in this chapter is from a manuscript that is in preparation for submission to *Journal of Immunology* by Shalini Sharma and Barry T. Rouse.

Sharma S and Rouse BT. Regulatory T cell expression of Herpes virus entry mediator following HSV-1 infection and its functional significance. (*Journal of Immunology*-in preparation).

In this chapter “our” and “we” refers to co-authors and me. My contribution in the paper includes (1) Selection of the topic (2) Compiling and interpretation of the literature (3) Designing experiments (4) understanding the literature and interpretation of the results (5) providing comprehensible structure to the paper (6) Preparation of graphs and figures (7) Writing and editing.

Abstract

In many infections especially those that are chronic, the outcome may be influenced by the activity of one or more types of regulatory T cells (Tregs). Infections may cause Treg expansion but how this is accomplished remains uncertain. In this report, we demonstrate one possible mechanism by which HSV-1 infection could act to signal and expand the Treg population. We show that CD4⁺FoxP3⁺ regulatory T cells up regulate the receptor, herpes virus entry mediator (HVEM) following HSV-1 infection [a binding site for major viral glycoprotein HSV-1gD (gD)]. Recombinant HSV-1 gD added to the cultures increased the proportions of Foxp3⁺ cells among CD4⁺CD25⁺T cells, up

regulated activation markers on FoxP3⁺ T cells in the cultures and expanded Treg population with suboptimal TCR stimulation. The Treg expansion was dependent on gD interaction with HVEM. In addition Treg expansion in HVEM knockout animals (HKO) was significantly less than WT mice. As a result HKO animals generated more elevated T cell responses than the wild type (WT) animals and cleared virus more rapidly. Our results are discussed in terms of understanding of the factors that control Treg activation and expansion in response to pathogens and their application to manipulate Treg function in acute infections.

Introduction

The magnitude of a T cell mediated immune response to an acute viral infection may be influenced by the activity of one or more types of regulatory T cells (15), particularly those that express FoxP3. Pathogens may signal Treg expansion with the response influencing the magnitude and perhaps pattern of the immune response. In some cases, responses to pathogens and vaccines are elevated if the Treg response is modulated (14, 17). The extent of the Treg response in different individuals may also explain in some circumstances the differential outcome of infection with chronic infection such as in hepatitis(4). However in situations where infections persist and immune reactions cause extensive tissue damage such as HSK, the Treg response can be beneficial and can limit the size of lesions (10). In many studies the Treg response to pathogens is assumed to consist mainly or predominately of antigen specific Tregs, although

there are instances where the Treg involved appear not be antigen reactive. This may be the case with HSV infection, and this possibility is investigated in the present report. We show that one of the major glycoprotein of HSV, normally involved in viral entry into susceptible cells, may cause proliferation and activation of Treg since such cells may express the entry molecule HVEM. Besides being an entry receptor for HSV, HVEM is identified as a co-stimulatory molecule that is known to be constitutively expressed on the cells of the immune compartment. HVEM can promote T cell activation by propagating signals from the TNF super family member ligand, LIGHT, a lymphotoxin related inducible ligand (19) that competes with glycoprotein D for binding to HVEM on T cells or can deliver inhibitory signals upon binding with BTLA (B and T lymphocyte attenuator). In a previous report HVEM knockout mice were shown to develop an unexpected enhancement of T cell responses (18), with increased susceptibility to autoimmunity. In addition over expression of HVEM enhances Treg suppressive function (16) suggesting a role of HVEM in Treg suppressive function.

Our studies demonstrate that a CD4⁺FoxP3⁺ regulatory T cell expand and up regulate HVEM following HSV-1 infection. Additionally HSV-1gD was detectable in the draining popliteal lymph nodes (PLN) following footpad infection with peak levels present around day 5 p.i. Primed cells, when re-stimulated with UV inactivated HSV resulted in further upregulation of HVEM on Tregs. Interestingly the presence of soluble gD increased the proportions of Foxp3⁺ cells among CD4⁺CD25⁺T cells in the culture and expanded Tregs in the presence of

suboptimal TCR stimulation. Consistent with this, HKO mice possessed significantly diminished ratios of CD4⁺FoxP3⁺/CD4⁺FoxP3⁻ cells in the PLN after HSV-1 infection and cleared virus faster than the WT animals. This could mean that engagement of HVEM with gD results in Treg activation and expansion which in turn modulates effector responses. T cells from scurfy mice, which have truncated form of FoxP3 (16) lacked HVEM expression even after activation and over expression of HVEM enhances Treg suppressive function (16) suggesting a role of HVEM in Treg suppressive function. Consistent with this, naïve HVEM knockout animals expressed reduced frequencies and expression levels of FoxP3⁺ T cells compared to their naïve WT counterparts.

Materials and Methods

Mice and Virus

Female 7-8-wk-old C57BL/6 (B6) (H-2b) mice were purchased from Harlan Sprague-Dawley and housed in the animal facilities at the University of Tennessee. Foxp3-GFP knock in mice were a kind gift from Dr. M. Oukka (Brigham and Women's Hospital, Harvard Medical School). HVEM knockout mice were obtained from Dr. Carl Ware at La Jolla institute of Allergy and Immunology (LIAI), California and were bred and maintained in the animal facility at the University of Tennessee. All investigations follow guidelines of the Committee on the Care of Laboratory Animals Resources, Commission on Life Science, National Research Council. HSV-1 strain KOS and RE was grown in vero cells obtained from American Type Culture Collection. The viruses were concentrated,

titrated, and stored in aliquots at -80°C until use. Titers were measured in vero cells and expressed as PFU per milliliter. Mice were infected in footpad (FP) with 2.5×10^5 PFU of HSV KOS in 30- μ l volume. Corneal infections of C57BL/6 mice were conducted under deep anesthesia. Mice were scarified on their corneas with a 27-gauge needle, and a 3 μ l drop containing the required viral dose was applied to the eye. The eyes were examined on different days post infection (dpi) with a slit-lamp biomicroscope (Kowa), and the clinical severity of keratitis and angiogenesis of individually scored mice was recorded as described elsewhere (12).

Antibodies and Reagents

Antibodies purchased from BD PharMingen were PerCP-CD4, FITC and PE anti-FoxP3, APC-anti-CD25 (PC61), APC-anti-CD103, FITC-anti GITR, antiCD62 ligand (CD62L), FITC-anti-CD44, and PerCP-anti-CD69. BrdU staining kit was purchased from BD Pharmingen. PE- anti HVEM (e-Bioscience), recombinant HSV-1gD and anti HVEM antibody were kindly provided by Dr. Gary Cohen (University of Pennsylvania), Recombinant human IL-2 was obtained from Hemagen. Complete RPMI 1640 was used for in vitro cultures.

Quantitation of HSV-1 in Foot Pad Tissues

The quantitation of HSV-1 in foot pad (FP) tissue was determined as reported by Jennings et al (5). Briefly, the mice were killed at the indicated time post infection (p.i.), the FP surface was cleaned with 70% isopropyl alcohol, and the tissues were removed with a scalpel. The tissues were stored in virus diluent (PBS supplemented with 0.6 mM CaCl₂, 0.5 mM MgCl₂/H₂O, 20 mg Phenol red,

and 50g gentamicin sulfate per ml) at -80°C. Tissues were disrupted by homogenization in 1 ml ground glass grinders (Wheaton) and centrifuged, and the supernatant was used to assay viral titration on vero cells. Finally, plaques were visualized with crystal violet.

Cell Surface and Bromodeoxyuridine Staining

Surface staining was performed as described previously (6). For bromodeoxyuridine (BrdU) staining, the BrdU kit from BD PharMingen was used according to the manufacturer's instructions. Briefly, HSV-1 infected mice received i.p. injection of BrdU (1 mg/ml) 12 hours before termination of mice. Draining popliteal lymph node cells were stained first with anti-CD4 and FoxP3 and subsequently labeled with anti-BrdU mAb. Samples were analyzed on a FACS caliber cytometer using FlowJO software (BD Biosciences).

Western blotting

For the detection of HSV-1gD, draining popliteal lymph nodes were dissected at the indicated time points in 300 ul of RIPA buffer containing protease inhibitor cocktail (aprotinin, PMSF and sodium orthovanadate), cell debris was removed by centrifugation and the samples stored at -80°C till used for SDS-PAGE. In brief, after 2 hrs of blocking with 3% nonfat milk in TBS, membranes were incubated with 1:1000 dilution of rabbit polyclonal anti HSV-1gD antibody (mouse monoclonal IgG1, 100 µg/ml, Santa Cruz biotechnology) and membranes were then incubated for 1 hr with secondary antibody coupled to horse raddish peroxidase. Specific bands were detected with Immobilon™

western; Millipore). Membranes were stripped and then reprobed to detect β actin.

Cell purification and *in vitro* cell culture

CD4 T cells were purified from Foxp3-GFP knock-in animals using a CD4 T cell isolation kit, and 5×10^5 cells were cultured with the indicated concentrations of recombinant HSV-1gD and suboptimal concentrations of anti-CD3. In some cultures anti-HVEM antibody was added to the cultures. In additional experiments FoxP3⁺ cells were sorted (FACS vantage) from the enriched CD4 T cell population based on the GFP expression. CD4⁺FoxP3⁺ Tregs were incubated with recombinant HSV-1gD. 48 hours post incubation Tregs in the culture were analyzed by flow cytometry for expression of surface activation markers.

Thymidine incorporation assay

Splenocytes from the naïve FoxP3-GFP knock in mice were enriched for CD4 T cells using CD4 T cell isolation kit according to the manufacturer's protocol (Miltenyi Biotec, Auburn, CA). Tregs were sorted (FACS vantage) from this enriched CD4 T cell population based on GFP expression. Sorted CD4⁺CD25⁺ Treg populations were incubated with anti-CD3 and recombinant HSV-1gD at the indicated concentrations. The cells were plated at a density of 5×10^5 in 96-well round-bottom tissue culture plates in a total volume of 200 μ l of RPMI medium (Gibco). Sixteen hours before harvest, [3H] thymidine (1 μ Ci/well; 1Ci=37GBq) was added. The cells were harvested onto a UniFilter

(PerkinElmer). [3H]thymidine incorporation was measured with a scintillation counter, and the results were expressed as mean cpm from triplicate cultures.

Results

HSV infection causes expansion of FoxP3⁺ Tregs

To follow changes in CD4⁺FoxP3⁺ Treg responses after HSV infection, FoxP3GFP knock in mice were used and analyses were performed in draining PLN populations. The infection changed the frequency of CD4⁺T cells that were FoxP3⁺ with numbers of such cells increased by more than two fold at day 5 p.i (fig 4.1B) and more than fourfold at day 8 p.i. compared to naive mice. A similar trend was observed with the absolute numbers of CD4⁺FoxP3⁺. The absolute numbers of CD4⁺ T cells (fig 4.1C) in the popliteal lymph nodes peaked at day 5 p.i. Whereas the highest absolute numbers of CD4⁺FoxP3⁺ cells (fig 4.1D) were present after the peak of effector activity i.e. at day 8 p.i. To determine whether or not different viral loads could influence the magnitude of Treg expansion, we infected WT animals with various inoculation doses of HSV-1 i.e 2x10⁶, 2x10⁵, 2x10⁴ as well as with UV inactivated virus. Increasing infection doses resulted in a gradual increase in the level of Treg expansion in the draining popliteal lymph nodes (data not shown).

HVEM expression is up-regulated on regulatory T Cells following HSV-1 infection

We next analyzed the expression of HVEM on Tregs. HVEM, a tumor necrosis factor receptor super family member that interacts with the gD protein of

HSV-1 to facilitate cell entrance, is shown to be constitutively expressed by the cells of the immune compartment. Flow Cytometry showed HVEM expression by 45-50% of naïve CD4⁺FoxP3⁺ cells. Following HSV-1 infection in the footpad, HVEM was up regulated on CD4⁺FoxP3⁺ cells with up to 70% at day 8p.i and 90% CD4⁺FoxP3⁺ cells expressing HVEM at day 11p.i (fig 4.2 A and B). The MFI of HVEM expression was also increased on FoxP3⁺ Tregs (fig 4.2C) following HSV-1 infection. HVEM knockout Tregs have been reported to be less suppressive and over expression of HVEM in Tregs increases their suppressive ability (16) thus increased expression of HVEM on Tregs following HSV-1 infection could be of functional significance.

In some experiments DLN cells from infected FoxP3-GFP knock in mice were obtained at indicated time points post infection and were stimulated with either UV inactivated HSV kos or anti-CD3/anti-CD28 for 72 hours. HVEM expression was analyzed on CD4⁺FoxP3⁺ and CD4⁺FoxP3⁻ cells by flow cytometry. Our results demonstrate that HVEM expression was further up regulated (fig 4.3A) on FoxP3⁺ CD4 T cells when stimulated with UV inactivated HSV kos but not on CD4⁺FoxP3⁻ cells. Stimulation with anti-CD3 anti-CD28 did not result in change in HVEM expression levels on either the FoxP3⁺ or FoxP3⁻ cells (fig 4.3B). Interestingly the highest MFI of HVEM expression after UV inactivated HSV stimulation was observed when the cells were obtained after day 6 p.i. Taken together our *in vivo* observations of the detectable HSV-1gD in the DLN after HSV-1 infection and *in vitro* experiment suggests that presence of HSV-1 gD could influence the up regulation of its own receptor HVEM.

It has been shown that HSV-1 is able to enter activated T lymphocytes as well as immature and mature DCs. Additionally gD is expressed on the surface of infected T cells and it is postulated that the cellular gD interacts with HVEM in a juxtacrine and autocrine way (7). To explore the mechanism that might be responsible for triggering Treg expansion, we hypothesized that possibly HSV itself could trigger this and may represent an early means by which the virus infection could signal Treg activation and expansion. Experiments were performed to detect if viral protein gD is detectable in the draining lymph node. Western blotting on the draining popliteal lymph node homogenates from the naïve and HSV infected animals at day 2, 5, 7 and day 10 p.i. showed that whereas the PLN homogenates from the naïve mice completely lacked gD expression and a negligible amounts of gD was detectable at day 2 p.i. However gD was detectable at day 5, 7 and 10 post HSV-1 infection, a significant expression of gD being detectable in the PLN homogenates at days 7 and 10 p.i. (fig 4.3C).

Recombinant HSV-1 gD increases the proportions of FoxP3⁺ T cells among CD4⁺CD25⁺T cells

Our observations that regulatory T cells expand following HSV-1 infection, that HVEM is preferentially up regulated by regulatory T cells and more interestingly the detectable levels of HSV-1 gD in the draining popliteal lymph node led us to hypothesize that the interaction of HVEM with one of its known viral ligand gD could be of functional significance in terms of causing a T cell

perhaps only Treg to change gene expression, proliferate or show activation changes.

To address this question we performed three sets of experiments, in one experiment we enriched CD4 T cells (fig 4.4A) from the splenocytes of naïve mice (up to around 90% purity) and incubated 5×10^5 cells with varying concentrations of recombinant gD and anti CD3 (1 ug/ml). As shown in fig 4.4B, addition of recombinant gD in the presence of anti-CD3 increases the proportion of FoxP3⁺ cells among the CD4 T cells in the cultures. This effect was relatively specific for HSV-1gD HVEM interaction, as addition of anti HVEM antibody to the cultures did not result in increased proportions of FoxP3⁺ cells (fig 4.4C). In some experiments FoxP3⁺ cells were sorted from enriched CD4 T cells based on GFP expression and 2×10^5 FoxP3-GFP⁺ cells were incubated with different concentrations of HSV1-gD and IL-2. 48hrs post-incubation, the cells were stained for activation markers. CD69 and CD25 were up regulated on Tregs that were incubated with recombinant gD in a dose dependent manner (fig 4.4 D and E). In the third set of experiments sorted FoxP3⁺ cells (2×10^5 cells) were incubated with anti-CD3 alone or anti-CD3 plus recombinant HSV-1 gD and recombinant IL-2 in the cultures. In presence of gD, Tregs showed proliferation when relatively higher concentrations of anti-CD3 was used (fig 4.5C). This proliferative effect was not observed when anti-HVEM antibody was added (fig 4.5D) to the culture suggesting an effect that is mediated by gD binding with HVEM. Taken together our results could mean that besides being an entry

receptor for HSV, HVEM binding with HSV-1 gD can trigger activation and proliferation of Tregs.

HVEM knockout mice generate weaker Treg responses

Our *in-vivo* and *in-vitro* observations suggest that HVEM is up regulated on regulatory T cells following HSV-1 infection and that gD-HVEM interaction results in the increased representations of CD4⁺FoxP3⁺ regulatory T cells among CD4 T cells. To evaluate if HKO and WT animals showed differences upon HSV-1 infection, the animals were infected with HSV-1 in the foot pad and the frequencies and absolute numbers of CD4⁺ and CD4⁺Foxp3⁺ cells were recorded in the draining popliteal lymph node at day 5.5 and 8p.i. At day 5.5 and day 8 p.i HKO mice had significantly reduced frequencies of CD4⁺Foxp3⁺T cells (fig 4.6 C-F). The absolute numbers of total lymphocytes ($p < 0.0006$) as well as CD4⁺T cells ($p < 0.0006$) and CD4⁺FoxP3⁺Tcells ($p < 0.017$) were significantly higher in the HKO animals (fig 4.7A). The numbers sustained to be significantly higher for CD4 T cells ($p < 0.0179$) even at day 8 p.i in the HKO mice. These findings are consistent with the previous findings (18) that reported a hyper proliferative CD4 T cell responses in HKO mice. However when the representation of CD4⁺FoxP3⁺ among the CD4⁺FoxP3⁻ T cells was compared, HKO mice showed a significantly lower Treg to Teff ratios at day 8 p.i ($p < 0.002$) (fig 4.7 D and E), whereas the ratios were largely non significant at day 5.5 p.i. consistent with our observations that significantly higher numbers of CD4⁺FoxP3⁺ T cells are observed after the peak of effector responses in the WT animals. Taken together and consistent with *in vitro* experiments, our *in vivo* data suggests that there are diminished

representations of CD4⁺FoxP3⁺ regulatory T cells among CD4 T cells in the HKO mice. The expansion of Tregs observed in the draining popliteal lymph node following HSV-1 infection might be mediated by recruitment and/or proliferation of these cells. BrDU incorporation assay was performed to analyze whether Treg undergo proliferation *in vivo*. HSV-1 infected mice were pulsed with BrDU 12 hours before sacrifice. At day 8 p.i. draining popliteal lymphoid populations were analyzed by FACS for evidence of BrDU incorporation. CD4 T cells were gated on FACS plot, and the assay revealed an average 1.5 to 2 fold increase in proliferation of CD4⁺FoxP3⁺ cells in PLN of WT animals compared to HKO (fig 4.6 G and H).

Additionally the proportions of CD4⁺T cells co expressing FoxP3 and the activation markers CD25 (fig 4.8A, B and E), CD103 (fig 4.8C, D and F), were significantly reduced in HKO animals. Interestingly a higher proportion of FoxP3⁺ cells were CD62L^{lo} (fig 4.8G) at the indicated time points post infection and reduced expression of CD44 on FoxP3⁺ cells (fig 4.8H and I) in HKO mice compared to the WT animals, thus indicative of them being less activated.

Influence of regulatory T cell expression of HVEM on the outcome of immune response to HSV

We monitored whether the diminished representations of FoxP3⁺ T cells in HKO mice affected the course of viral infection. Our data imply that the acute cutaneous viral load in the FP was comparable in both WT and HKO until day 5. However, no viral plaques were observed in the HKO mice on day 6 whereas

significant viral load was still present in the control animals. By day 8 no virus was detected in the FP of both groups (data not depicted).

In the mouse model of SK, CD4⁺CD25⁺ regulatory T cells have been shown to control the severity of viral immuno-inflammatory lesions (14) and previous studies have suggested a non-redundant inhibitory effect of HVEM on T cell responses (18). Thus given our data that HKO Tregs are less suppressive and the lack of HVEM mediated negative regulation of T cell activation we tested the susceptibility of HKO mice to the development of HSK following ocular HSV-1 infection. There were two possibilities, either the HKO mice will not develop the disease because they lack the HSV-1 entry receptor (HVEM) or will develop more disease due to the deficiency of negative regulatory interaction.

WT or HKO mice were infected with 1×10^4 PFU of HSV RE ocularly and the progression of HSK and angiogenesis were recorded by slit lamp biomicroscopy. The cellular infiltration in the collagenase digested corneas was recorded at day 15 p.i in WT and HKO animals. There were around 2 fold higher frequencies of CD4 T (fig 4.9A) cells with significantly increased expression of CD49d (fig 4.9B) on them in the HKO animals compared to the WT animals. These findings are consistent with our own findings where absence of Tregs resulted in altered phenotype of CD4 T cells (with increased CD49d expression on CD4⁺T cells) following ocular HSV-1 infection (14).

Discussion

To survive an infection, host needs to generate an efficient immune response against the pathogen but at the same time the host immune response

to pathogens needs precise regulation to minimize tissue damage whilst still achieving defense (10). Tregs play a very important role in balancing these 2 contradictory effects occurring in most infectious diseases. In our previous report we have shown that HSV infection activates and expands CD4⁺CD25⁺ regulatory T cells (15) and the majority of expanded Tregs are not antigen specific. In the current study we report one possible mechanism by which HSV-1 infection could act to signal and expand the Treg population. Using footpad infection model we show that CD4⁺FoxP3⁺ regulatory T cells up regulates HVEM following HSV-1 infection and the viral ligand HSV-1gD was detectable in the draining popliteal lymph nodes (PLN). Presence of recombinant HSV-1 gD increased the proportions of Foxp3⁺ cells among CD4⁺CD25⁺T cells and up regulated activation markers on FoxP3⁺ T cells in the cultures. Consistent with this, HKO mice represented significantly diminished ratios of CD4⁺FoxP3⁺/CD4⁺FoxP3⁻ cells in the PLN after HSV-1 infection and cleared virus faster than the WT animals suggesting that functional interaction of HSV-1gD with HVEM expressed on T regs might be one possible means of non-specific Treg expansion.

In the present study we observed significantly increased frequencies and absolute numbers of FoxP3⁺ Tregs following HSV infection of the footpad in the draining PLN. These findings are consistent with our previous report (15) suggesting that the CD8 T cell response to the immunodominant peptide SSIEFARL was significantly enhanced when CD4⁺CD25⁺ Tregs were depleted. Treg activation prevents immunopathology by dampening pathogen specific immune responses but this can also lead to enhanced pathogen survival (3). This

leads to the question for the cells or the factors involved in expansion of Treg and whether proliferation, de novo induction or enhanced survival of Tregs is the predominant reason for the increased numbers of Tregs in the virus infected tissues and the draining lymph nodes following a viral infection. It has been reported that virus infected DCs can expand the population of FoxP3⁺ cells in vitro upon presentation of antigens to naïve T cells (2), alternatively it is shown that CD8⁺T cells play a vital role in Treg expansion (22, 23) where Friend's virus (FV) infected mice without CD8⁺T cells, no expansion of Tregs was observed in any of the investigated organs. One such study has also reported that the expansion of Tregs exclusively depended on the presence of virus specific effector CD4⁺T cells (1). Viral replication itself or presentation of antigen to virus specific Tregs have also been attributed to induce Treg expansion (22).

One curious observation we made was the up regulation of HVEM by Tregs and its viral ligand HSV-1gD was detectable in the draining popliteal lymph node following HSV infection of the foot pad. Previous reports have shown that HVEM is up regulated on Tregs and down regulated on T effectors upon activation. Interestingly our data points towards the maximum Treg numbers and HVEM up regulation after the peak of effector responses. Additionally highest levels of HSV-1gD levels were also detected after day 5-post infection (i.e after peak of effector responses). One plausible explanation of high Treg numbers after peak of effector responses could be that effector T cells are undergoing a contraction after peak activity and thus increased Treg representation. Enhanced up regulation of HVEM could be ligand mediated, as increased availability of

HSV-1gD was evident at later time points post infection. More direct evidence for this was obtained by additional *in-vitro* experiments where stimulation of primed T cells with UV inactivated HSV kos resulted in further up regulation of HVEM on Tregs, maximum up regulation again observed when cells were obtained after peak effector activity. Currently, it is not clear how regulatory T cells are induced and act to modulate effector cell function following HSV-1 infection, we therefore undertook these studies to better understand whether the ability of HSV-1gD to interact with HVEM could alter immune responses. Although HVEM mediates both positive and negative immune signals (9), our observations are more consistent with the hypothesis that binding of viral ligand gD to HVEM causes T cells and perhaps only Treg to show activation changes. Evidence suggests that HSV-1 gD can modulate the activities of the T cell via HVEM during binding, entry, or egress (7). It has been shown that HVEM is involved in NFkB activation by HSV-1 gD (11) thus it is conceivable that one consequence of this interaction might be the NFkB activation in Tregs however; such effects were not formally investigated.

Further support for the immunomodulatory role of gD HVEM interaction came from the studies using HVEM knockout mice. Previous reports have established a role of HVEM in Treg function. One such study reported that HVEM expression on CD4⁺CD25⁺ T regulatory cells was important to mediate the suppressive functions of Tregs, accordingly HVEM knockout Tregs had decreased suppressive activity (16). T cells from scurfy mice have been shown to lack HVEM expression even after activation, suggesting involvement of FoxP3 in

regulation of HVEM expression. These findings are consistent with our own observation that Tregs from naïve HVEM knockout mice had reduced frequencies and FoxP3 expression levels compared to the WT animals. However more interesting was the observation that following HSV infection the expression levels of FoxP3 increased on WT Tregs whereas decreased on the HKO Tregs. Additionally significantly diminished ratios of CD4⁺FoxP3⁺Tcells to CD4⁺FoxP3⁻ cells were observed in the HKO mice and again the differences more evident at day 8p.i. (after the peak of effector responses). This could mean that absence of gD-HVEM interaction in HKO animals further augments the scenario of diminished FoxP3 expression on Tregs already existing due to lack of HVEM. These findings were further supported by our in-vitro experiments that utilized soluble gD and the effects abolished with anti HVEM antibody. It is still a matter of debate whether Treg that suppress pathogen specific T-cell responses have to be pathogen specific themselves. In several infectious diseases, such as Leishmania (13) or hepatitis C virus (8) pathogen specific Tregs have been found and in some auto-immune diseases, only antigen specific Tregs were able to suppress autoreactive T cells, whereas non-specific Tregs were ineffective (21). However several studies have reported that polyspecific Tregs that are efficiently recruited to proliferate in the organs with virus induced inflammation can suppress virus specific T cell responses (22).

Soluble gD has been shown to inhibit T cell proliferation (7). It is conceivable that gD binding to HVEM might be able to provide a strong negative signal, the outcome of which is manifested as a defect in T cell proliferation.

Alternatively our observation might suggest that gD binding to HVEM on Tregs result in treg activation and expansion which in turn inhibit T cell proliferation. Thus it is conceivable that same type of receptor ligand interaction might have different outcome depending on the cell type. In the present study we observed similar or even attenuated numbers of IFN γ ⁺ CD4 T cells in the draining PLN of HKO animals. Because engagement of HVEM on T cells by its natural ligands may augment (in the case of LIGHT) or attenuate (in the case of BTLA or CD160) immune response (20) therefore it remains to be studied in more depth how the balance of these competing interactions condition the kinetics of the immune response in different cell types.

LIST OF REFERENCES

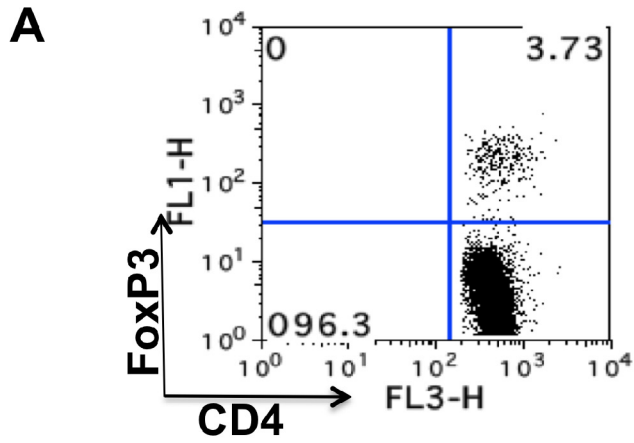
1. **Antunes, I., M. Tolaini, A. Kissenpfennig, M. Iwashiro, K. Kuribayashi, B. Malissen, K. Hasenkrug, and G. Kassiotis.** 2008. Retrovirus-specificity of regulatory T cells is neither present nor required in preventing retrovirus-induced bone marrow immune pathology. *Immunity* **29**:782-794.
2. **Balkow, S., F. Krux, K. Loser, J. U. Becker, S. Grabbe, and U. Dittmer.** 2007. Friend retrovirus infection of myeloid dendritic cells impairs maturation, prolongs contact to naive T cells, and favors expansion of regulatory T cells. *Blood* **110**:3949-3958.
3. **Belkaid, Y.** 2008. Role of Foxp3-positive regulatory T cells during infection. *Eur J Immunol* **38**:918-921.
4. **Belkaid, Y., and B. T. Rouse.** 2005. Natural regulatory T cells in infectious disease. *Nat Immunol* **6**:353-360.
5. **Bonneau, R. H., and S. R. Jennings.** 1989. Modulation of acute and latent herpes simplex virus infection in C57BL/6 mice by adoptive transfer of immune lymphocytes with cytolytic activity. *J Virol* **63**:1480-1484.
6. **Kumaraguru, U., and B. T. Rouse.** 2000. Application of the intracellular gamma interferon assay to recalculate the potency of CD8(+) T-cell responses to herpes simplex virus. *J Virol* **74**:5709-5711.
7. **La, S., J. Kim, B. S. Kwon, and B. Kwon.** 2002. Herpes simplex virus type 1 glycoprotein D inhibits T-cell proliferation. *Mol Cells* **14**:398-403.
8. **Li, S., E. J. Gowans, C. Chougnnet, M. Plebanski, and U. Dittmer.** 2008. Natural regulatory T cells and persistent viral infection. *J Virol* **82**:21-30.
9. **Murphy, T. L., and K. M. Murphy.** 2010. Slow down and survive: Enigmatic immunoregulation by BTLA and HVEM. *Annu Rev Immunol* **28**:389-411.
10. **Rouse, B. T., and S. Sehrawat.** 2010. Immunity and immunopathology to viruses: what decides the outcome? *Nat Rev Immunol* **10**:514-526.
11. **Sciortino, M. T., M. A. Medici, F. Marino-Merlo, D. Zaccaria, M. Giuffrè-Cuculetto, A. Venuti, S. Grelli, and A. Mastino.** 2008. Involvement of HVEM receptor in activation of nuclear factor kappaB by herpes simplex virus 1 glycoprotein D. *Cell Microbiol* **10**:2297-2311.
12. **Sharma, S., S. Mulik, N. Kumar, A. Suryawanshi, and B. T. Rouse.** 2011. An anti-inflammatory role of VEGFR2/Src kinase inhibitor in herpes simplex virus 1-induced immunopathology. *J Virol* **85**:5995-6007.
13. **Suffia, I. J., S. K. Reckling, C. A. Piccirillo, R. S. Goldszmid, and Y. Belkaid.** 2006. Infected site-restricted Foxp3+ natural regulatory T cells are specific for microbial antigens. *J Exp Med* **203**:777-788.
14. **Suvas, S., A. K. Azkur, B. S. Kim, U. Kumaraguru, and B. T. Rouse.** 2004. CD4+CD25+ regulatory T cells control the severity of viral immunoinflammatory lesions. *J Immunol* **172**:4123-4132.
15. **Suvas, S., U. Kumaraguru, C. D. Pack, S. Lee, and B. T. Rouse.** 2003. CD4+CD25+ T cells regulate virus-specific primary and memory CD8+ T cell responses. *J Exp Med* **198**:889-901.
16. **Tao, R., L. Wang, K. M. Murphy, C. C. Fraser, and W. W. Hancock.** 2008. Regulatory T cell expression of herpesvirus entry mediator suppresses the

- function of B and T lymphocyte attenuator-positive effector T cells. *J Immunol* **180**:6649-6655.
17. **Toka, F. N., S. Suvas, and B. T. Rouse.** 2004. CD4⁺ CD25⁺ T cells regulate vaccine-generated primary and memory CD8⁺ T-cell responses against herpes simplex virus type 1. *J Virol* **78**:13082-13089.
 18. **Wang, Y., S. K. Subudhi, R. A. Anders, J. Lo, Y. Sun, S. Blink, J. Wang, X. Liu, K. Mink, D. Degrandi, K. Pfeffer, and Y. X. Fu.** 2005. The role of herpesvirus entry mediator as a negative regulator of T cell-mediated responses. *J Clin Invest* **115**:711-717.
 19. **Ware, C. F., and J. R. Sedý.** 2011. TNF Superfamily Networks: bidirectional and interference pathways of the herpesvirus entry mediator (TNFSF14). *Curr Opin Immunol*.
 20. **Watts, T. H., and J. L. Gommerman.** 2005. The LIGHT and DARC sides of herpesvirus entry mediator. *Proc Natl Acad Sci U S A* **102**:13365-13366.
 21. **Westendorf, A. M., D. Fleissner, L. Groebe, S. Jung, A. D. Gruber, W. Hansen, and J. Buer.** 2009. CD4⁺Foxp3⁺ regulatory T cell expansion induced by antigen-driven interaction with intestinal epithelial cells independent of local dendritic cells. *Gut* **58**:211-219.
 22. **Zelinskyy, G., K. K. Dietze, Y. P. Hüsecken, S. Schimmer, S. Nair, T. Werner, K. Gibbert, O. Kershaw, A. D. Gruber, T. Sparwasser, and U. Dittmer.** 2009. The regulatory T-cell response during acute retroviral infection is locally defined and controls the magnitude and duration of the virus-specific cytotoxic T-cell response. *Blood* **114**:3199-3207.
 23. **Zelinskyy, G., A. R. Kraft, S. Schimmer, T. Arndt, and U. Dittmer.** 2006. Kinetics of CD8⁺ effector T cell responses and induced CD4⁺ regulatory T cell responses during Friend retrovirus infection. *Eur J Immunol* **36**:2658-2670.

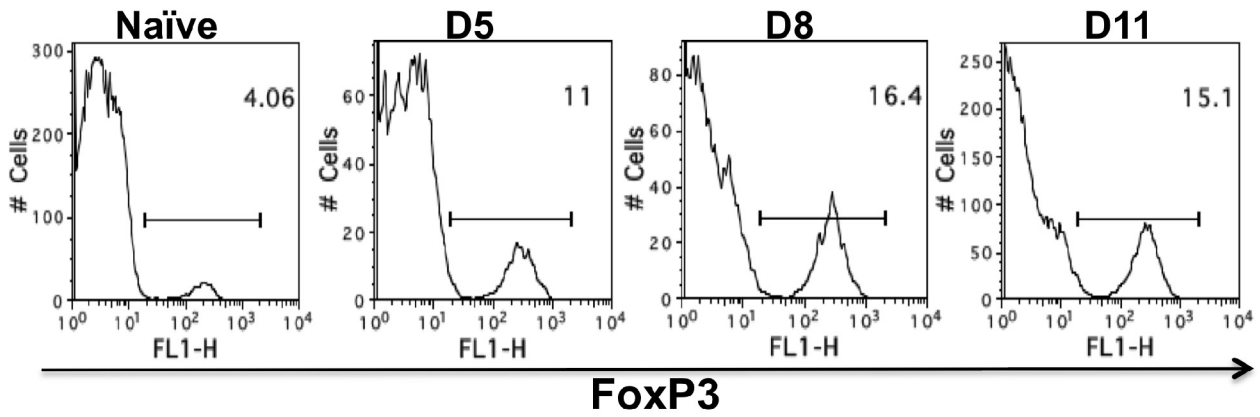
APPENDIX

Figure 4.1 HSV-1 infection results in the expansion of CD4⁺FoxP3⁺ regulatory T cells

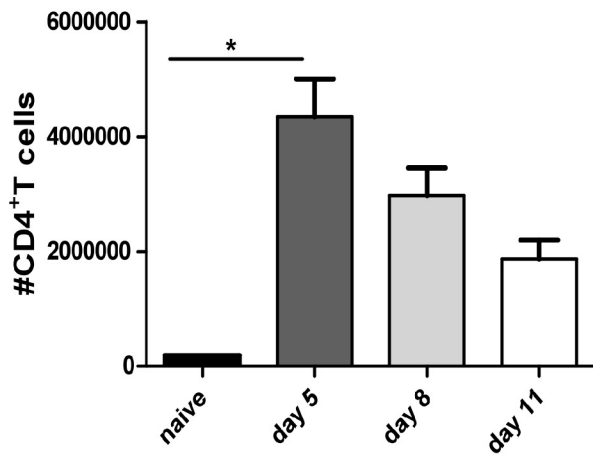
FoxP3-GFP knock in mice were infected with 2×10^5 PFU of HSV kos in a 30 μ l drop in the footpad. The kinetics of FoxP3⁺ Tregs was measured at indicated time points in the draining popliteal lymph nodes (PLN) following HSV-1 infection of the footpad. (A) Representative FACS plot showing CD4⁺FoxP3⁺ and CD4⁺FoxP3⁻ T cells in the pooled (n=4) popliteal lymph nodes of naïve mice. (B) Histograms depicting the increased frequencies of FoxP3⁺ Tregs at indicated time points in the draining PLN following HSV-1 infection. Bar graphs depicting absolute numbers of CD4 T (C) and CD4⁺FoxP3⁺T (D) cells in the draining PLN of naïve and HSV infected mice at indicated time points post infection. Data are representative of three independent experiments with 4-5 mice per group in each experiment. Error bars represent SEM. The level of significance was determined using one-way ANOVA with Bonferroni post hoc settings.



B



C



D

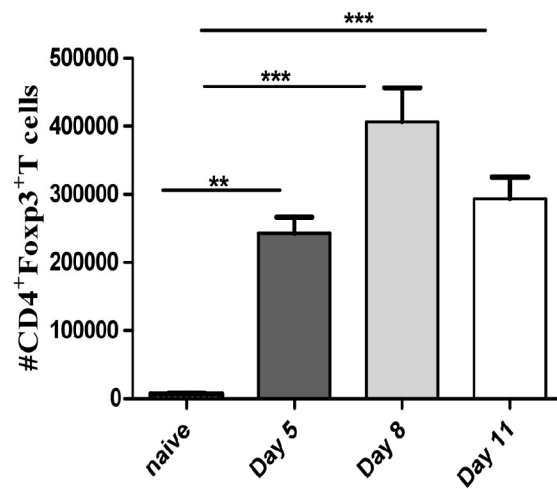


Figure 4.2 HVEM expression is up-regulated on regulatory T Cells following HSV-1 infection and its viral ligand is expressed in PLN following infection

Mice were infected with 2×10^5 PFU of HSV-1 KOS. At indicated time points following infection, draining popliteal lymph nodes were collected and flow cytometry was performed on these samples for expression of HVEM. (A) Representative FACS plots depicting HVEM expression by FoxP3⁺ Tregs. Numbers in the quadrants indicate percent of each subset. (B) HVEM expression by CD4⁺FoxP3⁺T at indicated time points post infection is shown by histograms. (C) Bar graphs shows the MFI of HVEM expression on FoxP3⁺T cells. Data are representative of three independent experiments. Error bars represent SEM. The level of significance was determined using student's t test.

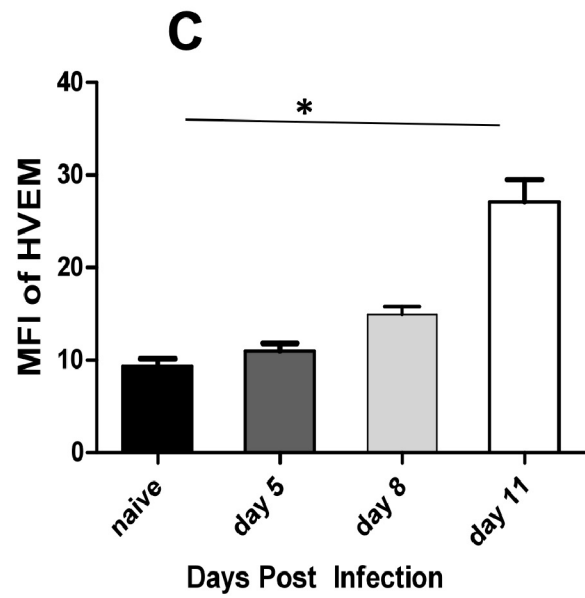
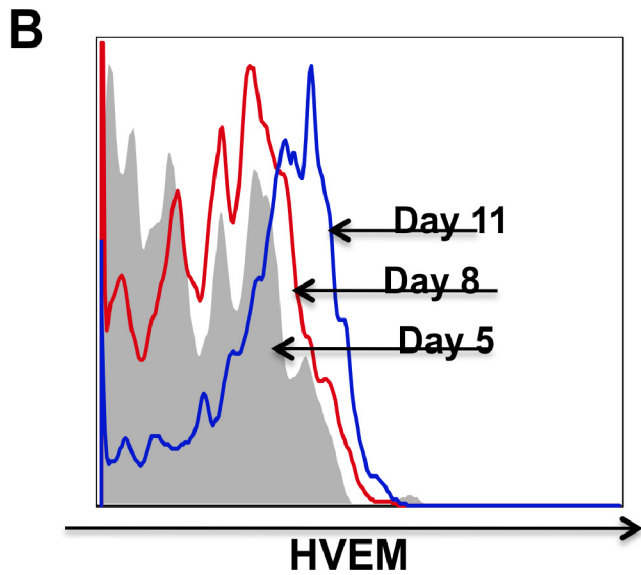
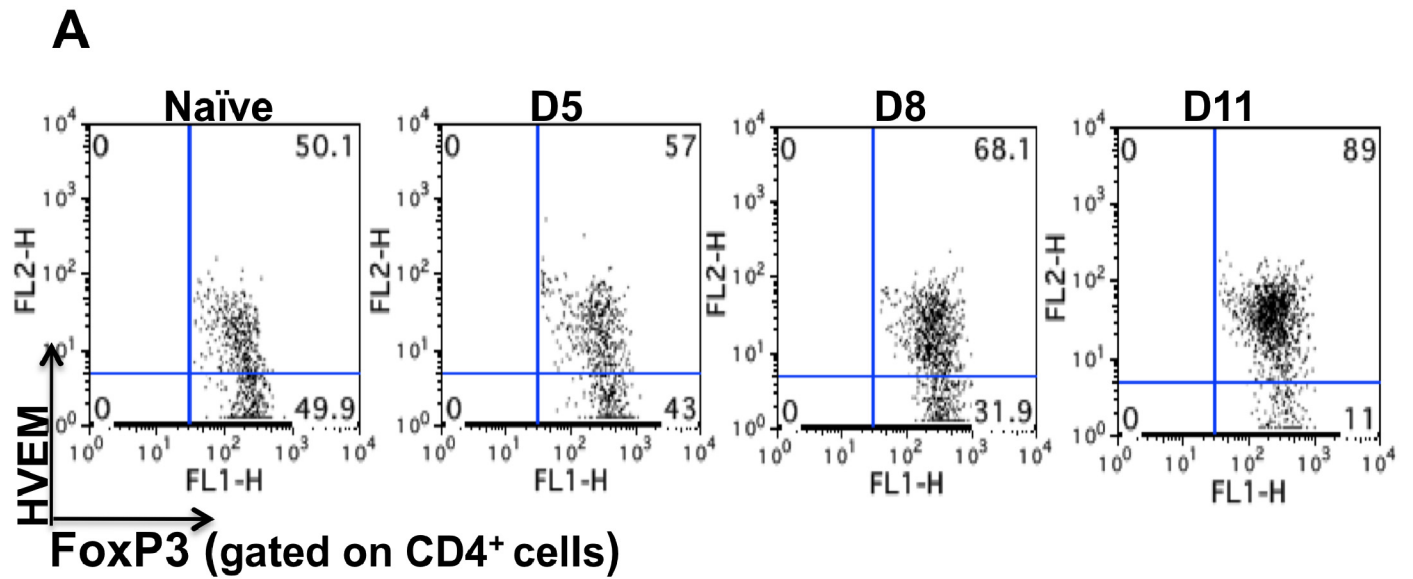


Figure 4.3 Primed cells stimulated with HSV causes HVEM up regulation on Tregs

FoxP3-GFP knock in mice were infected with 2×10^5 PFU of HSV KOS in a 30- μ l drop in the footpad. Draining PLN cells were isolated at indicated time points p.i and stimulated with either UV inactivated HSV kos (MOI = 2) or anti-CD3 (1 μ g/well) anti-CD28 (0.5 μ g/well) for 72 hours. (A) The cells were then analyzed flow cytometrically for HVEM expression on CD4⁺FoxP3⁺ (upper panel) and CD4⁺FoxP3⁻ (lower panel) cells. Histograms depicting HVEM expression by unstimulated (shaded area) and UV inactivated HSV kos stimulated (black line). (B) FACS analysis for HVEM expression on CD4⁺FoxP3⁺ (upper panel) and CD4⁺FoxP3⁻ (lower panel) cells. Histograms depicting HVEM expression by unstimulated (shaded area) and anti-CD3 anti-CD28 stimulated (black line). (C) Western blot analysis for detection of HSV-1gD in the draining PLN lysates at different time points following HSV-1 infection. Draining PLN (2PLN/mice) were collected and levels of HSV-1gD were detected using rabbit polyclonal anti HSV-1gD antibody. Soluble HSV-1gD served as a positive control.

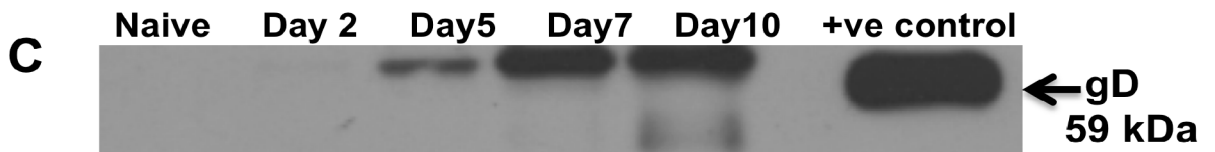
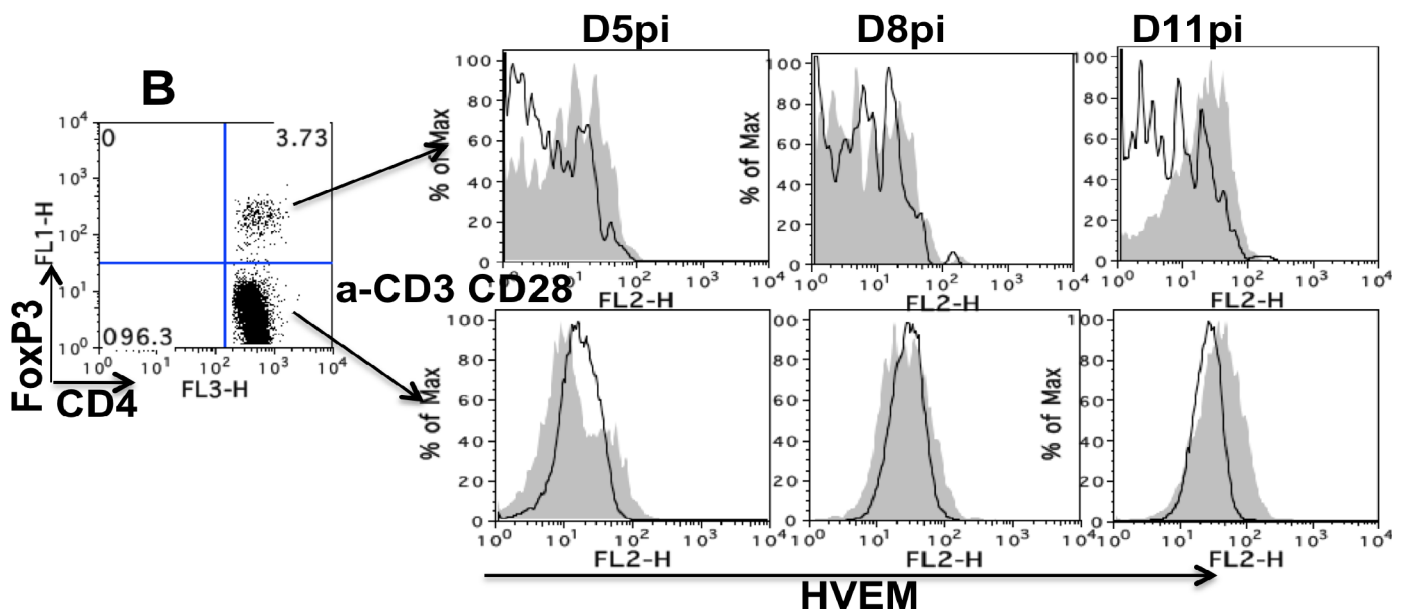
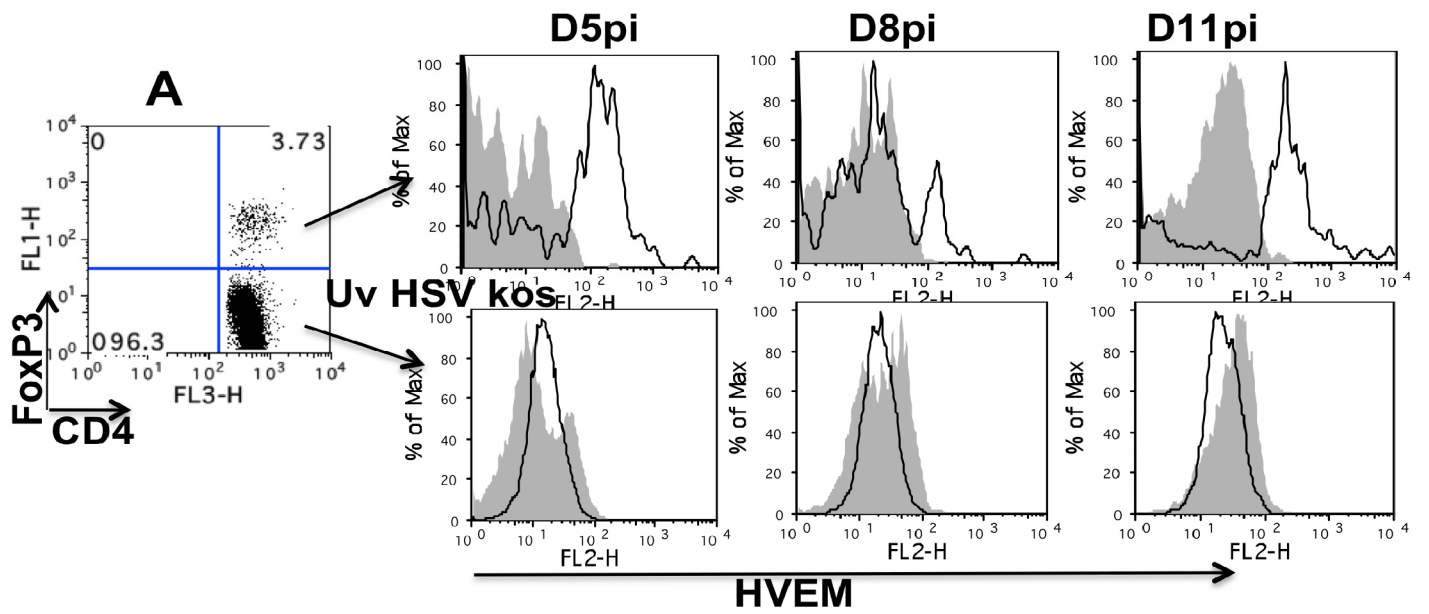


Figure 4.4 Recombinant HSV-1 gD increases the proportions of FoxP3⁺ T cells among CD4⁺T cells

CD4 T cells were enriched from the splenocytes of naïve mice using miltenyi biotech kit. Up to around 90% pure CD4 T cells were obtained following enrichment (A). Enriched naïve CD4 T (5×10^5) cells were incubated cells with varying concentration of soluble gD, recombinant human IL-2 and suboptimal concentrations of anti CD3 ($0.5 \mu\text{g/ml}$) for 48 hours. As shown (B) addition of recombinant gD in the presence of IL-2 increases the proportion of FoxP3⁺ cells among the CD4 T cells. (C) Bar graphs depicting the percentages of CD4⁺ CD25⁺ FoxP3⁺ CD4 T cells in the cultures under indicated incubation conditions. Error bars represent SEM. The level of significance was determined using one-way ANOVA using Bonferroni post hoc settings. In some experiments enriched CD4 T cells from FoxP3-GFP mice were sorted for FoxP3⁺ from enriched CD4 T cell population based on GFP expression. Sorted FoxP3⁺ cells (2×10^5 cells) were then incubated with different concentrations of HSVgD and IL-2 (**conc.**). CD69 (D) and CD25 (E) expression on sorted FoxP3⁺T cells following 48hrs post-incubation is shown. Data are representative of three independent experiments.

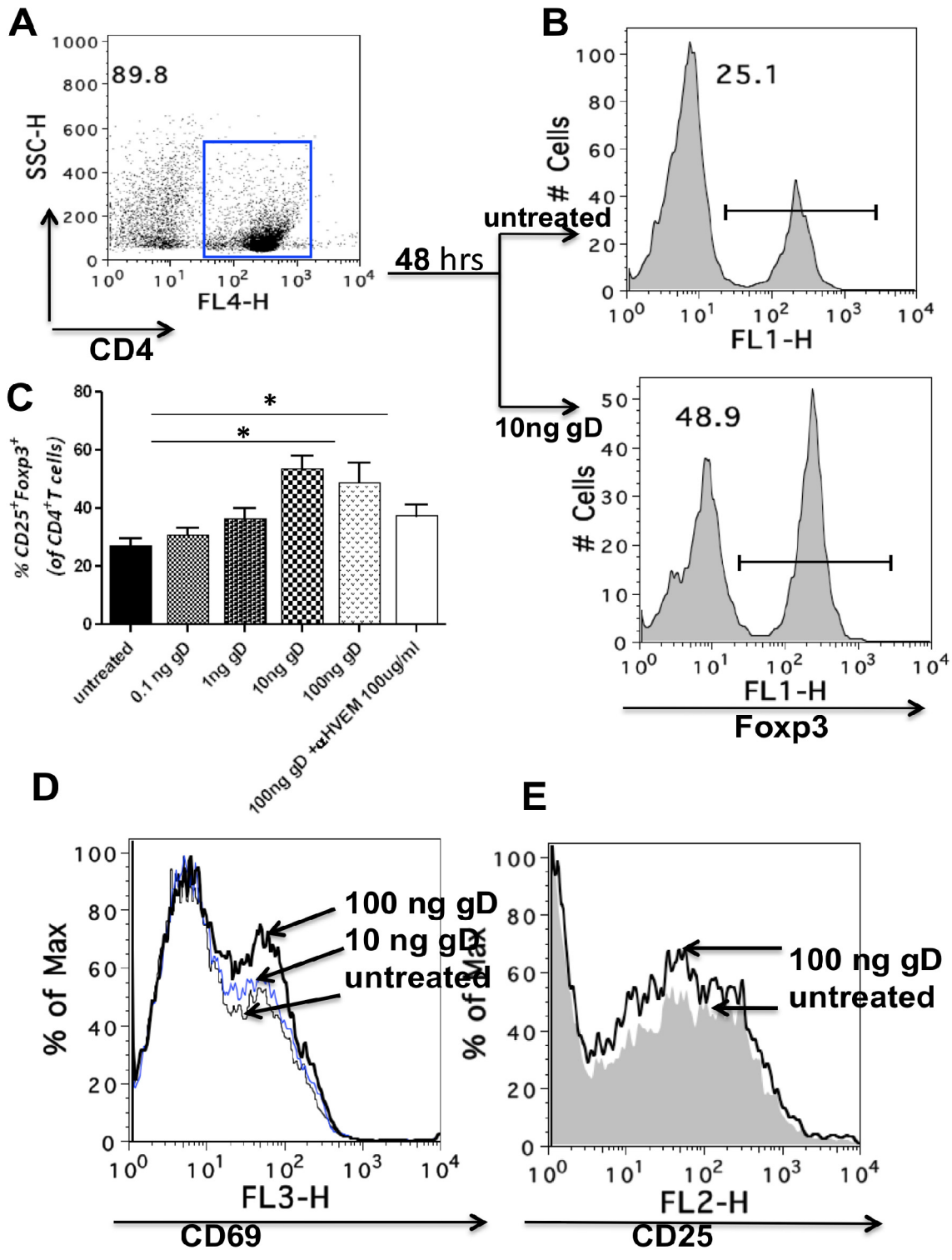


Figure 4.5 HSV-1gD can help to expand Tregs

CD4 T cells were enriched from the splenocytes of naïve mice using miltenyi biotech kit and FoxP3⁺ cells were sorted from enriched CD4 T cell population based on GFP expression. Representative FACS plots showing presort (A) and post sort (B) population. (C) CD4⁺FoxP3⁺ Treg populations from naive WT mice were stimulated with anti-CD3 alone, anti-CD3 plus recombinant HSV-1gD, or anti-CD3 plus anti-CD28 at the indicated concentrations. The proliferation was determined by [3H]thymidine incorporation. Tregs proliferated significantly at relatively high concentrations of anti-CD3 with HSV-1gD compared with anti-CD3 alone. (D) CD4⁺FoxP3⁺ Treg populations from naive WT mice were stimulated with anti-CD3 (1 ug/ml), anti-CD3 (1 ug/ml) plus HSV-1gD (1 ug/ml), or anti-CD3 plus HSV-1gD (1 ug/ml) and soluble anti-HVEM Ab (100 ug/ml) as indicated. The proliferation was determined by [3H] thymidine incorporation. These experiments were repeated two times. Error bars represent SEM. The level of significance was determined using student's t test.

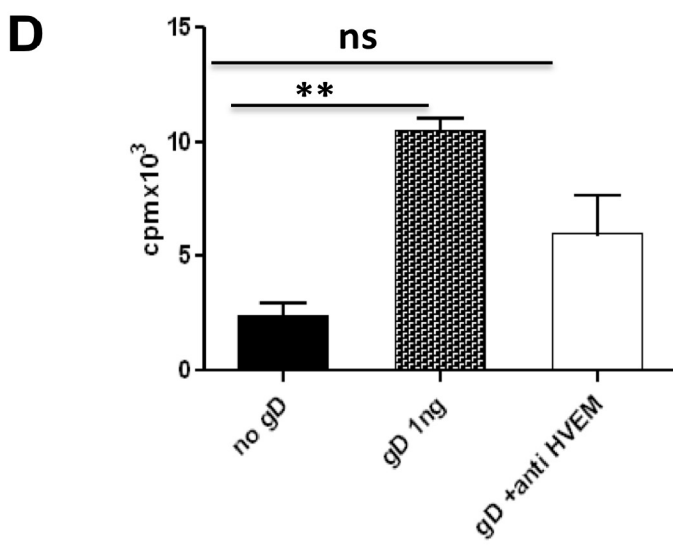
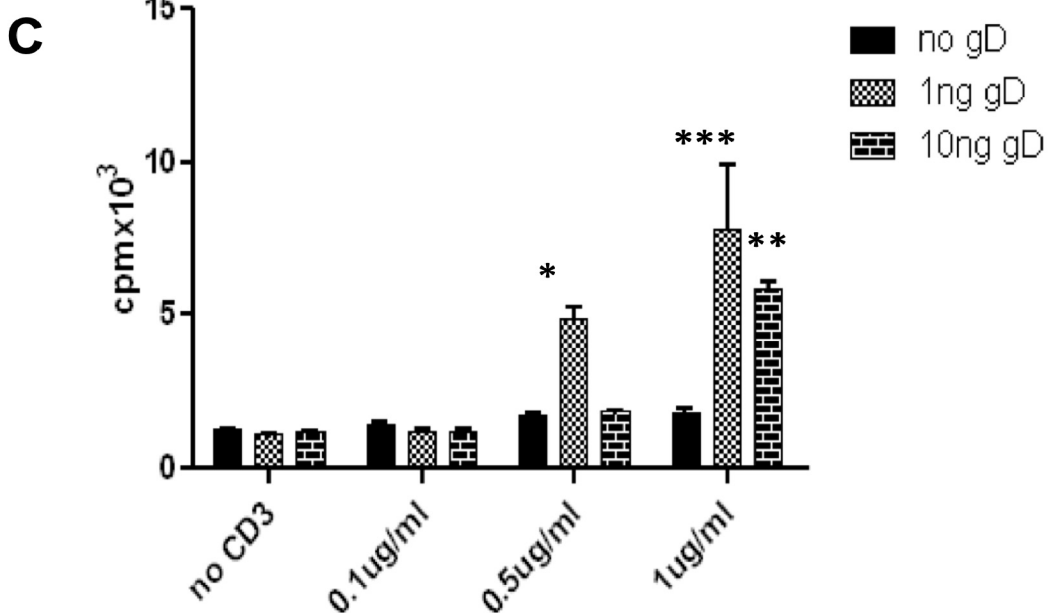
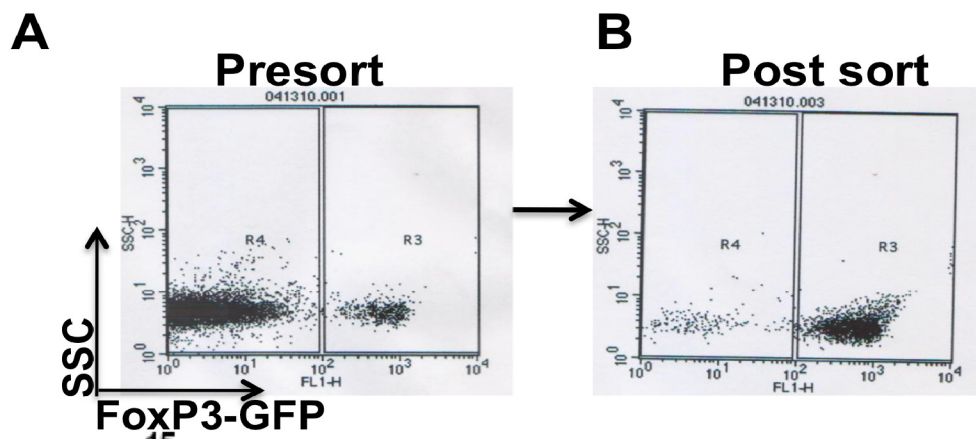


Figure 4.6 Diminished representations of CD4⁺FoxP3⁺ regulatory T cells in the HVEM knockout mice

CD4⁺ and CD4⁺FoxP3⁺ T cell responses were compared among age and gender matched HSV-1 infected WT and HKO animals at indicated time points post infection. Representative FACS plots showing frequencies of CD4⁺ T cells from WT and HKO animals in the draining PLN at day 5.5 (A) and day 8 (B) following HSV-1KOS infection in the footpad. Representative FACS plots showing CD4⁺FoxP3⁺ T cells from WT and HKO animals in the draining PLN at day 5.5 (C) and day 8 (D) following HSV-1kos infection in the footpad. (E) Histograms depicting FoxP3 expression on CD4T cells in WT (black line) or HKO (shaded area) mice in draining PLN at day 8 post HSV infection in the foot pad. (F) MFI of FoxP3 expression in WT and HKO animals at day 8 p.i is shown. HSV-1 infected mice were pulsed with BrDU 12 hours before sacrifice. At day 8 p.i. (I and J) draining popliteal lymphoid populations were analyzed by FACS for evidence of BrDU incorporation. Data are representative of three independent experiments with 5 mice per group in each experiment. Error bars represent SEM. The level of significance was determined using student's t test.

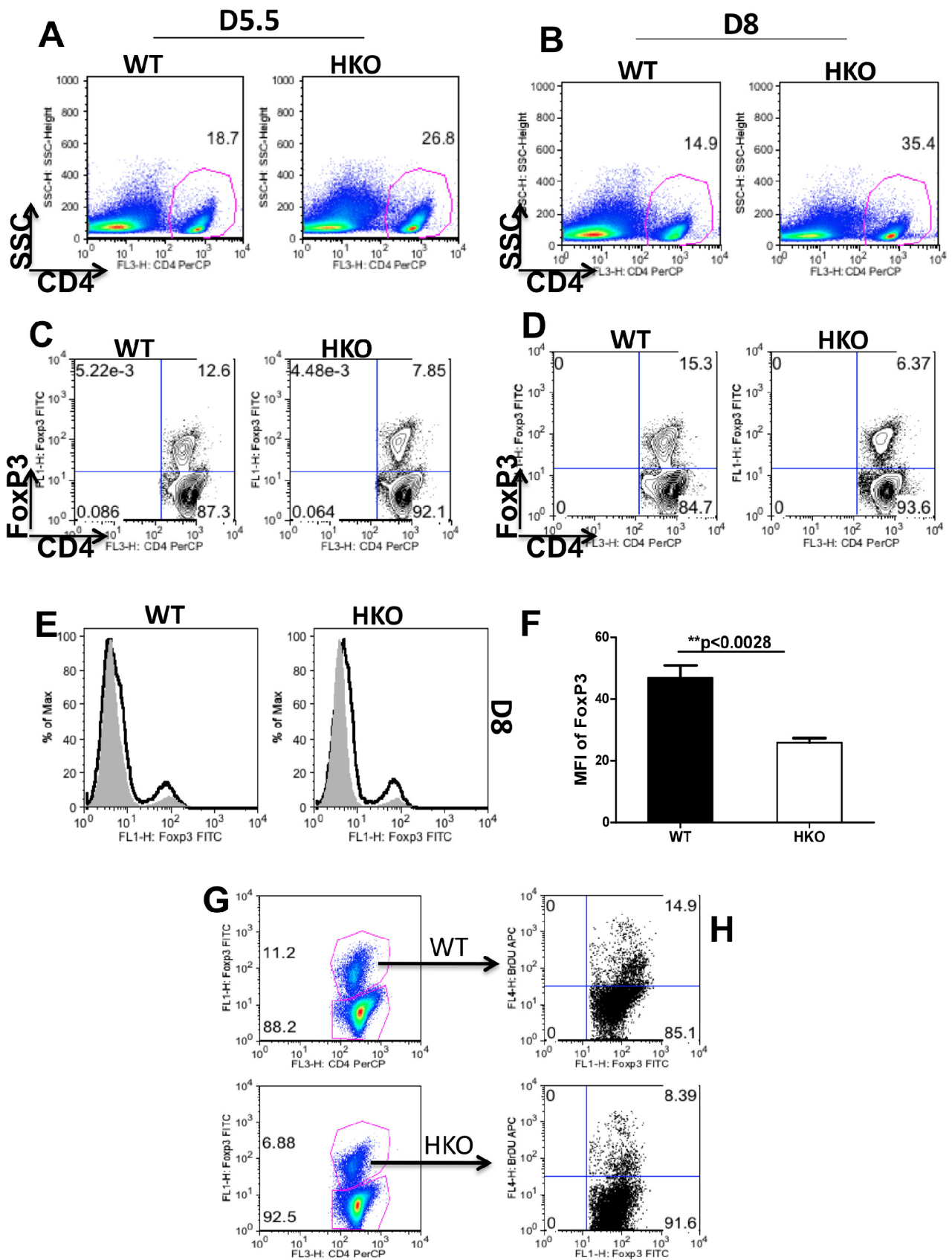


Figure 4.7 Reduced numbers of CD4⁺FoxP3⁺ per CD4⁺FoxP3⁻T cells in HVEM knockout mice

(A) Absolute numbers of CD4⁺ and CD4⁺FoxP3⁺T cells in the draining PLN of WT and HKO animals at indicated time points as calculated from 4.6 C and D. (B) Ratios of absolute numbers of CD4⁺FoxP3⁺ cells to CD4⁺T cells at day 5.5 (B) and day 8 (C) p.i. Ratios of absolute numbers of CD4⁺FoxP3⁺ cells to CD4⁺FoxP3⁻T cells at day 5.5 (D) and day 8 (E) p.i. is shown.

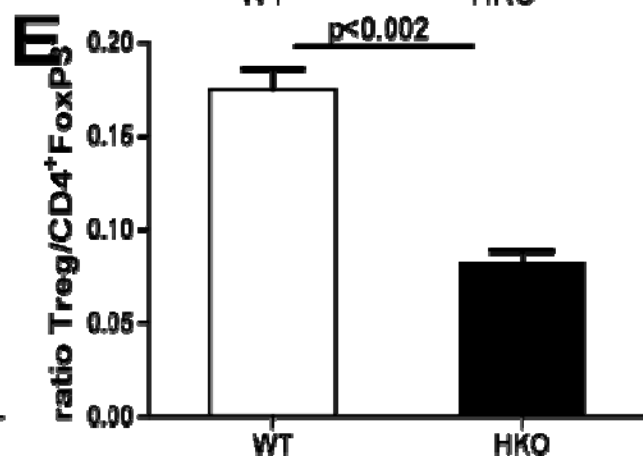
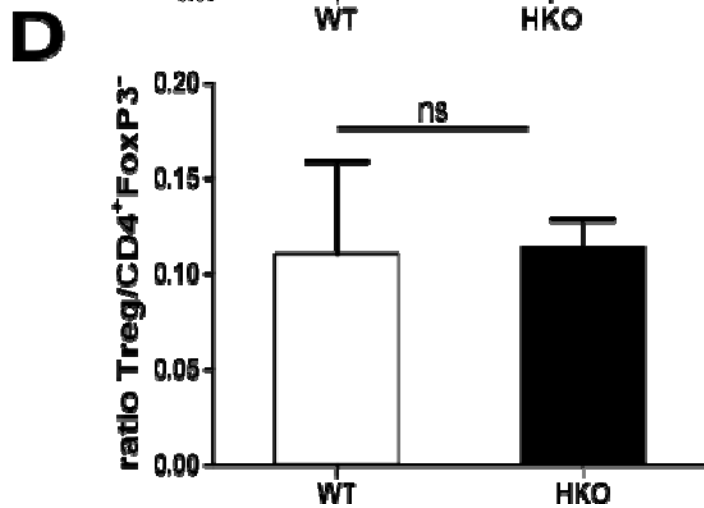
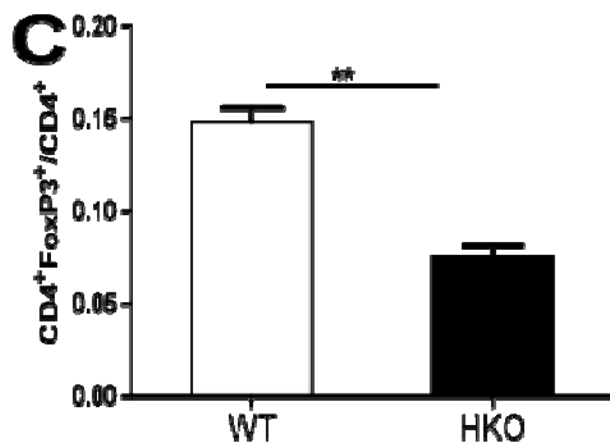
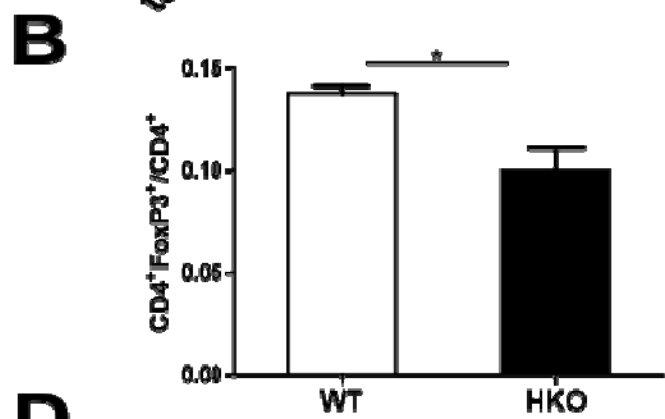
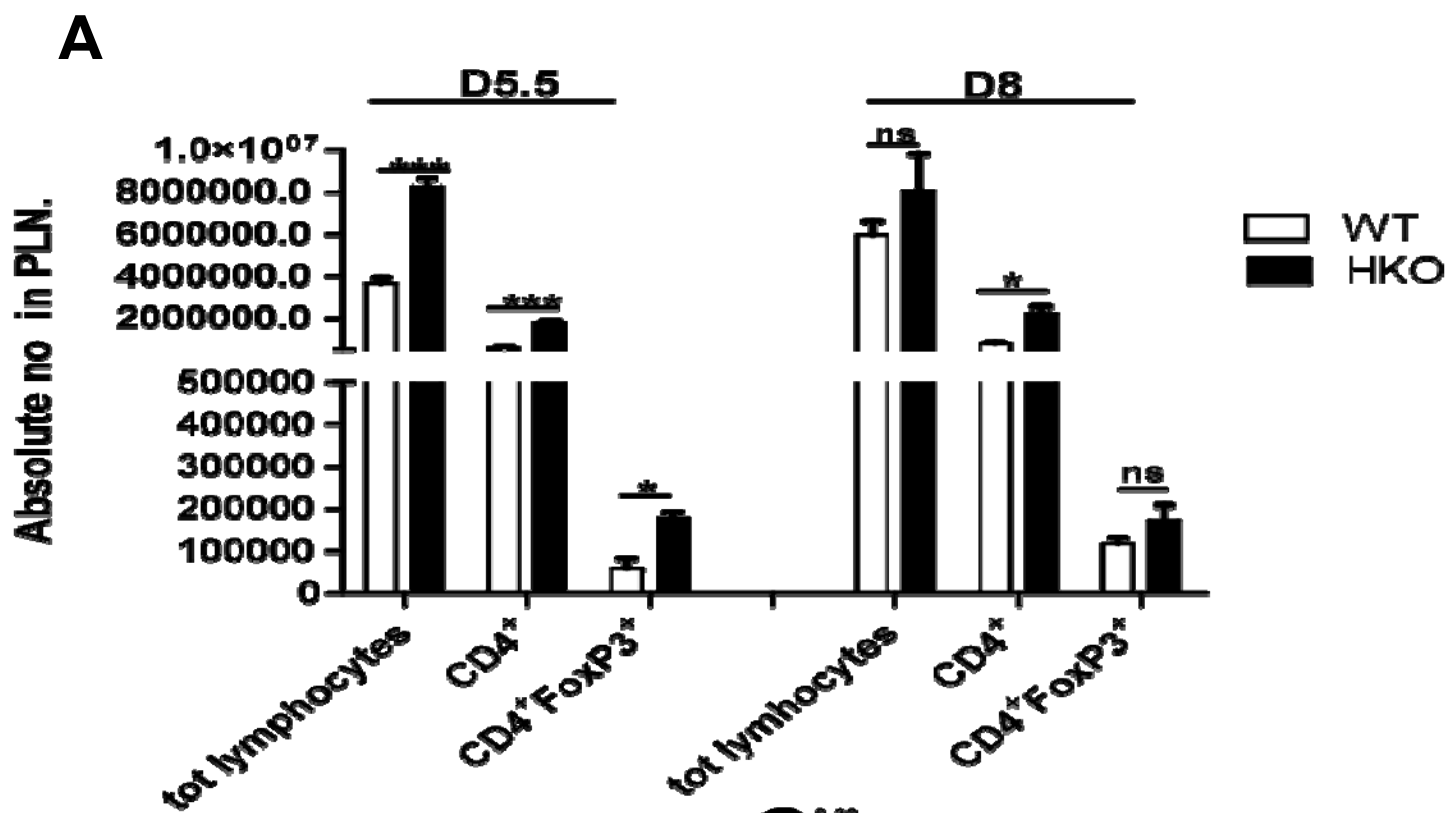


Figure 4.8 Diminished frequencies of activated Tregs in HKO animals

(A) Gated CD4⁺T cells from WT and HKO mice were analyzed at indicated time points by flow cytometry for co-expression of the Treg surface markers CD25 (A, B and E), CD103 (C, D and F) and activation marker CD44 (H) with the Treg associated transcription factor FoxP3. (H) MFI of CD44 expression on WT and HKO Tregs is shown. CD62L expression on CD4⁺FoxP3⁺ cells in WT and HKO mice at indicated time points is shown. The FACS plots of a representative mouse are shown. Five animals/group were analyzed, which all gave very similar results.

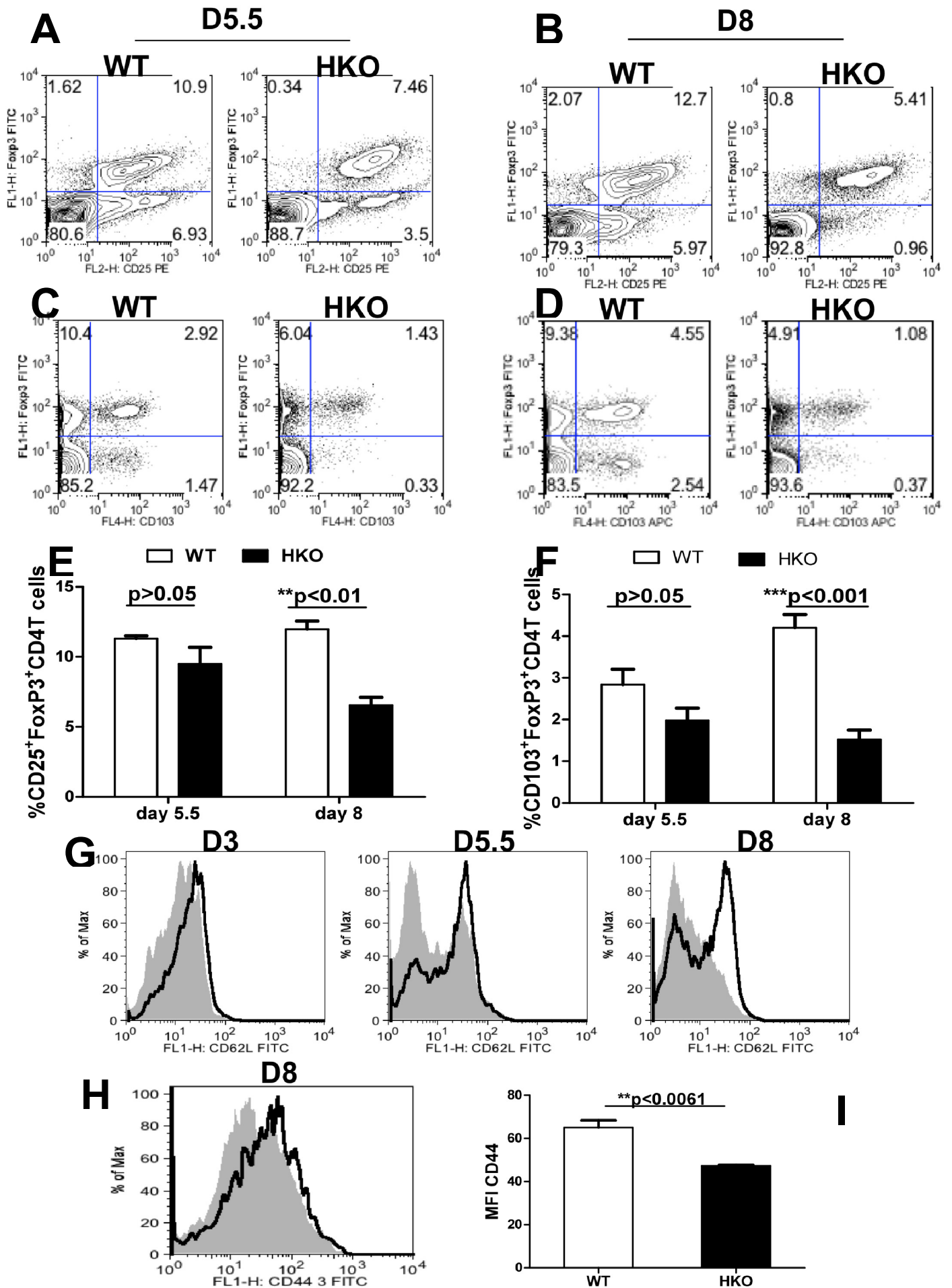
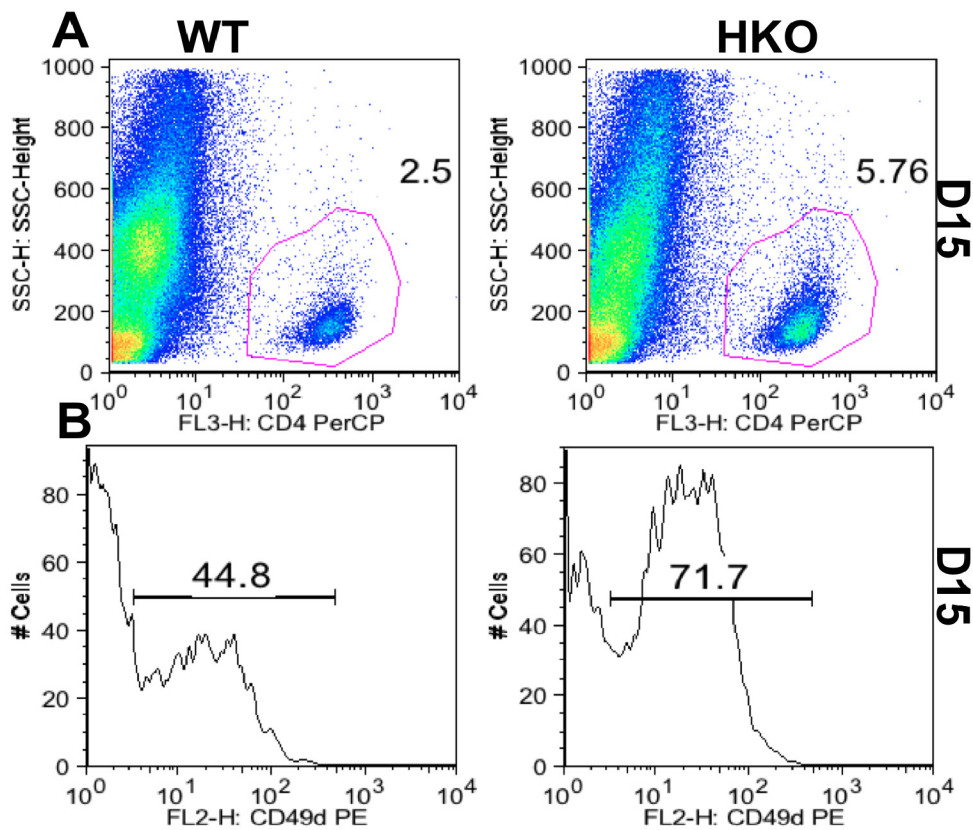


Figure 4.9 Influence of HVEM expressing T regs on outcome of immune response to HSV.

WT or HKO mice were infected ocularly with 1×10^4 PFU of HSV RE in a 3- μ l drop in the footpad. Single cell suspension of the infected corneas were prepared from pooled 6 corneas (n=3) at day 15 p.i. from each group (WT and HKO) of mice. The cells were labeled for: **(A)** CD4⁺ and **(B)** CD49d (VLA4). The numbers on the dot plots indicates the percentage of the cells expressing the particular markers in WT and HKO mice. The experiment was repeated three times and data are representative of a single experiment.



PART-V
CONCLUSION

Many viruses infect humans and most are controlled satisfactorily by the immune system with limited damage to host tissues. Some viruses, however, do cause overt damage to the host, either in isolated cases or as a reaction that commonly occurs after infection. The outcome is influenced by properties of the infecting virus, the circumstances of infection and several factors controlled by the host. In this dissertation, we focus on host factors that influence the outcome of viral infection, including the induction of anti-inflammatory cells and proteins, as well as the presence of counter-inflammatory mechanisms. Here we discuss our current understanding of the circumstances of infection and host-controlled factors that could explain why an infection can be resolved with minimal impact or cause substantial tissue damage.

Understanding of the circumstances of infection and host-controlled factors that could explain why an infection can be resolved with minimal impact or cause substantial tissue damage could prove to be useful in the future for the control and perhaps prevention of tissue-damaging virus infection. Accordingly by inhibiting the factors involved in immunopathology following an acute viral infection or manipulating the immunomodulatory factors such as some cytokines, groups of molecules derived from omega-3 polyunsaturated fatty acids, as well as some of the carbohydrate binding proteins of the galectin family and co stimulatory molecules like HVEM could be beneficial in preventing immunopathology and to enhance immune responses to vaccines.

VITA

Shalini Sharma was born in Jodhpur, Rajasthan, India. She received her DVM Degree from the Rajasthan Agricultural University in Bikaner, Rajasthan India, in 2002. She completed her M.V.Sc. (Master of Veterinary science) in Veterinary Biochemistry from the Rajasthan Agricultural University in Bikaner, Rajasthan India, in 2004. She worked for one year as a Veterinary Officer in Jodhpur, Rajasthan, India. She also worked as research specialist at Emory University, Atlanta GA, USA. She was accepted to graduate school at the University of Tennessee, Department of Comparative and Experimental Medicine, in summer 2008. She received her Doctorate Degree in Comparative and Experimental Medicine in 2011. She is going to pursue her postdoctoral training under Dr. Paul G Thomas at Department of Immunology, St. Jude Children's Research Hospital Memphis, TN.